National Research FLAGSHIPS
Wealth from Oceans

CSIRO

WAMSI NODE 1 PROJECT 2

FINAL REPORT

Coastal ecosystem characterisation, benthic ecology, connectivity and client delivery modules

ANNEXURE A – RESEARCH CHAPTERS

Editor: John K. Keesing
Chapter senior authors: Russ C Babcock *et al.,* Peter D Craig *et al.,* Philip E England et al. and Mat A Vanderklift *et al.*
30 June 2011

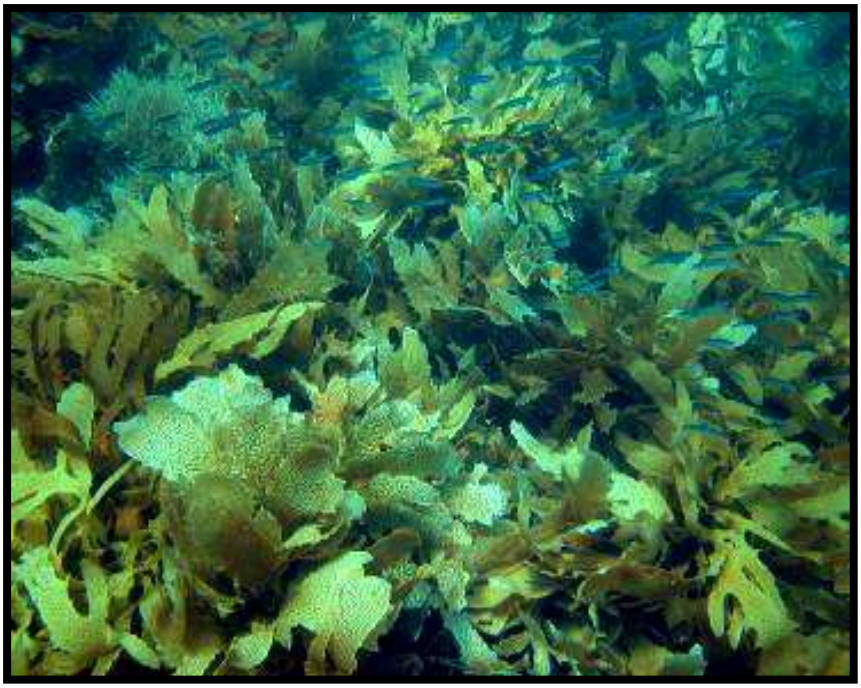

www.csiro.au

western australian marine science institution

This is an unpublished report for the Western Australian Marine Science Institution [WAMSI] It should not be cited without permission of the authors.

Enquiries should be addressed to:

Dr John Keesing, CSIRO Private Bag 5, Wembley, Australia 6913

john.keesing@csiro.au

Important Disclaimer

Acknowledgements

The editor and authors would like to thank WAMSI for financial support for this project, the vessel and crew of the RV Linnaeus especially Stelios Kondylas and Ryan Crossing, Toni Cannard, Lucy Kay and Mizue Iijima for helping prepare the report and the following people who assisted with field and laboratory work and sample and data analyses: Douglas Bearham, Claudio Del Deo, Quinton Dell, Ryan Downie, Geordie Clapin, Kylie Cook, Tennille Irvine, Hector Lozano-Montes, Natalie Millar, Richard Pillans, Dirk Slawinski, Joanna Strzelecki, Ted Wassenberg, Mads Thomsen, Fernando Tuya and Peter Kiss. Edith Cowan University and the Australian Research Council contributed additional resources to the genetics component. Jason Waring, Irshad Nainar and Dirk Slawinski are acknowledged as initiating the concept and original development of the DIVE software that was subsequently extended through this WAMSI project.

Contents

.

List of Figures

List of Tables

1. AN ASSESSMENT OF THE IMPORTANCE OF PHYSICAL FORCING AND ECOLOGICAL INTERACTIONS AMONG KEY FUNCTIONAL GROUPS IN DETERMINING PATTERNS OF SPATIAL MOSAICS IN BENTHIC HABITATS

Russ C Babcock, Damian P Thomson, Peter D Craig , Mat A Vanderklift, Graham Symonds and Jim Gunson.

CSIRO Marine and Atmospheric Research

1.1 Introduction

Ecologically sustainable management of resources requires the ability to rapidly address the current state of resources as well as key ecological processed which maintain these resources. Increasingly, resource managers also require information on the relative importance of physical versus biological processes in order to predict how ecosystems may respond to environmental variability including a changing climate. In order to better characterise the south west Australian marine coastal and shelf ecosystem structure and function, and enhance our shared capacity to understand, predict and assess ecosystem response to anthropogenic and natural pressures, we assessed the relative importance of physical forcing and ecological interactions among key functional groups in determining patterns of spatial mosaics in benthic habitats.

The project focused on the habitat dynamics of temperate algal communities on reefs off Western Australia. These algal communities display a complex mosaic of different algal assemblages, or habitat types, broadly characterised as either canopy or gap habitats. This mosaic structure has a strong influence on the overall biodiversity of rocky reefs in temperate south west Australia. Changes in this pattern and the relative proportion of the two habitat types will therefore have profound implications for the biodiversity and productivity of coastal marine ecosystems in the region. In order to understand the dynamics of this habitat mosaic structure, we employed three complimentary approaches. First, we describe natural patterns of habitat variation and correlate these patterns with physical and ecological variables. Second, we conduct experimental manipulations to better understand the ecological processes underpinning patterns in habitat mosaics. Finally we develop habitat models of ecosystem dynamics to help predict environmental change under varying physical or ecological conditions.

Mosaics of habitat dominated by canopy-forming macroalgae and canopy-free (open-gap) habitat are prominent features of temperate subtidal reefs. However, the persistence and mechanisms underlying the arrangement of these patterns are not well understood. We described patterns in the proportion of reef covered by each of these habitats, and the length of patches of each habitat, at 20 sites encompassing a gradient in wave exposure in south-western Australia. Our aims were to characterise patterns, and the strength of associations with potential influences, in order to develop models of habitat mosaic generation and maintenance. Modelled seabed orbital velocities explained approximately 35% of the variation in the length of open-gap patches. This observation supports the hypothesis that waves create open-gaps by dislodging canopy algae. Herbivorous damselfish (Parma spp.) were 5.6 times more likely, and the sea urchin *Heliocidaris erythrogramma* was 20 times more likely, to be encountered at sheltered inshore sites than at exposed sites further from shore. Parma were 8.2 times more likely to be found in open-gap habitat. However, there was no relationship between the occurrence of either herbivore and the proportion of open-gap habitat among sites. These

observations do not support a hypothesis that grazing by herbivores creates open-gaps. Massive sponges were three times as likely to be found in open-gap habitat, and hard corals were 91 times more likely to be encountered in open-gap habitat. The strength of these associations suggests that canopy algae might negatively influence sessile invertebrates. Further, the large size and likely old age of sessile invertebrates, particularly hard corals, indicates that patches of open-gap habitat can persist for decades. The patterns observed suggest that wave-induced disturbances create open-gaps and that these gaps are persistent features of temperate reefs.

Whether they are observational, experimental or modelling based, studies of the natural environment are characterised by their 'grain' and 'extent', the smallest and largest scales represented in time and space. These are imposed scales that should be chosen to ensure that the natural scales of the system are captured in the study. We developed a simple cellular automata model of habitat to represent the presence or absence of vegetation, with global and local interactions described by four empirical parameters. Such a model can be formulated as a nonlinear Markov equation for the habitat probability. The equation produces inherent space and time scales that may be considered as transition scales or the scales for recovery from disturbance. However, if the resolution of the model is changed, the empirical parameters must be changed to preserve the properties of the system. Further, changes in the spatial resolution lead to different interpretations of the spatial structure. In particular, as the resolution is reduced, the apparent dominance of one habitat type over the other increases. The model provides an ability to compare both field and model investigations conducted at different resolutions in time and space. The model allows us to better interpret our observations and also forms the basis for ongoing modelling studies.

The results of the study have been published or are in review in the peer reviewed international literature and are presented in the three sections below:

1) Evidence for persistent kelp forest habitat patches and multiple hypotheses for their creation and maintenance. (*In review* Marine Ecology Progress Series.)

2) Deterministic aspects of kelp forest patch dynamics and models of patch turnover (*In review*)

3) Imposed and inherent scales in cellular automata models of habitat. (Craig PD. 2010 Ecological Modelling 221:2425–2434).

1.2 Evidence for persistent kelp forest habitat patches and multiple hypotheses for their creation and maintenance

In Review: Marine Ecology Progress Series

Thomson DP, Babcock RC, Vanderklift MA, Symonds G.

CSIRO Marine and Atmospheric Research, Private Bag 5, Wembley, WA, 6913

Keywords: *Ecklonia radiata*, patch dynamics, alternate states, wave exposure, habitat heterogeneity, grazing, coral.

1.2.1 Abstract

Mosaics of habitat dominated by canopy-forming macroalgae and canopy-free (open-gap) habitat are prominent features of temperate subtidal reefs. However, the persistence and mechanisms underlying the arrangement of these patterns are not well understood. We described patterns in the proportion of reef covered by each of these habitats, and the length of patches of each habitat, at 20 sites encompassing a gradient in wave exposure in south-western Australia. Our aims were to characterise patterns, and the strength of associations with potential influences, in order to develop models of habitat mosaic generation and maintenance. Modelled seabed orbital velocities explained approximately 35% of the variation in the length of open-gap patches. This observation supports the hypothesis that waves create open-gaps by dislodging canopy algae. Herbivorous damselfish (Parma spp.) were 5.6 times more likely, and the sea urchin *Heliocidaris erythrogramma* was 20 times more likely, to be encountered at sheltered inshore sites than at exposed sites further from shore. Parma were 8.2 times more likely to be found in open-gap habitat. However, there was no relationship between the occurrence of either herbivore and the proportion of open-gap habitat among sites. These observations do not support a hypothesis that grazing by herbivores creates open-gaps. Massive sponges were three times as likely to be found in open-gap habitat, and hard corals were 91 times more likely to be encountered in open-gap habitat. The strength of these associations suggests that canopy algae might negatively influence sessile invertebrates. Further, the large size and likely old age of sessile invertebrates, particularly hard corals, indicates that patches of open-gap habitat can persist for decades. The patterns observed suggest that wave-induced disturbances create open-gaps and that these gaps are persistent features of temperate reefs.

1.2.2 Introduction

Models of succession describe a process whereby episodic disturbances (such as storms) clear vegetation, thus providing an opportunity for colonisation by pioneer species that are then gradually replaced by competitively-dominant species. In some cases, disturbed areas eventually return to the same pre-disturbance or 'climax' state (Connell & Slatyer 1977). However, succession to a single state is frequently not the only possible outcome. For example, patches of algae can coexist with other space-occupying organisms, such as mussels (Petraitis & Dudgeon 2005) or seagrasses and other algae (Menge *et al.*, 2005), which are alternatives to an algae-dominated state (Johnson & Mann 1988, Drake 1990, Sutherland 1990, Menge *et al.*, 2005, Petraitis & Dudgeon 2005). These non-algal dominated states can represent different stages in a deterministic process of recovery to a single state, or the outcomes of divergent succession determined by events that occur during recovery. The species that are advantaged during recovery can be determined by a set of so-called 'assembly rules' see Keddy (1992).

Canopy-forming algae (e.g. kelp) are a characteristic feature of subtidal temperate reefs (Schiel 1988, Wernberg *et al.*, 2003, Connell & Irving 2008). Due to their large size and strong influence over the physical environment beneath the canopy (by altering light, water motion, sedimentation, and abrasion) adult kelps readily outcompete understory flora and fauna (Dayton 1985, Toohey *et al.*, 2004, Wernberg *et al.*, 2005). Descriptions of assemblages of macroalgae are often based on their association with (canopy tolerant) or without (canopy intolerant) kelp (Irving & Connell 2006, Toohey & Kendrick 2008). The competitive dominance of canopy algae may be periodically challenged through disturbances, such as storms or grazing.

Algal assemblages in southern Australia are characterised by two distinct alternate states. The dominant canopy state, consisting largely of the small kelp *Ecklonia radiata*, coexists with patches devoid of kelp (open-gap state) that are dominated by small filamentous and foliose algae (Connell & Irving 2008, Wernberg & Connell 2008). Canopy and open-gap patches vary in size from metres to hundreds of metres (Hatcher 1989, Connell & Irving 2008, Toohey & Kendrick 2008, Wernberg & Connell 2008) and can persist from months to years (Toohey *et al.*, 2007).

One potential influence on the size and distribution of canopy and open-gap patches is wave energy. Wave-generated hydrodynamic forces can affect algae directly through damage or dislodgement (Dayton & Tegner 1984, England *et al.*, 2008, Wernberg & Goldberg 2008) or indirectly by affecting the behaviour of herbivores (Vadas *et al.*, 1986, Konar & Estes 2003, Lauzon-Guay & Scheibling 2010). Despite this, few studies have examined relationships between the distribution of canopy algae and water flow at the sea floor. The few studies that have attempted to do so have either relied on proxies for water flow, such as indices of wave exposure (Fowler-Walker *et al.*, 2006, Wernberg & Connell 2008) or used localised flow measurements that are difficult to extrapolate to the influence of flow over an entire reef (Siddon & Witman 2003, Toohey 2007).

Another process that can influence the size and distribution of canopy and open-gap patches is grazing. For example, high densities of sea urchins can denude extensive areas, creating patches devoid of macroalgae (open-gaps) that can persist for decades across hundreds of kilometres of coastline (Dayton 1975, Scheibling & Raymond 1990, Babcock *et al.*, 1999, Andrew & O'Neill 2000). However, while sea urchin grazing has been shown to have devastating and broad scale effects on kelp canopies in many parts of the world (Breen & Mann 1976, Scheibling *et al.*, 1999), this phenomenon has not been reported along thousands of kilometres of the southern Australian coastline (Vanderklift & Kendrick 2004, Connell *et al.*, 2007). Herbivorous fish do not typically create open-

gaps on temperate reefs, although they can maintain open-gaps that are already present (Jones & Andrew 1990, Jones 1992).

Disturbed areas or open-gaps in canopies are often colonised by turf algae, which in turn can inhibit kelp recruitment (Kennelly 1987a, Gorman & Connell 2009) thus slowing, or even preventing, the recovery of canopies (Dayton *et al.,* 1984). Since kelp also inhibits the growth of understory algae, such as some turf, these interactions may further stabilise the presence of alternate canopy and open-gap patches. Episodic disturbances might initiate open-gap patches, while chronic perturbations, such as increased nutrients or sediment runoff, might confer turfs a competitive advantage over canopy forming algae (Benedetti-Cecchi *et al.,* 2001, Gorman & Connell 2009).

The presence of canopy-forming algae can have both negative and positive consequences for sessile invertebrates. Smothering, shading and abrasion by brown algae can negatively affect reef-building corals (Coyer *et al.,* 1993, McCook *et al.,* 2001, Jompa & McCook 2002) and in some cases can poison coral tissues through direct contact (Rasher & Hay 2010). Yet, in some instances, shading by canopy algae can have a positive effect on tropical corals; for example by ameliorating the effects of elevated water temperatures (McCook *et al.,* 2001).

In this study, we adopted a mensurative approach to evaluating and developing hypotheses relating to patch structure of temperate Australian reefs, cf Underwood *et al.,* (2000). We hypothesised that spatial patterns in the composition and size of patches (canopy and open-gap) would be related to variations in wave exposure, the abundance of herbivores (sea urchins and fish) and large sessile invertebrates (corals and massive sponges), and the three-dimensional complexity of the reef (rugosity). The aims of this study were therefore to test for the presence of relationships between the cover and size distribution of patches of canopy algae and: (1) wave exposure (measured as bottom orbital wave velocity), (2) the abundance of herbivores, and (3) the abundance of dominant sessile invertebrates.

1.2.3 Methods

Study area

This study was conducted in Marmion Lagoon, Western Australia (31˚50', 115˚42'). The lagoon is characterised by three parallel lines of limestone reef, located approximately 0.5 km, 2.4 km and 4.2 km offshore (Figure 1.1). The shallowest reefs are located on the inshore and mid-shelf reef lines (1 to 5 m) and deeper reefs are located on the offshore reef line (10 to 18 m). Inshore reefs are high relief (3 – 5 m vertical relief) isolated patch reefs surrounded by large areas of sand and seagrass. In comparison, mid-shelf and offshore reefs are larger (> 1 ha) and are typically separated by narrow channels of sand and seagrass. The mid-shelf reef line hosts the largest area of reef (approximately 7 ha) and for the purposes of this study was divided into inner and outer sections because of the difference in their exposure to waves. For a detailed description see Hatcher (1989) and Toohey *et al.,* (2004).

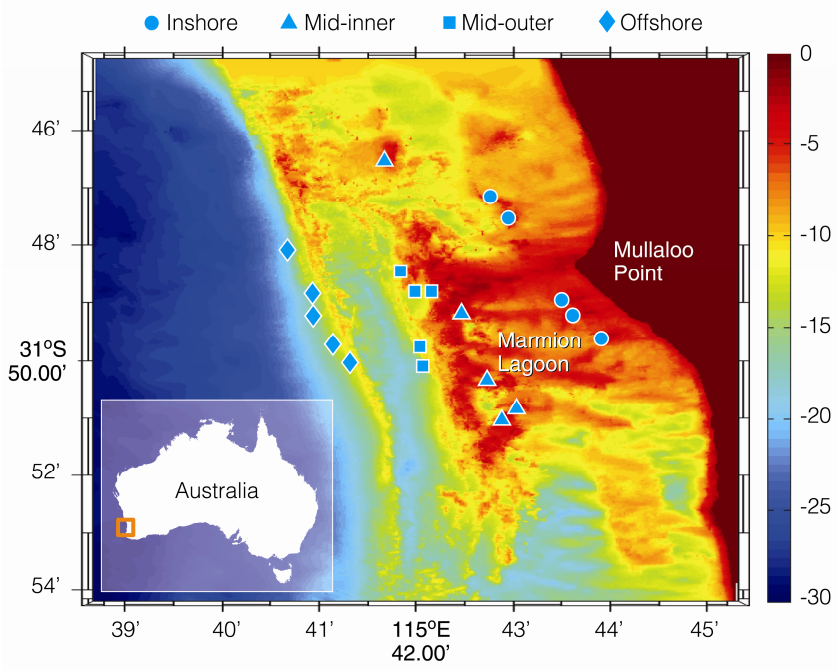

Figure 1.1. Map showing the regional context, bathymetry and location of the 20 sites surveyed within Marmion Lagoon. At increasing distances from the coast are the inshore sites ●, mid-inner sites ▲, mid-outer sites ■ and offshore sites ◆. Water depth (m) is indicated by colours on the right-hand axis.

Wave model

Estimates of wave exposure were derived using the wave model SWAN (Booij N, Ris RC and Halthuijsen LH, Delft, Netherlands). SWAN takes into account the effects of spatial propagation, refraction, shoaling, generation, dissipation and non-linear wave-wave interaction to provide estimates of mean ($Urms^{mean}$) and maximum ($Urms^{max}$) annual bottom velocity at defined grid points (Booij *et al.*, 1999, Ris *et al.*, 1999). The model domain used in this study consisted of two grids – a 300 x 300 m large-scale grid encompassing 231,630 ha, and a 30 x 30 m high-resolution grid encompassing 16,178 ha.

To estimate the annual bottom velocities (Urms, in m s-1) across the high-resolution grid, the wave model SWAN was run for one year (1 July 2007 to 31 July 2008) and the results averaged for each 30 m grid cell. The model was forced at its western boundary by wave parameters obtained from the Rottnest wave buoy (located 20 km south-west of the study area) to produce maps of the annual mean significant wave height (Hs^{mean}, in m) and bottom velocity ($Urms^{mean}$, in m s^{-1}) across the high resolution grid (Figure 1.2). A rapid decrease in wave height across the mid-reef line (Figure 1.2) results from depth-induced breaking that effectively limits the annual mean wave height across the top of these reefs to 0.8 Hs^{mean}. Similarly, bottom orbital velocities are also limited so although the offshore wave height increases during storms there is not a corresponding increase in bottom orbital velocity over the mid-shelf reef line. However, the offshore reefs are typically too deep for the waves to break, so during storms the wave height and bottom orbital velocities at offshore reefs could be larger than the annual means.

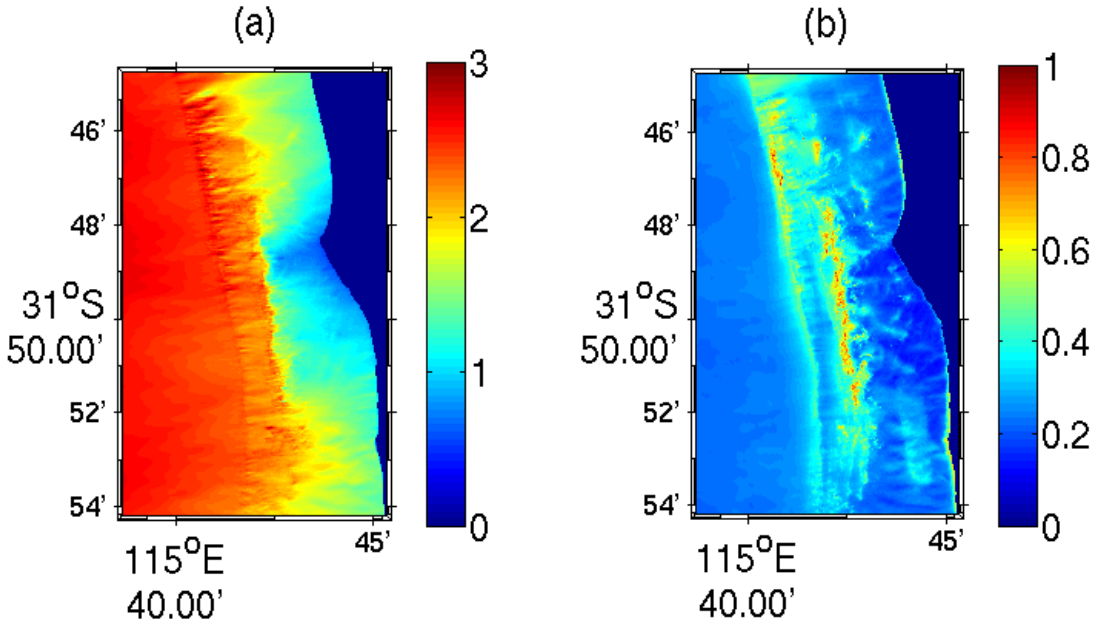

Figure 1.2. SWAN model output across the high resolution grid. (a) Significant wave height (Hs metres) and (b) root mean square bottom orbital velocity (Urms m s^{-1}).

Wave exposure for each of our study sites was estimated using the $Urms^{mean}$ and $Urms^{max}$ values from the nearest model grid point. In the case of video transects (see below for description), which spanned an extent greater than 200 metres, the Urms values were averaged for the six grid points closest to the transect position.

Habitat structure

The survey design incorporated a gradient encompassing five sites at each of the four locations (i.e. offshore, mid-outer, mid-inner and inshore). The length and proportion (% cover) of canopy and open-gap patches were measured using small-scale belt-transects by divers on SCUBA (see Wernberg and Connell (2008); n = 5 per site, length = 25 m), and large-scale towed video belt-transects (n = 5 per location, mean length = 257 m ± 26.9). Two offshore sites were not surveyed due to poor weather. Transects were measured at the two different scales mentioned above in order to ensure that we had the ability to detect patterns at both small and large scales. Transects were completed between December 2006 and January 2007.

Large-scale video transects

Towed video transects began at the same geographical coordinates as the diver transect sites. However, where conditions prevented vessel access (2 sites), video transects started immediately to the north. A downward-facing video camera was towed by a boat at a speed of 1 knot and the footage relayed via cable to a video recorder on the boat. The GPS position and depth were logged to an onboard computer connected to the video recorder and were included in the recorded images. The relative positions recorded on the video images were accurate to ± 5 m (determined using a Garmin 72 GPS). Camera height was maintained approximately two metres from the substrate such that the field of view was held constant at 1 m width.

Video footage was viewed in the laboratory and the geographical coordinates at the start and end points of each canopy and open-gap patch were recorded. The length of each patch was then calculated as the distance travelled between the start and end point of each patch. The proportions of canopy habitat and open-gap habitat were calculated as a proportion of the transect length.

Small-scale diver transects

Divers using 25 m x 1 m belt transects surveyed patterns at resolutions lower than that able to be detected using the towed video equipment; each 1 m2 section of each transect was classified into one of two categories: canopy habitat (> 50% cover of *Ecklonia radiata* and *Sargassum* spp.) or open-gap habitat (> 50% cover of filamentous and short foliose algae) (Figure 1.3). Open-gap patches consisted of predominantly small foliose and filamentous algae from the genera *Laurencia, Plocamium, Pterocladia, Ulva, Jania,* and *Curdiea*, as well as calcareous red algae from the genera *Amphiroa, Metagoniolithon* and *Tricleocarpa,* and crustose coralline algae (Figure 1.3b). The open-gap patch is equivalent to the 'open' classification used by Irving *et al.*, (2004), while canopy habitat is equivalent to the 'monospecific' or 'mixed' classifications used by these same authors. The length of each patch was calculated by summing the lengths of contiguous 1m sections. The proportions of canopy habitat and open-gap patches were calculated as a proportion of the transect area.

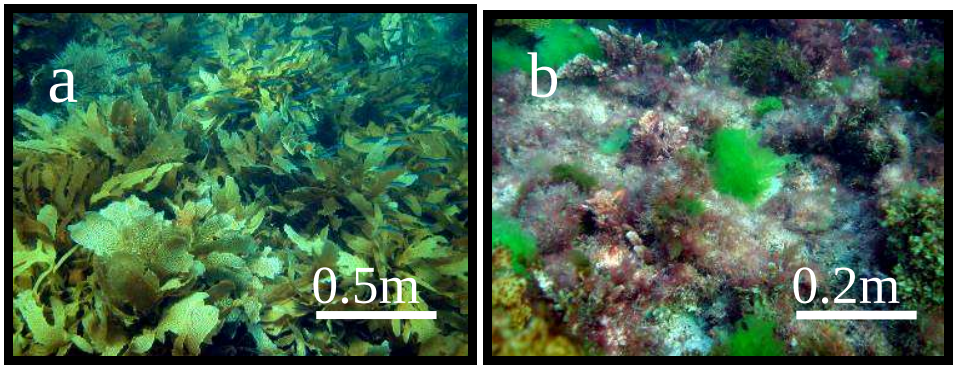

Figure 1.3. The two habitat states used in this study. (a) canopy habitat consisting of *Ecklonia radiata* and *Sargassum* spp., and (b) open-gap patches consisting of small foliose red and green algae.

Herbivores and sessile invertebrates

The numbers of herbivorous damselfish (*Parma* spp.), sea urchins (*Heliocidaris erythrogramma*), corals (*Plesiastrea* spp., *Goniastrea* spp., *Pocillopora* spp., *Favia* spp., *Faviites* spp., *Coscinarea* spp.) and massive sponges (*Mycale* spp.) present within each 1 m2 section of a transect were also recorded. Corals were identified *in situ* to genus and sponges were identified as either massive or non-massive based on appearance. The sizes of all sponges and corals were estimated to the nearest centimetre in two dimensions (maximum diameter and perpendicular diameter).

The topographic complexity (rugosity) of each site was measured using a 10 m chain laid adjacent to the transect, with care taken to ensure the chain was in contact with the substrate at all points along its length. The linear distance between the two ends of the chain were measured and an index of rugosity estimated as the ratio of the linear distance to the total chain length (McCormick 1994).

1.2.4 Statistical analysis

Permutational MANOVA (Anderson 2001) was used to test for differences in the cover (%) and average length (m) of open-gap patches among locations, sites and transects. Variables were also tested independently. Because this test uses permutation to calculate statistical significance, it is not dependent on the assumptions of parametric significance tests. Analyses were performed using Euclidian distances calculated from untransformed data, and were done using the PRIMER statistical software. For video surveys the design included replicate transects (n = 5, random) at the four locations (n = 4, fixed). For diver surveys, transects (n = 5, random) were nested within sites (n = 5), which were nested within locations (n = 4, fixed).

Non-linear regression was used to test for the significance of relationships between modelled wave exposure and site averages of open-gap lengths (using both video and diver transect data), and between rugosity and the proportion and average length of open-gap patches (diver transect data only). Best-fit regressions were obtained using a Marquardt-Levenberg algorithm. Statistical assumptions of normality, constant variance and independence of residuals were checked using Kolmogorov-Smirnov goodness-of-fit, Spearman Rank correlation and Durban-Watson statistics respectively, using the statistical software SigmaPlot v10.

Patterns of association among locations, patch types and the presence of herbivores (fish and sea urchins) or sessile invertebrates were analysed using logistic regression. The nature of differences between locations was resolved using Tukey contrasts. Analyses were performed using R statistical software. We were most interested in testing whether coefficients for each of the factors were statistically significant, so we focussed on the significance of the deviances, tested using a $\chi 2$ test (Hosmer *et al.*, 1988). Odds ratios were calculated as (p1/(1-p1))/(p2/(1-p2)), where p1 is the proportion of 'presences' in Habitat 1 (or Location 1) and p2 is the proportion of 'absences' in Habitat 2 (or Location 2).

Differences in the median size (radius in cm $\frac{maximum\ dimension}{2}$) of corals and massive sponges between locations were tested using Kruskal-Wallis one-way analysis of variance and pair-wise comparisons between locations were performed using Kolmogorov-Smirnov goodness-of-fit tests, using the statistical software SAS version 9.1.

1.2.5 Results

Wave exposure and transects

Large-scale video transects. The proportion of open-gap patches measured during the large-scale towed video transects was not significantly different among locations ($p > 0.1$, Table 1.1a). Lengths of open-gap patches, however, varied significantly among locations with a trend for increasing gap length at the offshore locations (Table 1.1b). The largest gaps were located at the mid-outer and offshore locations (Figure 1.4) where there was also a lower frequency of small (< 5 m) open-gap patches (Table 1.2, Figure 1.4).

There was a significant relationship between the average lengths of open-gap patches and modelled annual mean bottom velocity ($r^2 = 0.34$, $p = 0.037$, Figure 1.5). While the relationship between the average lengths of open-gap patches and annual maximum bottom velocity was also statistically significant, it explained a smaller proportion of the overall variation ($r^2 = 0.28$, $p = 0.021$).

Small-scale diver transects. The proportion of open-gap patches (%) measured in the small-scale diver transects did not differ among locations; however there was significant variability among sites (Table 1.3a). The size frequency distribution of open-gap lengths also did not vary significantly among locations (Table 1.1b). The modal length of open-gap patches at all locations was 1 m (Figure 1.6).

There was no significant relationship between rugosity and either the proportion ($r^2 = 0.007$, $p = 0.738$) or length ($r^2 = 0.014$, $p = 0.259$) of open-gap patches, nor was there a significant relationship between either average gap length or gap proportion and either annual mean ($r^2 = 0.132$, $p = 0.116$; $r^2 = 0.159$, $p = 0.081$) or annual maximum bottom orbital velocity ($r^2 = 0.041$, $p = 0.390$; $r^2 = 0.005$, $p = 0.758$).

Table 1.1. Results of PERMANOVA testing for differences in the proportion (a) and length (b) of open-gap patches based on towed video estimates.

(a) Proportion

Source	df	SS	MS	Pseudo-F	P(perm)	Unique perm
Location	3	3226	1075.5	2.347	0.108	999
Residual	15	6873	458.2			
Total	18	10099				

(b) Length

Source	df	SS	MS	Pseudo-F	P(perm)	Unique perm
Location	3	8862	2954	3.980	**0.048**	999
Transect	12	10508	875.69	3.22	**0.018**	998
Residual	68	18456	271.4			
Total	83	35407				

Table 1.2. Analysis of towed video estimates of cross-shore variation in open-gap patch size frequency.

Kolmogorov-Smirnov	KS	D	KSa	p
Inshore - Mid-inner	0.093	0.224	0.66	0.777
Inshore - Mid-offshore	0.252	0.525	2.01	< **0.001**
Inshore - Offshore	0.187	0.428	1.38	< **0.04**
Mid-inner – Mid-offshore	0.213	0.455	1.23	0.092
Mid-inner - Offshore	0.181	0.364	0.90	0.389
Mid-offshore - Offshore	0.082	0.171	0.50	0.961

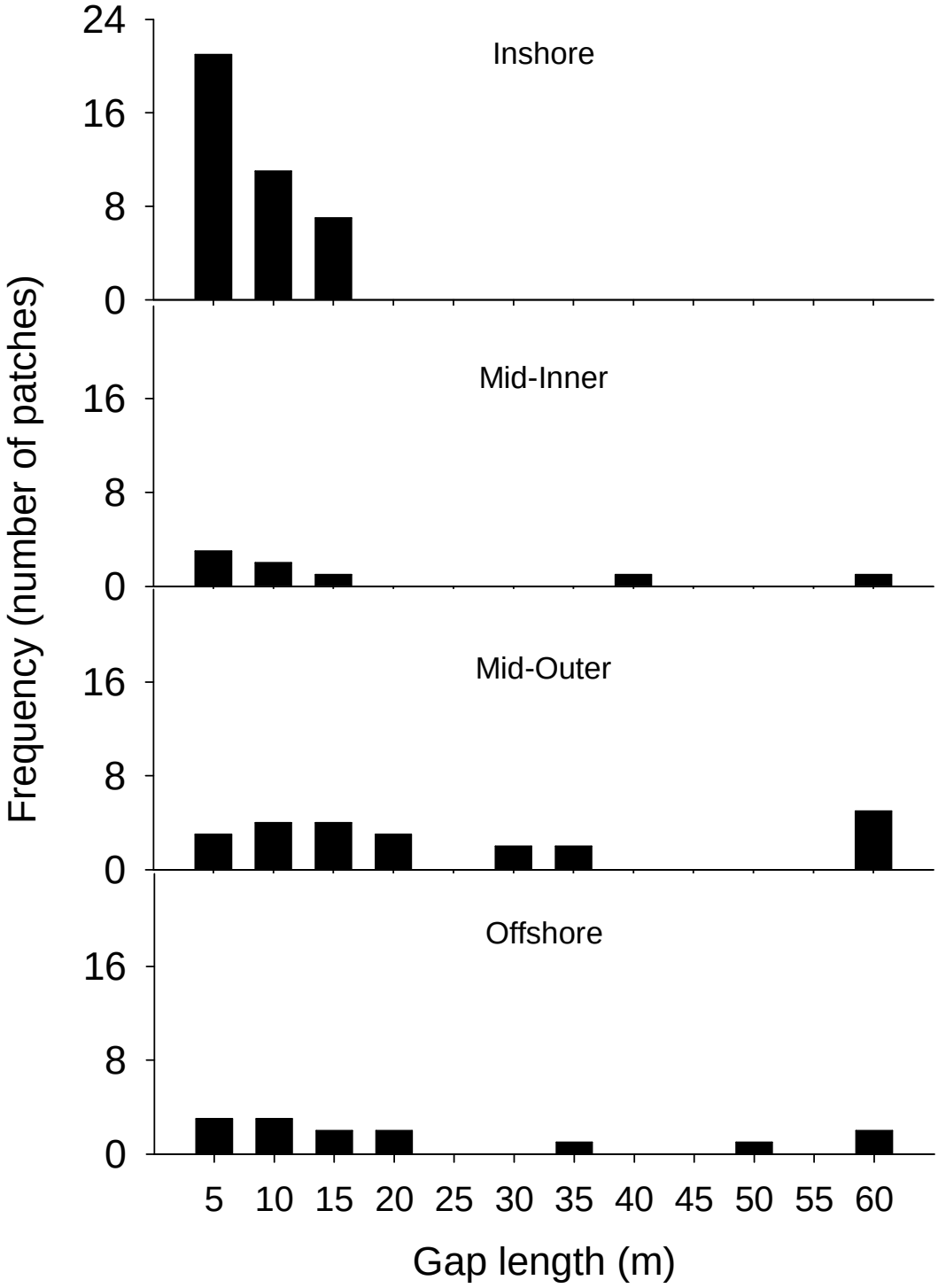

Figure 1.4. Frequency distribution of lengths of open-gap patches at each of the four locations based on towed video.

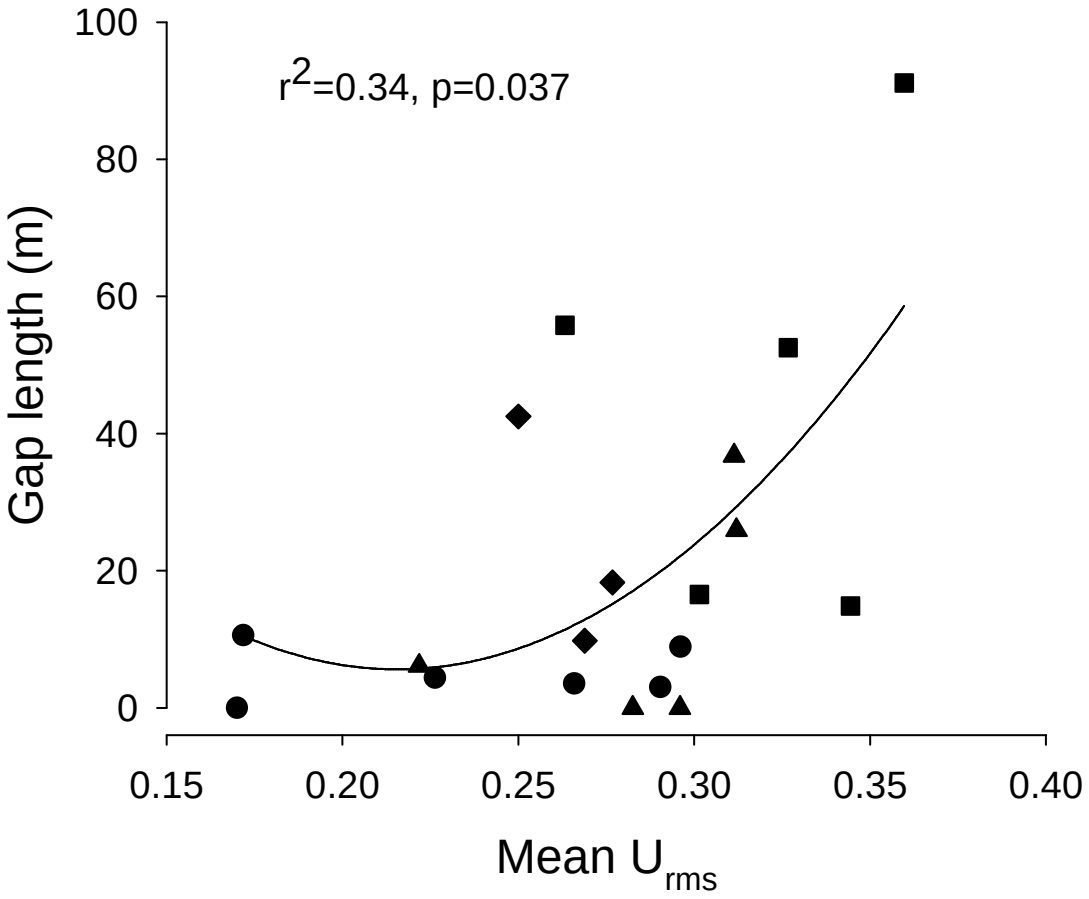

Figure 1.5. Regression (Levenberg-Marquardt fit) between modelled bottom water velocity and average length of open-gap canopy patches for. Inshore●, Mid-Inner▲, Mid-Outer■, Offshore◆.

Table 1.3. Results of PERMANOVA testing for differences in the proportion (a) and length (b) of open-gap patches based on diver estimates

(a) Proportion

Source	df	SS	MS	Pseudo-F	P(perm)	Unique perms
Location	3	6549	2183.0	1.153	0.351	999
Site	16	30302	1893.8	5.027	**0.001**	999
Residual	80	30137	376.7			
Total	99	66987				

(b) Length

Source	df	SS	MS	Pseudo-F	P(perm)	Unique perms
Location	3	8687	2895.8	1.34	0.26	998
Site	16	39487	2468.0	1.836	**0.022**	996
Transect	73	106270	1455.8	1.841	**0.001**	995
Residual	228	180260	790.6			
Total	320	329280				

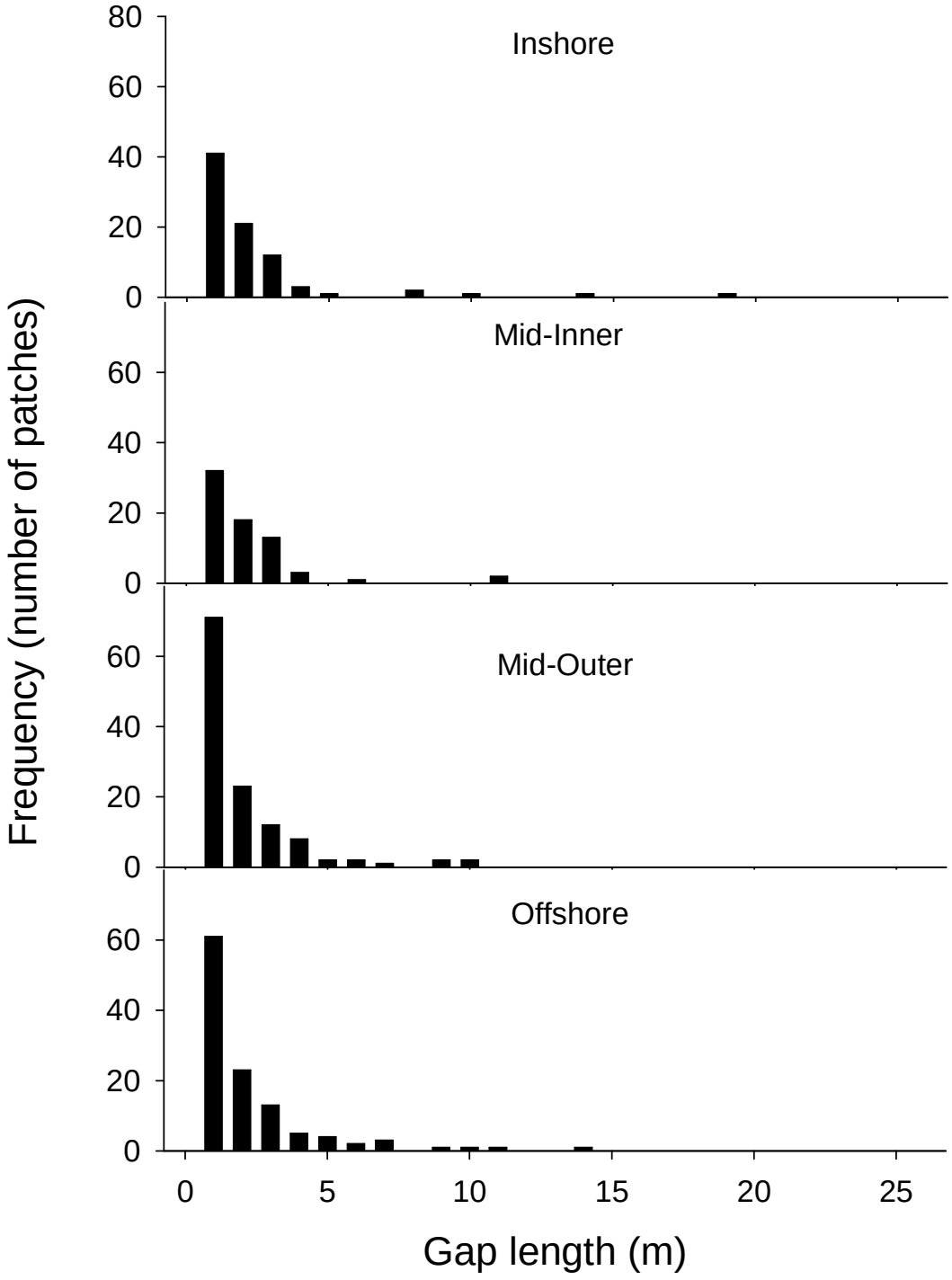

Figure 1.6. Frequency distribution of lengths of open-gap patches at each of the four locations based on diver survey transects.

Herbivores and sessile invertebrates

The sea urchin *Heliocidaris erythrogramma* was most frequently encountered inshore, where it was 20 times more likely to be recorded than at other locations (Table 1.4, Table 1.5). Similarly, herbivorous damselfish (*Parma* spp.) were most frequently encountered on inshore reefs (Table 1.4, Table 1.5) were they were 5.6 times more likely to be encountered than at other locations. In addition *Parma* were 8.2 times more likely to be encountered in open-gap patches than in canopy habitat, while *H. erythrogramma* was encountered equally as often in canopy habitats and open-gap patches (Table 1.4, Table 1.5). We found no relationship between rugosity and the number of either *H. erythrogramma* ($r^2 = 0.015$, $p = 0.612$) or *Parma* ($r^2 = 0.141$, $p = 0.112$).

The density of hard corals differed among locations and was lowest on the inshore reefs and highest on offshore reefs (Figure 1.7a). The probability of encounter also increased with increasing distance from shore with hard corals being 7.9 times more likely to be found offshore or mid-shore than inshore (Table 1.4, Table 1.6). In contrast, the density of massive sponges did not exhibit a consistent unidirectional trend (Figure 1.7a b). Hard corals were 91 times more likely and massive sponges 2.9 times more likely to be found in open-gap habitat than in canopy habitat (Table 1.4, Table 1.6). The majority of sponges in canopy-dominated habitat were low-profile sand-encrusted *Mycale spp*. There was no significant relationship between rugosity and the abundance of either hard corals ($r^2 = 0.052$, $p = 0.344$) or massive sponges ($r^2 = 0.018$, $p = 0.576$).

Table 1.4. Number of 1 m^2 quadrats in which selected biota were present/absent.

	Inshore		Mid-Inner		Mid-Outer		Offshore	
	Gap	Canopy	Gap	Canopy	Gap	Canopy	Gap	Canopy
Parma spp.	86/272	12/255	6/145	3/471	23/230	6/366	17/246	5/357
H.erythrogramma	90/268	92/175	0/151	8/466	5/248	20/352	3/260	2/360
C. tenuispinus	0/358	0/267	0/151	0/474	0/253	0/372	18/245	1/361
Hard Coral	25/63	2/36	10/34	0/81	42/20	0/63	28/23	0/74
Massive Sponge	37/33	4/51	1/38	2/84	35/18	18/54	29/22	21/55

Table 1.5. Results of logistic regression testing for association between locations, habitats and the presence or absence of herbivorous sea urchins (*Heliocidaris erythrogramma*) and fish (Parma spp.).

Heliocidaris erythrogramma

Source	df	Dev	Resid df	Resid	P
Habitat	1	0.9	2498	800.30	0.3427
Location	3	118.89	2495	681.41	< **0.0001**
Site	16	116.06	2479	565.35	< **0.0001**
Transect	80	120.05	2400	445.30	< **0.01**

Parma spp.

Source	df	Dev	Resid df	Resid	P
Habitat	1	129.55	2498	1048.86	< **0.0001**
Location	3	74.785	2495	974.07	< **0.0001**
Site	16	47.469	2479	932.6	< **0.0001**
Transect	79	129.36	2400	803.24	< **0.0001**

Table 1.6. Results of logistic regression testing for association between locations, habitats and the presence or absence of sessile invertebrates.

Corals

Source	df	Dev	Resid df	Resid	P
Habitat	1	129.59	497	383.89	< **0.0001**
Location	3	28.32	494	355.56	< **0.0001**
Site	16	83.164	478	272.39	< **0.0001**

Massive sponges

Source	df	Dev	Resid df	Resid	P
Habitat	1	79.887	498	525.81	< **0.0001**
Location	3	77.88	495	447.93	< **0.0001**
Site	16	64.70	479	383.22	< **0.0001**

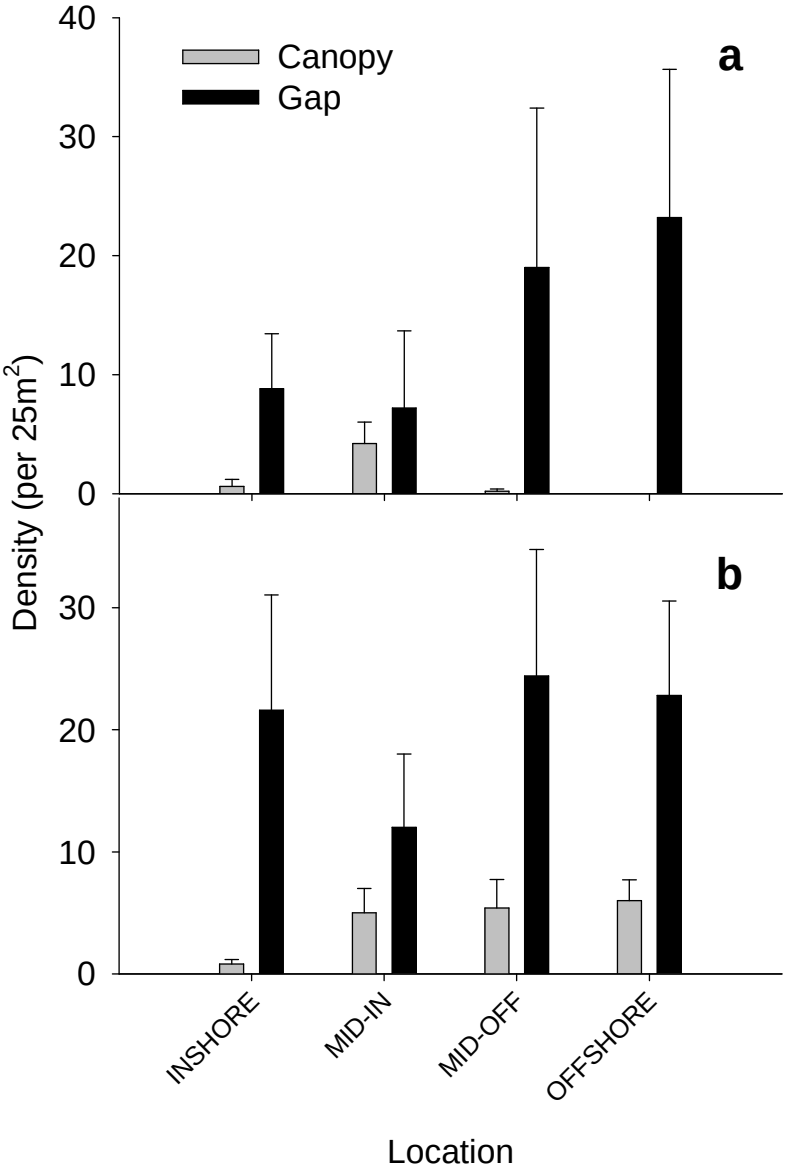

Figure 1.7. Cross shore distribution of sessile invertebrates (corals – a, massive sponges – b) relative to open-gap patches and canopy habitats. Data are means per 25 m^2 transect (+ SE) based on diver survey transects

Size frequency distributions of corals differed among locations. All locations were dominated by small size classes (mainly *Plesiastrea versipora*) with the exception of the mid-inner location where larger colonies occurred more frequently (Figure 1.8). This pattern was reflected by significant variation in size frequency (Kruskal Wallis $\chi 2 = 94.5$, df = 3, $p < 0.0001$). The ten largest corals (> 25cm radius) were recorded at the inshore and mid-inner sites. However, the average mean radius of

the most abundant hard coral (*P. versipora*) was 2.08 ± 0.08 cm. The size frequencies of massive sponges also varied among locations (Kruskal Wallis $\chi 2 = 57.22$, df = 3, $p < 0.0001$) and similar to hard corals the largest colonies (> 25cm radius) occurred most frequently at the mid-inner location (Figure 1.9).

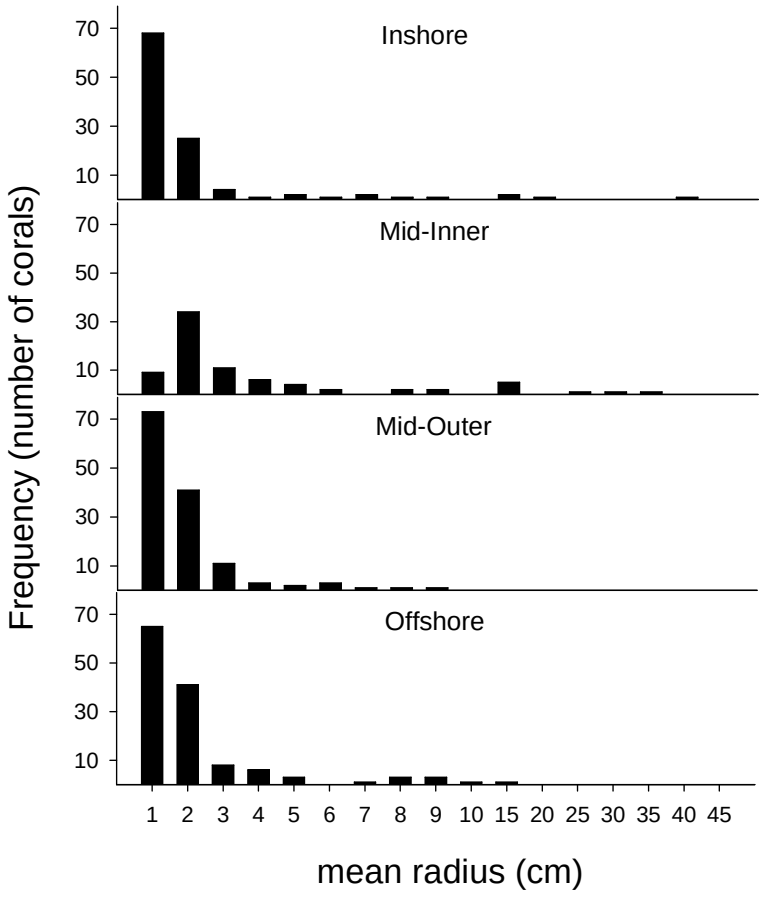

Figure 1.8. Size frequency distribution of corals at cross shore locations at Marmion Lagoon.

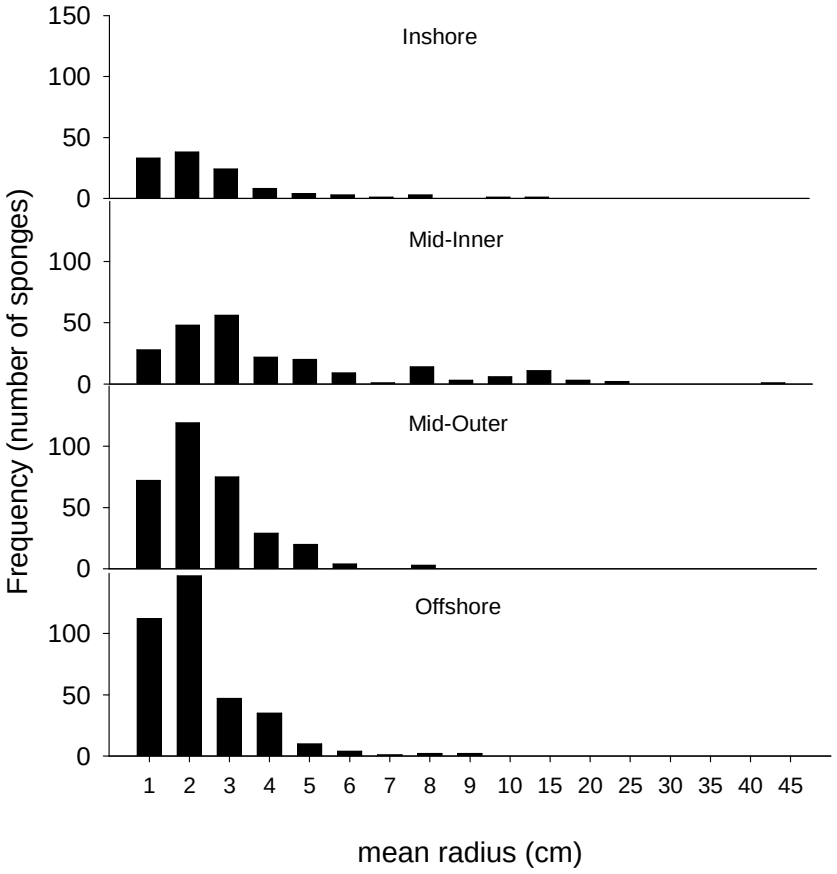

Figure 1.9. Size frequency distribution of sponges at cross shore locations at Marmion Lagoon.

1.2.6 Discussion

Variation in patch size associated with gradients in wave energy

The length of open-gap patches assessed by video transects was positively (but non-linearly) related to modelled wave exposure, indicating that the mechanisms important in the creation and/or maintenance of larger open-gap patches may be more prevalent in areas with higher seabed water velocities. Consistent with this, open-gap lengths and the proportion of open-gap patches were greater at the mid-outer and offshore locations, where wave energy tended to be highest.

Mechanisms responsible for these patterns are likely to include the direct effects of hydrodynamic forces on canopy algae. For example, the removal of canopy-forming kelp during storms can result in the creation of large open-gaps (Dayton & Tegner 1984, Dayton *et al.,* 1992, Graham *et al.,* 1997, Leliaert *et al.*, 2000). During this study, significant wave heights (Hs) up to 3.8 m occurred at offshore Site 1. For such a sea-state the maximum wave height would be twice the significant wave height (Holthuijsen 1997), i.e. 7.6 m, producing maximum bottom velocities of greater than 2 m s^{-1}. Bottom velocities are likely to be further increased due to the effects of plunging wave crests (Denny 1988). These bottom velocities are within the range required to dislodge *Ecklonia* holdfasts or break stipes (2 to 5 m s^{-1}; (Thomsen *et al.,* 2004). However, the relationship between kelp density and resistance to dislodgment is complex (Wernberg 2005). At low to moderate velocities, densely

aggregated kelp are less likely to be dislodged than solitary kelp (Wernberg 2005). As bottom velocities increase, the potential for the imposition of additional drag forces on aggregated kelp through entanglement by detached kelp increases. The creation of open-gaps through the removal of whole plants may therefore occur more frequently, or over larger areas, at sites with higher modelled seabed water velocities.

Additionally, the recruitment dynamics of canopy-forming species may contribute to the maintenance of recently formed large open-gaps. Kelps often recruit to areas where conspecifics occur (Cole & Babcock 1996, Gagnon *et al.*, 2003) and are also inhibited by the presence of turfing algae and sediment (Gorman & Connell 2009). The recruitment of kelp to existing areas of canopy, rather than existing large open-gaps, would serve to maintain any existing large canopy patches through infilling of small open-gaps within larger canopy patches (Wernberg & Connell 2008), and maintain large open-gaps through reduced kelp recruitment. If so, both mechanisms would likely favour the maintenance of larger open-gaps.

Despite wave exposure being one of the most important influences on benthic ecosystems (Harrold *et al.*, 1988, Menge *et al.*, 1993, Lindegarth & Gamfeldt 2005, Wernberg & Connell 2008) it is difficult to isolate its effects on patch structure. Wave exposure can contribute to habitat heterogeneity through direct effects on key habitat-forming species (e.g. canopy dislodgement) as well as indirect effects on predators (e.g. grazing fish and sea urchins) and competitors (e.g. corals and sponges). Furthermore, the relative importance of wave impacts versus other influences such as light availability, nutrient availability, sediment loading and water oxygenation, is expected to vary considerably over short distances and may explain further variation in patch structure.

Variation in the length and proportion of open-gap patches was greatest over distances of metres, with diver transects revealing significant variation in the length and proportion of open-gaps among sites and transects, but not among locations. Habitat heterogeneity over distances of metres is typical of subtidal rocky coasts (Connell & Irving 2008, Wernberg & Connell 2008) and suggests that mechanisms responsible for the creation or maintenance of open-gaps may be small in extent (i.e. reef rugosity) or spatially variable (i.e. wave exposure). Our observations suggest that it is unlikely that variation in topographic complexity is responsible for either the lengths of patches or proportions of each habitat, since there was no correlation between reef rugosity and open-gap length or proportion.

Open-gap patches as persistent alternate states

Corals and massive sponges were far more likely to be encountered in open-gap patches, occupying less than 6% of the total cover (canopy + open-gap) and 14% of open-gap cover. The predominance of corals and sponges in open-gap patches suggests competitive interactions between canopy-forming algae, corals and massive sponges are unlikely to be frequent enough to influence the maintenance of open-gaps. Conversely, the almost exclusive occurrence of corals and massive sponges in open-gap patches, consistent across all four locations, suggest that canopy-forming algae may negatively influence recruitment, survival or physiological performance of corals and sponges to the extent that they are rarely encountered in canopy habitats. Mechanisms by which canopy-forming algae may exclude corals are not well understood, particularly in temperate environments where corals are generally rare. However, abrasion (Miller & Hay 1996), shading (Miller & Hay 1996), overgrowth (Coyer *et al.*, 1993) and allelopathic chemical effects (Littler & Littler 1997) are all likely to be important (reviewed in McCook et al 2001). In tropical ecosystems, macroalgae readily out-compete both corals and sponges, particularly where rates of grazing are low (Hughes *et al.*, 1987). Our results are consistent with these observations and suggest that similar to *Sargassum* assemblages in tropical

systems, canopy-forming algae inhibit hard corals and massive sponges through competitive exclusion on temperate reefs.

The near-total lack of corals within patches of algal canopy habitat, and the large size of some coral and sponge colonies, are two lines of evidence that indicate that gaps in canopy habitat are persistent alternate states. A colony of the most common coral found in this study, *Plesiastrea versipora*, with a radius of 2.08 cm (mean radius recorded) would be between 3 and 13 years old, assuming an average linear growth rate of 1.6 mm to 7 mm yr^{-1} (Burgess *et al.*, 2009). *P. versipora* colonies up to 8.5 cm radius were also recorded, indicating these larger colonies may be between 12 and 53 years. The age of these corals suggests that these open-gap patches are persistent alternate states, rather than a transient stage in a succession towards a canopy-dominated state. These patches might be created by disturbances such as extreme wave events, and they are almost certainly maintained by positive feedback mechanisms that might include selective grazing and competition.

Limited influence of grazers

Our study confirmed that the herbivorous damselfish *Parma* spp. are strongly associated with open-gap patches. *Parma* were eight times more likely to be encountered over open-gap patches than canopy habitats and were observed in highest densities where there was also a high proportion of open-gap patches (> 80%). Our results are consistent with previous work on *Parma* that found densities of *Parma* were negatively correlated with the cover of kelp at the scale of 10's of metres (Jones 1992). Despite having an ability to create small open-gaps within kelp canopies through localised pruning of kelp recruits (Andrew & Jones 1990), and a preference for feeding on algae found exclusively in open-gap habitats, *Parma* rarely clear existing stands of kelp (Jones 1992). This suggests that the strong association between *Parma* and open-gaps observed in this study are likely to be the result of kelp distributions influencing those of *Parma*, rather than *Parma* influencing distributions of kelp. The lack of any relationships between the occurrence of *Parma* and the overall proportion of open-gap patches at larger scales (among locations) in our study supports this conclusion.

In comparison to Parma, the sea urchin *Heliocidaris erythrogramma* was associated equally with canopy habitats and open-gap patches. However, *H. erythrogramma* feeds mainly on detached algae (Vanderklift & Kendrick 2005, Vanderklift & Wernberg 2008) and in Western Australia is not known to create gaps in kelp canopy (authors pers ob). It is likely therefore that any effect of grazing by *H. erythrogramma* will be weak and that at best the role of this sea urchin will be confined to maintaining existing open-gaps.

Competition as a possible mechanism for maintenance of open-gap patches

Competition between canopy algae and assemblages of smaller algae such as turfs can be intense. Algal turfs may inhibit (Kennelly 1987a) or even prevent the re-establishment of canopy algae, particularly where sediment inhibits the recruitment of kelp and nutrients increase the ability of turfs to monopolise space (Gorman & Connell 2009). At our study site, the assemblages of algae within open-gap patches were not exclusively composed of turf algae, but were rather mixed assemblages of foliose, corticated, articulated coralline and turfing algae. These assemblages might prevent the recruitment or establishment of canopy forming algae, similar to turf assemblages. If so, canopy and open-gap assemblages observed in this study may represent persistent alternate states, despite an absence of excessive sediment or nutrients (Miller & Hay 1996, Airoldi 2003, Gorman & Connell 2009).

1.2.7 Conclusion

In this study we characterised the proportion and size of canopy and open-gap states at multiple sites along a gradient in wave exposure, and found open-gap patch lengths were positively correlated with modelled seabed water velocities. These open-gap patches are not clearly associated with characteristics of reef structure, nor do they clearly correspond with general patterns of distribution of herbivorous fish or sea urchins. The conceptual model of kelp forest patch dynamics in south-western Australia suggested by our observations is that while wave-induced disturbances may create open gaps, these gaps persist for extended periods. Regardless of the processes that created the open-gaps, once created, these patches are almost certainly maintained for periods of several years to decades by a combination of biotic processes. These processes may include selective grazing, suppression of canopy recruitment by algal assemblages in open gaps, and wave-induced hydrodynamic forces. Evidence supporting our conclusion that patches are long-lived is provided by the presence of long-lived corals which were 91 times more likely to be encountered in open-gap patches than in canopy habitat. Experimental studies are required to discriminate among a range of competing factors that may maintain open-gaps such as pre-emptive colonisation by turf algae, damselfish grazing and deterministic patterns of hydrodynamic disturbance.

1.2.8 Acknowledgements

This research was supported by the Western Australian Marine Science Institution and CSIRO's Wealth from Oceans Flagship. Thanks are extended to G. Clapin, J. Strzelecki, T. Harriden and N. Murphy for field support, J. Gunson and N. Mortimer for assistance with the SWAN model and J. Fromont for identifying our sponge specimens. S. Wilson, J. Eagle and S. Talbot provided valuable comments on the manuscript.

1.2.9 References

Airoldi L (2003) The effects of sedimentation on rocky coast assemblages. Oceanography and Marine Biology, Vol 41 41:161-236

Anderson MJ (2001) A new method for non-parametric multivariate analysis of variance. Austral Ecology 26:32-46

Andrew NL, Jones GP (1990) Patch formation by herbivorous fish in a temperate Australian kelp forest. Oecologia 85:57-68

Andrew NL, O'Neill AL (2000) Large-scale patterns in habitat structure on subtidal rocky reefs in New South Wales. Marine and Freshwater Research 51:255-263

Babcock RC, Kelly S, Shears NT, Walker JW, Willis TJ (1999) Changes in community structure in temperate marine reserves. Marine Ecology-Progress Series 189:125-134

Benedetti-Cecchi L, Pannacciulli F, Bulleri F, Moschella PS, Airoldi L, Relini G, Cinelli F (2001) Predicting the consequences of anthropogenic disturbance: Large-scale effects of loss of canopy algae on rocky shores. Marine Ecology-Progress Series 214:137-150

Booij N, Ris RC, Holthuijsen LH (1999) A third-generation wave model for coastal regions - 1. Model description and validation. Journal of Geophysical Research-Oceans 104:7649-7666

Breen PA, Mann KH (1976) Changing lobster abundance and destruction of kelp beds by sea-urchins. Marine Biology 34:137-142

Burgess SN, McCulloch MT, Mortimer GE, Ward TM (2009) Structure and growth rates of the high-latitude coral: *Plesiastrea versipora*. Coral Reefs 28:1005-1015

Connell JH, Slatyer RO (1977) Mechanisms of succession in natural communities and their role in community stability and organization. American Naturalist 111:1119-1144

Connell SD, Irving AD (2008) Integrating ecology with biogeography using landscape characteristics: A case study of subtidal habitat across continental Australia. Journal of Biogeography 35:1608-1621

Connell SD, Vanderklift MA, Gillanders BM (2007) Negative interactions: The influence of predators and herbivores on prey and ecological systems. In: Marine Ecology. Oxford University Press, South Melbourne, p 72-100

Coyer JA, Ambrose RF, Engle JM, Carroll JC (1993) Interactions between corals and algae on a temperate zone rocky reef - mediation by sea-urchins. Journal of Experimental Marine Biology and Ecology 167:21-37

Dayton PK (1975) Experimental studies of algal canopy interactions in a sea otter dominated kelp community at Amchitka Island, Alaska. Fishery Bulletin 73:230-237

Dayton PK (1985) Ecology of kelp communities. Annual Review of Ecology and Systematics 16:215-245

Dayton PK, Currie V, Gerrodette T, Keller BD, Rosenthal R, Ventresca D (1984) Patch dynamics and stability of some California kelp communities. Ecological Monographs 54:253-289

Dayton PK, Tegner MJ (1984) Catastrophic storms, el-nino, and patch stability in a southern California kelp community. Science 224:283-285

Dayton PK, Tegner MJ, Parnell PE, Edwards PB (1992) Temporal and spatial patterns of disturbance and recovery in a kelp forest community. Ecological Monographs 62:421-445

Denny MW (1988) Biology and the mechanics of the wave-swept environment. Biology and the mechanics of the wave-swept environment:i-xiii, 1-329

Drake JA (1990) Communities as assembled structures - do rules govern pattern. Trends in Ecology & Evolution 5:159-164

England PR, Phillips J, Waring JR, Symonds G, Babcock R (2008) Modelling wave-induced disturbance in highly biodiverse marine macroalgal communities: Support for the intermediate disturbance hypothesis. Marine and Freshwater Research 59:515-520

Fowler-Walker MJ, Wernberg T, Connell SD (2006) Differences in kelp morphology between wave sheltered and exposed localities: Morphologically plastic or fixed traits? Marine Biology 148:755-767

Gorman D, Connell SD (2009) Recovering subtidal forests in human-dominated landscapes. Journal of Applied Ecology 46:1258-1265

Graham MH, Harrold C, Lisin S, Light K, Watanabe JM, Foster MS (1997) Population dynamics of giant kelp macrocystis pyrifera along a wave exposure gradient. Marine Ecology-Progress Series 148:269-279

Harrold C, Watanabe J, Lisin S (1988) Spatial variation in the structure of kelp forest communities along a wave exposure gradient. Marine Ecology-Pubblicazioni Della Stazione Zoologica Di Napoli I 9:131-156

Hatcher A (1989) Variation in the components of benthic community structure in a coastal lagoon as a function of spatial scale. Marine and Freshwater Research 40:79-96

Holthuijsen L (1997) Waves in oceanic and coastal waters, Vol. Cambridge University Press, Cambridge

Hosmer DW, Lemeshow S, Klar J (1988) Goodness-of-fit testing for the logistic-regression model when the estimated probabilities are small. Biometrical Journal 30:911-924

Hughes TP, Reed DC, Boyle MJ (1987) Herbivory on coral reefs - community structure following mass mortalities of sea-urchins. Journal of Experimental Marine Biology and Ecology 113:39-59

Irving AD, Connell SD (2006) Predicting understorey structure from the presence and composition of canopies: An assembly rule for marine algae. Oecologia 148:491-502

Johnson CR, Mann KH (1988) Diversity, patterns of adaptation, and stability of nova-scotian kelp beds. Ecological Monographs 58:129-154

Jompa J, McCook LJ (2002) Effects of competition and herbivory on interactions between a hard coral and a brown alga. Journal of Experimental Marine Biology and Ecology 271:25-39

Jones GP (1992) Interactions between herbivorous fishes and macroalgae on a temperate rocky reef. Journal of Experimental Marine Biology and Ecology 159:217-235

Jones GP, Andrew NL (1990) Herbivory and patch dynamics on rocky reefs in temperate australasia - the roles of fish and sea-urchins. Australian Journal of Ecology 15:505-520

Keddy PA (1992) Assembly and response rules - 2 goals for predictive community ecology. Journal of Vegetation Science 3:157-164

Kennelly SJ (1987) Inhibition of kelp recruitment by turfing algae and consequences for an Australian kelp community. Journal of Experimental Marine Biology and Ecology 112:49-60

Konar B, Estes JA (2003) The stability of boundary regions between kelp beds and deforested areas. Ecology 84:174-185

Lauzon-Guay JS, Scheibling RE (2010) Spatial dynamics, ecological thresholds and phase shifts: Modelling grazer aggregation and gap formation in kelp beds. Marine Ecology-Progress Series 403:29-41

Leliaert F, Anderson RJ, Bolton JJ, Coppejans E (2000) Subtidal understorey algal community structure in kelp beds around the cape peninsula (western cape, south africa). Botanica Marina 43:359-366

Lindegarth M, Gamfeldt L (2005) Comparing categorical and continuous ecological analyses: Effects of "Wave exposure" On rocky shores. Ecology 86:1346-1357

Littler MM, Littler DS (1997) Epizoic red alga allelopathic (?) to a caribbean coral. Coral Reefs 16:168-168

McCook LJ, Jompa J, Diaz-Pulido G (2001) Competition between corals and algae on coral reefs: A review of evidence and mechanisms. Coral Reefs 19:400-417

McCormick MI (1994) Comparison of field methods for measuring surface-topography and their associations with a tropical reef fish assemblage. Marine Ecology-Progress Series 112:87-96

Menge BA, Allison GW, Blanchette CA, Farrell TM, Olson AM, Turner TA, van Tamelen P (2005) Stasis or kinesis? Hidden dynamics of a rocky intertidal macrophyte mosaic revealed by a spatially explicit approach. Journal of Experimental Marine Biology and Ecology 314:3-39

Menge BA, Farrell TM, Olson AM, Vantamelen P, Turner T (1993) Algal recruitment and the maintenance of a plant mosaic in the low intertidal region on the oregon coast. Journal of Experimental Marine Biology and Ecology 170:91-116

Miller MW, Hay ME (1996) Coral-seaweed-grazer-nutrient interactions on temperate reefs. Ecological Monographs 66:323-344

Petraitis PS, Dudgeon SR (2005) Divergent succession and implications for alternative states on rocky intertidal shores. Journal of Experimental Marine Biology and Ecology 326:14-26

Rasher DB, Hay ME (2010) Chemically rich seaweeds poison corals when not controlled by herbivores. Proceedings of the National Academy of Sciences of the United States of America 107:9683-9688

Ris RC, Holthuijsen LH, Booij N (1999) A third-generation wave model for coastal regions - 2. Verification. Journal of Geophysical Research-Oceans 104:7667-7681

Scheibling RE, Hennigar AW, Balch T (1999) Destructive grazing, epiphytism, and disease: The dynamics of sea urchin - kelp interactions in nova scotia. Canadian Journal of Fisheries and Aquatic Sciences 56:2300-2314

Scheibling RE, Raymond BG (1990) Community dynamics on a subtidal cobble bed following mass mortalities of sea-urchins. Marine Ecology-Progress Series 63:127-145

Schiel DR (1988) Algal interactions on shallow subtidal reefs in northern New Zealand - a review. New Zealand Journal of Marine and Freshwater Research 22:481-489

Siddon CE, Witman JD (2003) Influence of chronic, low-level hydrodynamic forces on subtidal community structure. Marine Ecology-Progress Series 261:99-110

Sutherland JP (1990) Perturbations, resistance, and alternative views of the existence of multiple stable points in nature. American Naturalist 136:270-275

Thomsen MS, Wernberg T, Kendrick GA (2004) The effect of thallus size, life stage, aggregation, wave exposure and substratum conditions on the forces required to break or dislodge the small kelp *Ecklonia radiata*. Botanica Marina 47:454-460

Toohey B, Kendrick GA, Wernberg T, Phillips JC, Malkin S, Prince J (2004) The effects of light and thallus scour from *Ecklonia radiata* canopy on an associated foliose algal assemblage: The importance of photoacclimation. Marine Biology 144:1019-1027

Toohey BD (2007) The relationship between physical variables on topographically simple and complex reefs and algal assemblage structure beneath an ecklonia radiata canopy. Estuarine Coastal and Shelf Science 71:232-240

Toohey BD, Kendrick GA (2008) Canopy-understorey relationships are mediated by reef topography in *Ecklonia radiata* kelp beds. European Journal of Phycology 43:133-142

Toohey BD, Kendrick GA, Harvey ES (2007) Disturbance and reef topography maintain high local diversity in *Ecklonia radiata* kelp forests. Oikos 116:1618-1630

Underwood AJ; Chapman MG; Connell SD (2000) Observations in ecology: you can't make progress on processes without understanding the patterns. Journal of Experimental Marine Biology and Ecology 250:97-115

Vadas RL, Elner RW, Garwood PE, Babb IG (1986) Experimental evaluation of aggregation behaviour in the sea-urchin *Strongylocentrotus-droebachiensis* - a reinterpretation. Marine Biology 90:433-448

Vanderklift MA, Kendrick GA (2004) Variation in abundances of herbivorous invertebrates in temperate subtidal rocky reef habitats. Marine and Freshwater Research 55:93-103

Vanderklift MA, Kendrick GA (2005) Contrasting influence of sea urchins on attached and drift macroalgae. Marine Ecology-Progress Series 299:101-110

Vanderklift MA, Wernberg T (2008) Detached kelps from distant sources are a food subsidy for sea urchins. Oecologia 157:327-335

Wernberg T (2005) Holdfast aggregation in relation to morphology, age, attachment and drag for the kelp *Ecklonia radiata*. Aquatic Botany 82:168-180

Wernberg T, Connell SD (2008) Physical disturbance and subtidal habitat structure on open rocky coasts: Effects of wave exposure, extent and intensity. Journal of Sea Research 59:237-248

Wernberg T, Goldberg N (2008) Short-term temporal dynamics of algal species in a subtidal kelp bed in relation to changes in environmental conditions and canopy biomass. Estuarine Coastal and Shelf Science 76:265-272

Wernberg T, Kendrick GA, Phillips JC (2003) Regional differences in kelp-associated algal assemblages on temperate limestone reefs in south-western Australia. Diversity and Distributions 9:427-441

Wernberg T, Kendrick GA, Toohey BD (2005) Modification of the physical environment by an *Ecklonia radiata* (laminariales) canopy and implications for associated foliose algae. Aquatic Ecology 39:419-430

1.3 Deterministic aspects of kelp forest patch dynamics and models of patch turnover

In Review.

Thomson DP, Babcock RC

CSIRO Marine and Atmospheric Research, Private Bag 5, Wembley, WA, 6913

Keywords: *Ecklonia radiata*, *Sargassum*, gap, canopy, clearances heterogeneity

1.3.1 Abstract

Kelp forest assemblages in south-western Australia frequently occur as a mosaic of patches that can broadly be characterised as either Canopy or Gap habitats. Canopy habitats may further be broken down into assemblages dominated either by *Sargassum* or *Ecklonia*. Although habitat mosaics may remain stable for significant periods, perhaps decades, there is still considerable debate over the relative importance of stochastic (disturbance and succession) versus deterministic processes in maintaining these mosaics. Here, we conduct artificial clearances in both Canopy and Gap habitats, as well as at the boundary of Canopy and Gap habitats, to assess the relative importance of stochastic versus deterministic processes during the early recovery phase. After 3 years we found canopy assemblages were slow to re-establish, with most canopy clearances remaining as Gap habitat. These results support the hypothesis that once disturbed, canopy areas are unlikely to re-establish quickly. However where returns to canopy habitat were observed, they were more likely to occur in clearances which were within or adjacent to Canopy habitat, suggesting early recovery may in part be a deterministic process, controlled by the proximity of the disturbed area to nearby canopy habitat. Modelling of habitat transitions indicated that undisturbed canopy habitats had a longer average residence time (longevity) than Gap habitats, being 3.7 years and 2.8 years respectively. However, this pattern was reversed when habitats were artificially disturbed, with projected residence times becoming six times greater for gap habitats (12 years) when compared with canopy habitats (2.4 years). This observed asymmetrical response of canopy and gap habitats to severe disturbance indicate that any increase in the frequency of gap creation is likely to have long term and disproportionate negative impacts on overall canopy cover.

1.3.2 Introduction

Early paradigms of algal community dynamics emphasised succession in which disturbances, for example storms, clear the substratum which is soon colonised by pioneer species. These pioneer species usually give way to others more able to compete for space, with the disturbed areas eventually returning to the pre-disturbance or "climax" state (Sousa-Dias & Melo 2008).

On many temperate reefs kelps are an important and often characteristic climax assemblage. These comparatively large, long-lived algae, have a competitive advantage over other smaller species, which they are able to shade out due to their size. Macroalgal habitats that display a mosaic structure of two or more distinct algal assemblages are commonly referred to in the literature, particularly in relation

to kelp forests (Kennelly 1987b, Irving *et al.*, 2004, Connell & Irving 2008). Disturbances in kelp forests are typically the result of storms or grazing, and recovery of the kelp forest generally takes place within 2-3 years (Dayton *et al.*, 1992, Tegner *et al.*, 1997). A succession hypothesis may explain these habitat mosaics as the result of random disturbances at multiple discrete points in space and time, producing a highly dynamic patchwork of habitats in different stages of recovery.

There is growing realisation that succession to a single climax state is not always the outcome of dynamic processes in marine communities. Patches of habitat can persist for significant periods of time, for example algal patches can coexist with other space occupying organisms such as mussels and algae (Petraitis & Dudgeon 2005) or seagrass and algae (Menge *et al.*, 2005) producing adjacent alternate states. Algal assemblages in most of southern Australia are characterised by a patchy structure (Irving *et al.*, 2004) varying over scales of metres to 100's metres and including areas dominated by kelp canopy overstory as well as other assemblages with no canopy. Once created these open gaps can persist for months to years (Kirkman 1981, Kennelly 1987, Kendrick *et al.*, 1999), which raises the question: what processes maintain them?

Kelp-canopy assemblages at Marmion lagoon consist of a mosaic of canopy patches and patches which are largely devoid of kelp (gaps) (Hatcher 1989). If we hypothesise that these patches represent alternate states, then a disturbance to either one may facilitate its transition to another state. For example, clearance of turf algae may allow for colonization by canopy species, thereby increasing the probability of a transition from open-gap to canopy habitat. Similarly, a clearance in canopy habitat should allow for colonisation by turf species, thereby increasing the probability of transition to gap habitat (e.g. turf or foliose algae). Alternatively, if each habitat type has an inherent ability to maintain itself in the face of competition from other species (either canopy or gap forming), the result of disturbance should always favour one habitat type e.g. Canopy.

Several studies have looked at the ability of canopy assemblages to recover after disturbances, however the outcomes of reciprocal clearances as a test of interactions stabilizing kelp-forest habitat mosaics have not yet been assessed. In this study, we investigate the post-disturbance recovery of algal assemblages in both artificially cleared canopy and gap habitats. Specifically, we test three hypothesis:

1. Under a canopy succession hypothesis, would all clearances return to a canopy state, regardless of original state?

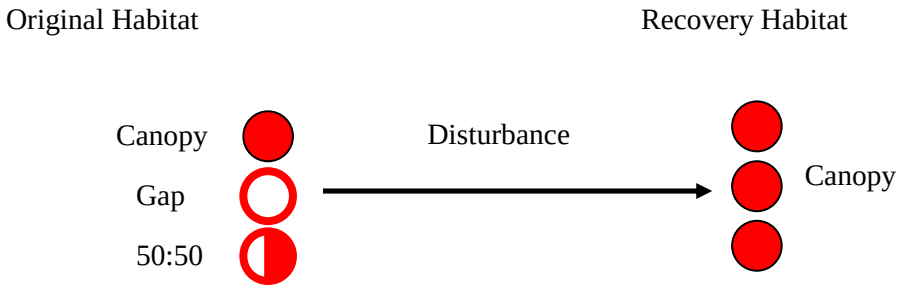

2. Under a deterministic hypothesis, would all clearances return to their original habitat state?

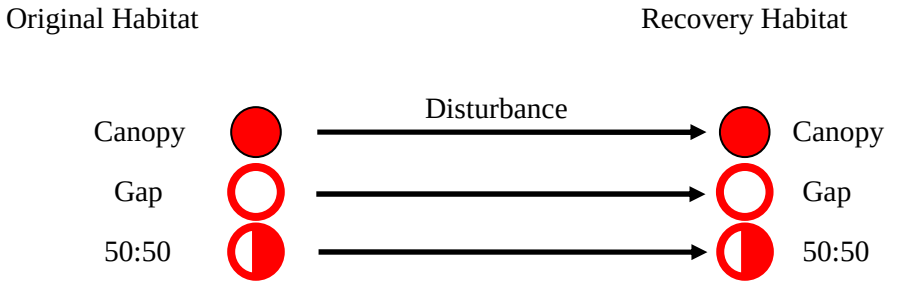

3. Under an alternate-state hypothesis, would clearances be equally likely to develop into either habitat state, regardless of original state.

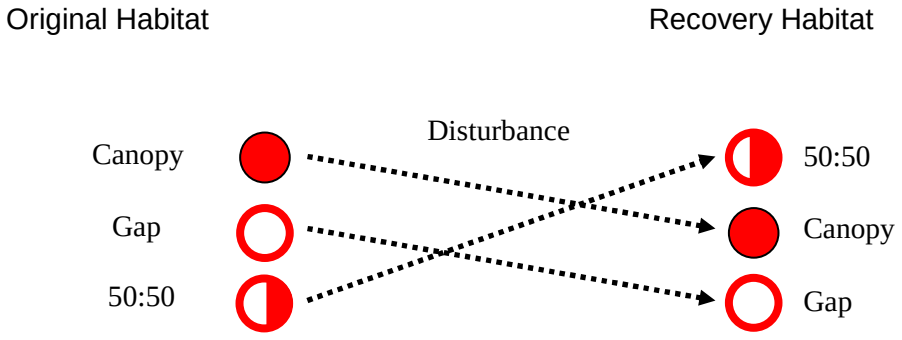

Due to the probability of transition to a particular habitat state after disturbance being dependent on the proximity of adjacent habitats, we also carried out a series of clearances across canopy/gap habitat transition zones.

1.3.3 Materials and methods

Study area

This study was conducted at Marmion lagoon (31˚48'18", 115˚42'11") a semi-enclosed body of water located 18km north-west of Perth. The lagoon is characterised by three lines of parallel limestone reef each between 8 to 10km long, located at increasing distance from the shore at 0.5km, 2.4km and 4.2km offshore (Figure 1.10). The shallowest reefs are located on the inshore and mid-shelf reef lines (1m to 6m) and deeper reefs are located on the offshore reef line (10 to 16m). Inshore reefs are high relief (3 – 5m) isolated patch reefs surrounded by large areas of sand and seagrass habitat. In comparison, mid-shelf and offshore reefs are larger (>1ha), and separated by only small channels of sand and seagrass habitat. The mid-shelf reef line is the largest area of reef (approximately 7 ha) and for the purposes of this study was divided into inner and outer midshelf locations. For a detailed description of all three reef lines see (Hatcher 1989, Toohey *et al.*, 2004).

Study sites

Based on a series of reconnaissance dives three sites were selected (Figure 1.10). All three sites were located along the middle reef line on low to medium relief reef (<3m) in approximately 3 – 5m water depth. Sites comprised of alternating patches of canopy forming brown algae e.g. *Ecklonia radiata* and *Sargassum* spp (Figure 1.11a). and low algae within gaps (Figure 1.11b). Gap areas consisted of predominantly small foliose and filamentous algae, such as *Laurencia*, *Plocamium*, *Pterocladia*, *Ulva*, *Jania*, *and Curdiea* as well as calcareous reds e.g. *Amphiroa*, *Metagoniolithon*, *Tricleocarpa* sp and crustose coralline algae (Figure 1.11b). Sites were selected to have varying degrees of complexity and similar exposure to prevailing wind and swell (as determined by distance from shore).

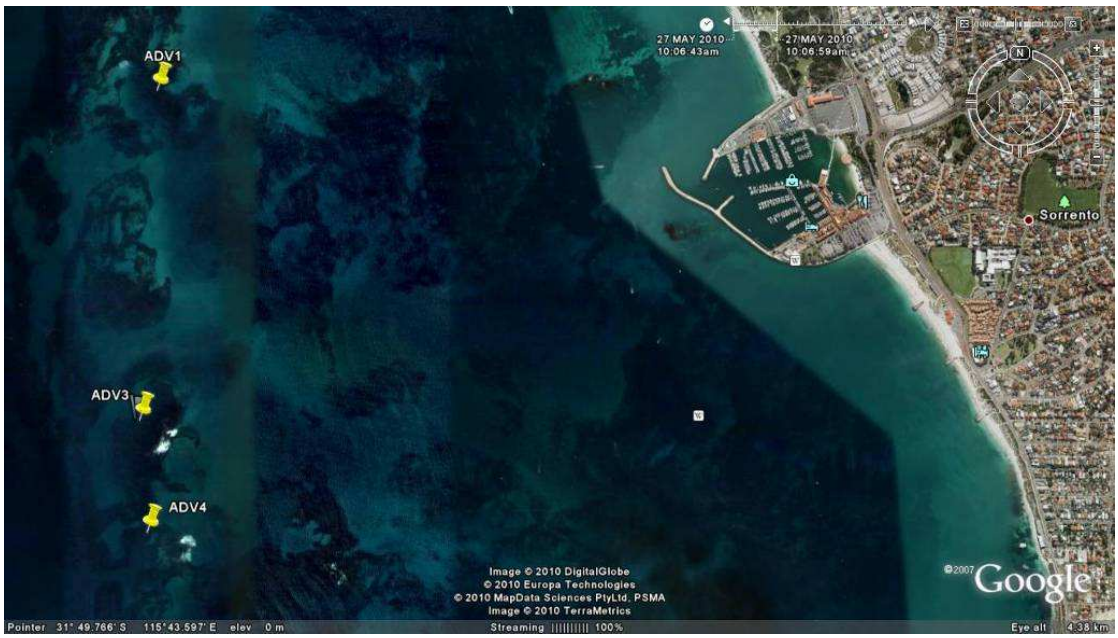

Figure 1.10. Location of the three study sites at Marmion Lagoon

(a) (b)

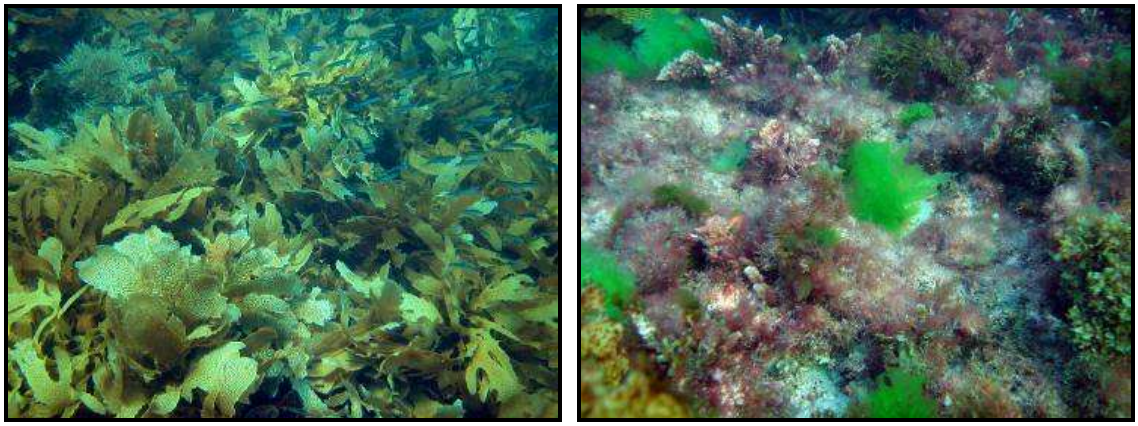

Figure 1.11.a and b: The two broad algal communities found at Marmion Reef (a) canopy forming algae consisting of *Ecklonia* sp and *Sargassum* sp (b) gap low algae consisting of small foliose and green algae.

Initial condition and Clearances

To simulate severe physical disturbance at each of the three sites 9 x 3m circular patches (plus 3 x 3m Controls) were cleared of all benthos using cold-chisels, hammers and wire brushes. The centre of each clearance was marked with a 1.2m steel fence post and a radial line of 1.5m length used to standardise the clearance area through 360˚.

The initial habitat of all plots was assessed prior to clearing. At each site equal numbers of plots were established in Canopy, Gap and 50:50 Canopy/Gap habitats (n = 3 treatment per site). (Figure 1.12 a,b,c). Initially, plots were visually classified as Canopy; >75% *Ecklonia* canopy, Gap; canopy forming brown algae absent, and 50:50; straddling Canopy and Gap habitats. Estimates of cover for major algal groups were obtaining from each plot prior to clearing using four randomly placed 0.5m x 0.5m photo quadrats. To provide a baseline for monitoring changes in percent cover of algae in each of the plots, additional 0.5m x 0.5m photo quadrats were obtained one week after clearing took place (Figure 1.12 clearance). Three control clearances plots were also established at each site.

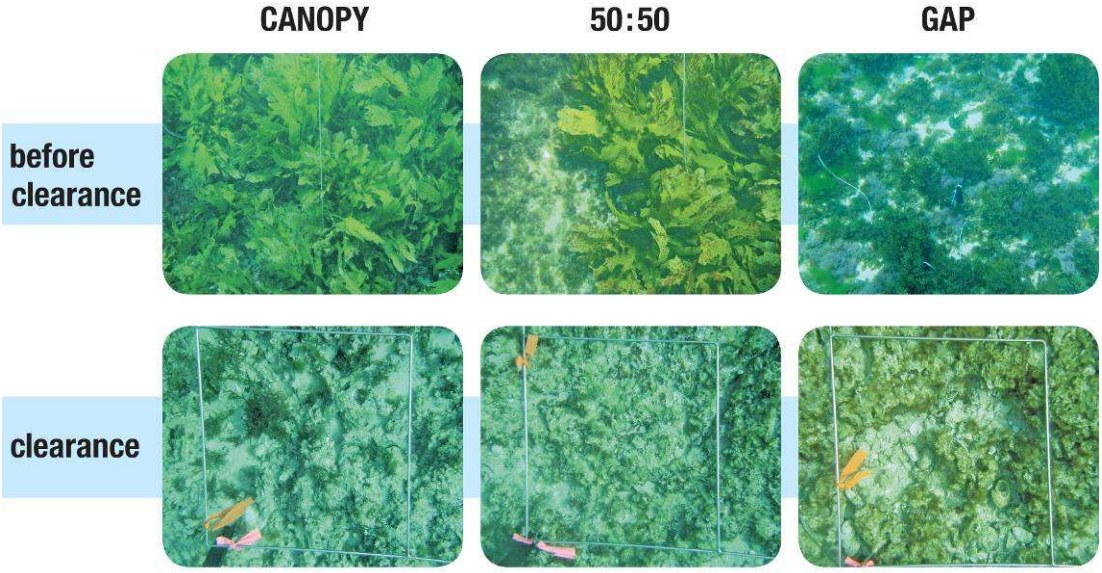

Figure 1.12. Canopy, 50% Gap: 50% Canopy and Gap habitats just prior to clearing and immediately after clearing.

Clearance recovery

Re-colonisation of all clearances by algal were monitored using fixed photo-quadrats, re-surveyed at approximately 4 monthly intervals (8 surveys between 0 and 38 months). At each census a digital camera (Cybershot, Sony, Japan) was used to photograph each clearance at varying distance from the clearance centre i.e. 2 photos in centre of clearance and 2 photos at clearance edge, 4 photographs per clearance. The camera was held 1.0 m above the substrate so that each photograph captured an area of 0.5m × 0.5m, verified *in situ* using a 0.5m quadrat. To obtain percent cover estimates sixteen fixed points were analysed per photograph; 64 points per clearance. Point analysis was carried out using Photo Transect Analysis Software (Australian Institute of Marine Science, Townsville) as per English *et al.*, (1987). The benthic category (i.e. turf algae, canopy algae, gap algae, sponge or coral) underlying each fixed point was recorded in each photograph. Differences in the recovery of canopy algae between clearance treatments were tested using one-way ANOVA, once assumptions of normality and homogeneity of variance had been tested.

Habitat modelling

Annual classification of clearances provided the basis for compiling transition matrices which summarised the annual probability of each habitat transitioning from one habitat to another. Data were then used to construct three models of habitat dynamics. The first model included data from the control plots only, and utilized a binary classification for either Gap or Canopy. This essentially represents the natural or un-manipulated state of habitat dynamics. The second and third models were based on the cleared plots, thereby replicating severe disturbances such as those which may occur during large winter storms. These models incorporated probabilities of clearances transitioning between either two habitat types (model two = gap, canopy) or three habitat types (model three = Gap, Sargassum, Ecklonia). The transition matrices formed the basis of habitat models that were used to derive basic population parameters such as residence times and to changes in habitat proportion over 10 years (PopTools).

1.3.4 Results

Initial condition and clearance

Canopy and gap habitats were different in terms of their composition, as shown by the relative cover of algal structural/functional groups prior to clearances (Table 1.7). Canopy habitat patches were dominated by *Ecklonia radiata*, with approximately 95% cover, with "other" understory algae (i.e. Rhodophytes such as Pterocladia and crustose coralline algae) making up the remaining 5% of benthic cover. Gap habitat patches consisted of approximately 50% turfing algae, with almost no canopy forming macroalgae (7% Sargassum spp., 0% Ecklonia sp.), while 50:50 habitat patches consisted of almost equal proportions of canopy and gap forming algae (55% and 45%).

Table 1.7. Composition of canopy prior to experimental clearances. (mean % cover +/- SE)

		Canopy	Gap	50:50
CANOPY	*Ecklonia*	94.00 (3.14)	0.00 (0.00)	55.00 (4.96)
	Sargassum	0.00 (0.00)	7.10 (5.90)	5.00 (2.92)
GAP	Turf	0.00 (0.00)	46.80 (13.20)	20.00 (6.61)
	Green algae	0.00 (0.00)	2.30 (1.00)	3.00 (1.38)
	Other	6.00 (2.56)	43.80 (8.00)	17.00 (4.42)

Clearances were highly effective in removing both canopy and gap associated algae. On completion of clearances, canopy algae comprised less than 1% of cover in all habitat treatments (Figure 1.13).

Recovery of Canopy algae

Recovery of canopy algae (Ecklonia + Sargassum) differed between clearance treatments, such that 38 months after clearance overall cover was significantly higher in Canopy treatments than in the Gap and 50:50 treatments ($F_{2,24}=5.68$, $p=0.0095$) (Figure 1.13). Mean canopy cover increased rapidly following clearance in all treatments, followed by general declines between 18 and 38 months (Figure 1.13). In Canopy and 50:50 treatments canopy cover remained less than 5% after 4 months, while in gap treatments, cover of canopy algae increased to greater than 20% (Figure 1.13). Between 4 and 10 months, the level of canopy cover increased such that by 10-14 months, canopy cover increased to between 50 to 60 percent across all treatments (Figure 1.13). At 18 months (late winter), canopy cover had decreased to less than 20%, followed by what appeared to be a gradual increase up to 38 months. This underlay strong seasonal variability. By 38 months, overall cover was significantly higher in Canopy treatments than in the Gap and 50:50 treatments ($F_{2,24}=5.68$, $p=0.0095$).

Seasonal trends in canopy cover were similar among clearance and control treatments, both in timing and relative magnitude however, differences did exist between clearance treatments. Canopy cover in clearance treatments and controls reached a maximum in late summer (10 to 14 months), followed by a minimum late winter and again increased in summer (26 and 34 months). Differences occurred between the three clearance treatments (Canopy, 50:50, Gap) with canopy cover consistently lower in canopy and 50:50 treatments than in controls (Figure 1.13). In contrast, the level of canopy cover in the Gap treatments remained consistently higher in the clearance treatments than in the controls (Figure 1.13).

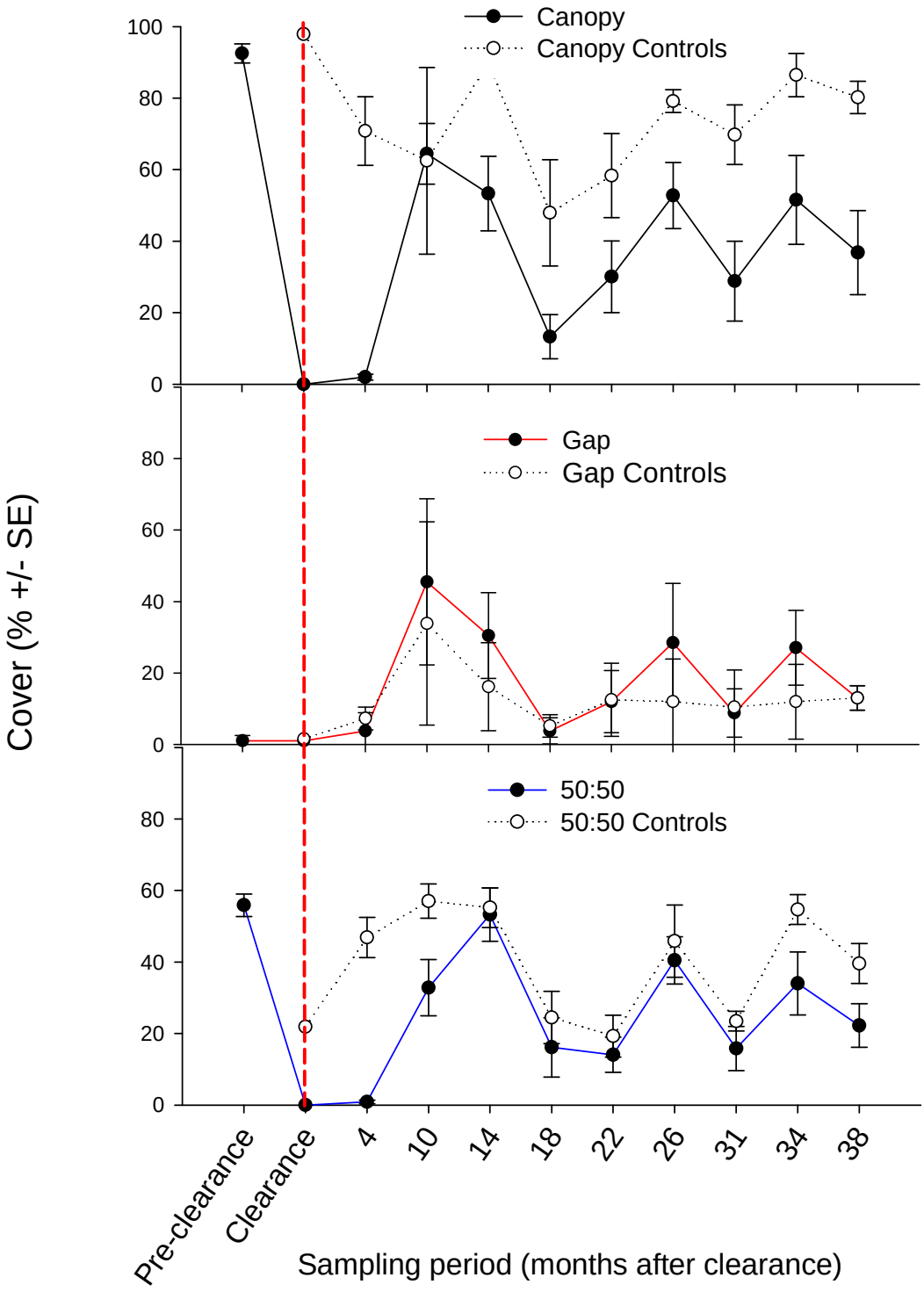

Figure 1.13. Recovery of canopy algae in the clearance treatments: Canopy, Gap and 50:50 habitats over 38 months

Recovery of Green algae, Sargassum and Ecklonia

Significant differences in the recovery of different algal groups were observed over the 38 months. Four months after clearance, green algae (mainly Ulva) dominated all clearance treatments comprising between 61% and 44% of total cover in Canopy and 50:50 treatments respectively (Figure 1.14) and plots were more frequently characterised by green algae in these treatments than in gap habitat clearances (Figure 1.15). Nevertheless the total cover of green algae in Gap treatments also increased at 4 months, although not to the same level as that observed in Canopy and 50:50 treatments. Average cover of green algae in Canopy and 50:50 clearances (~50%) was double that in the Gap treatment (27.9%), and ten times greater than in the control treatment (4 5%) (Figure 1.14). Between 4 and 18 months the total cover of green algae decreased in all treatments by 30-60% and although there was slight seasonal variability cover remained at levels below 20% up to 38 months.

Coinciding with the decrease in the cover of Green algae between 4 and 10 months, Sargassum cover increased to 55% in Canopy treatments (Figure 1.14). Ten months after clearance, Sargassum dominated Canopy, 50:50 and Gap treatments, comprising 55%, 30.9% and 44.3% of the total cover respectively. In contrast, Sargassum cover increased only marginally to 30% in control treatments (Figure 1.14). Sargassum cover decreased to less than 20% between 10 and 22 months, increasing seasonally to between 20% and 40% at 26 months and 34 months. Thereafter there was little overall trend in although There was clearly a seasonal variation in Sargassum cover; being highest in spring and lowest late winter.

In contrast to changes in the cover of Green algae and Sargassum, changes in the cover of Ecklonia were relatively gradual over the 38 months. Establishment and growth of Ecklonia in all treatments was slow and remained less than 3% after 4 months, increasing to approximately 10% in the canopy treatment after 10 months and remaining between 5% and 15% between 10 and 18 months. After 26 months Ecklonia cover contributed 12% and 5% of total cover in 50:50 and Gap treatments respectively, however in the Canopy treatments cover of Ecklonia continued to increase up to 38 months when it reached over 31.9%. At 38 months Ecklonia cover was similar in canopy clearances (31%) and canopy controls (39%) (Figure 1.14).

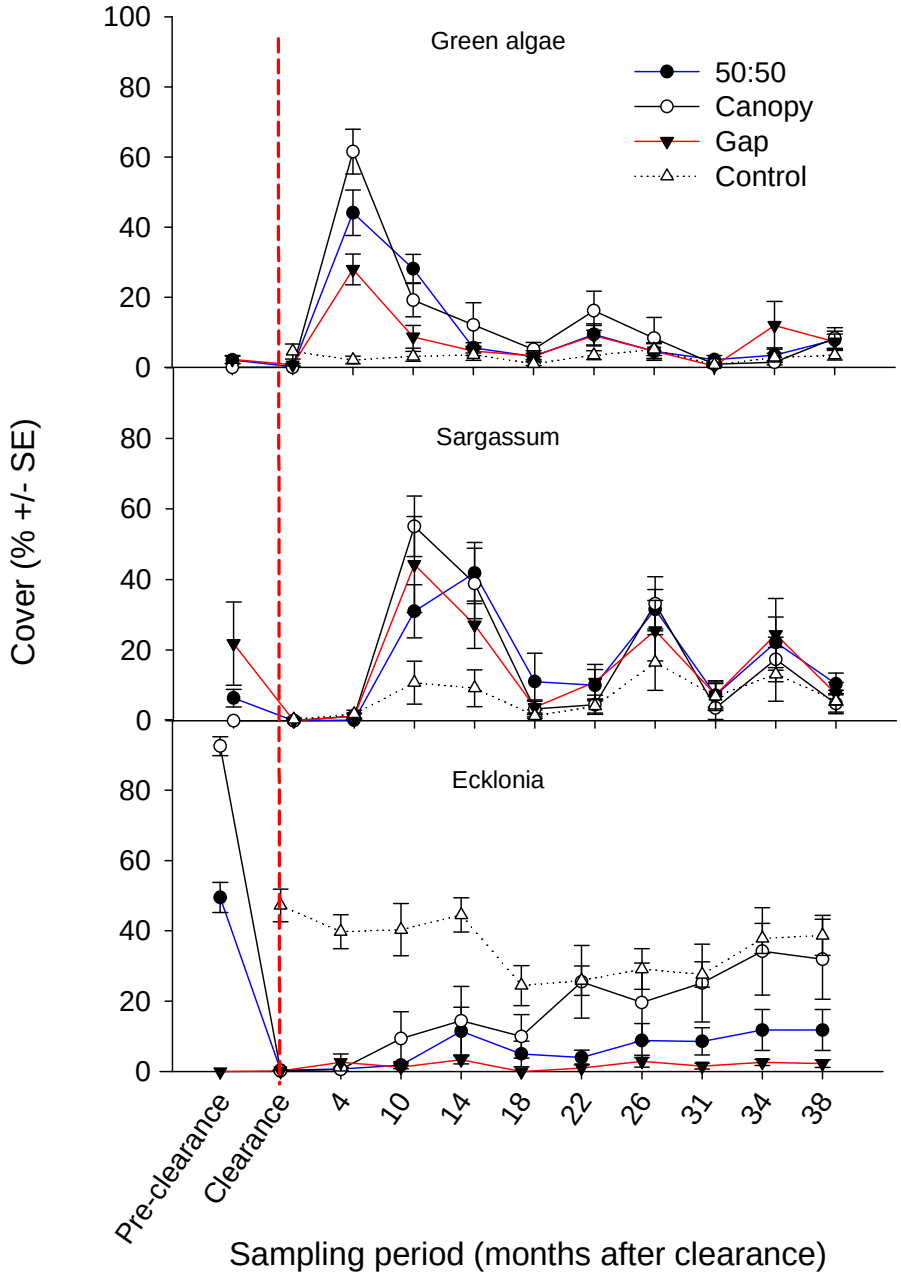

Figure 1.14. Trends in macroalgal cover in experimental clearances of canopy, gap, 50:50 and control treatments over 38 months.

Transition matrices

Transition states were assessed at approximately 12-month intervals (13, 26 and 38 months after clearance) (Figure 1.15) and indicated that early habitat transitions in control plots differed markedly to those in clearance plots. In un-manipulated control plots, the probability of transitioning to another state (gap or canopy) was much less than the probability of remaining in the same state, being 27% and 25% versus 72% and 75% respectively (Table 1.8). In comparison, the probability that a cleared area would transition to either Gap or Canopy states were relatively similar (Table 1.9, Table 1.10). The most likely outcome for clearances involved an initial transition to canopy state (57%), largely due to the high probability of establishment of a Sargassum canopy (Table 1.10).

Trends from the initial post clearance period did not persist in following years, when it was much more likely that Gap habitat would remain as Gap habitat (91%) (13-38 months, Table 1.9, Table 1.10). This probability was higher than that observed for the control plots (72%), highlighting the potential influence of clearances on gap-to-gap transitions. The influence of clearances on gap-to-gap transitions was also evident in gap longevity times, which were much greater for clearance plots than control plots. Based on the control plot data the average longevity (residence time) for a unit of Gap habitat was 3.65 yrs, while estimated residence time for Canopy habitat was slightly less at 2.8 yrs. In comparison, the average longevity (residence time) for a unit of Gap habitat in clearance plots was 12 years for Gap habitat and 2.4 years for Canopy habitat.

Elasticity values, which indicate the sensitivity of the overall matrix to changes in one of its components, also highlight the disproportionate influence of this gap-to-gap transition. For example in the control plot matrix, the highest elasticity value observed was 0.4393, this being for the Gap-Gap transition (Table 1.8). Clearance plots also indicated a high level of sensitivity to Gap-Gap transitions (Table 1.9, Table 1.10). Therefore, any given increase in the likelihood of this transition would result in a disproportionately strong change in the overall matrix. The clearances in experimental plots appeared to do exactly this, with quite strong increases in the probability that Gap habitats would remain as Gap habitats.

Projections of changes in the proportion of habitat over time showed that for both control and clearance plots, habitat proportions stabilised relatively rapidly. (Figure 1.16). From a starting point of an equal distribution of Gap and Canopy habitat, projections based on control plots stabilised within just one year, with a slightly higher proportion of Canopy than Gap habitat (Figure 1.16a). Similarly, the proportions of Gap and Canopy habitats in clearance plots stabilised after approximately four years, although with a much higher proportion of Gap habitat (84%) than Canopy habitat (Figure 1.16b). For the three-state habitat model (Gap, Sargassum, Ecklonia,) habitat proportions stabilized after approximately four years, with again the proportion of Gap habitat (82%) considerably higher than that for either Sargassum (8%) or Ecklonia (10%) (Figure 1.16c).

Projections of changes in the proportion of habitat over time, as well as early recovery trends in clearance plots, showed that Sargassum and Ecklonia canopy differed markedly in their dynamics. When Canopy habitat was differentiated into either Sargassum or Ecklonia (Table 4), residence times were considerably shorter for Sargassum habitat (1.6 yrs), than for Ecklonia habitat (6 yrs). Similarly, when transition probabilities were differentiated into either Sargassum or Ecklonia, Sargassum habitat was more likely to transition to Gap habitat (50%), in comparison to Ecklonia which once established was much more likely to remain as Ecklonia habitat (83%) than to transition to another state (Table 1.10).

Setting aside the examination of annual transition probabilities and examining the state of habitats after 3 years, the clearest trend was for clearance plots to be classified as Gap habitats. Despite many

of the plots having been occupied by Sargassum canopy habitat for some period of time (Figure 1.15), all clearance plots returned to Gap habitat after 38 months (Figure 1.15) For canopy clearance plots, four out of the nine had returned to Ecklonia canopy, with the others occupied by Gap habitat. In the 50:50 clearance plots, only one had transitioned to Ecklonia habitat, while all the others were Gap habitat. The overall pattern was of a return to the previous state, but this was overlain by the higher overall likelihood that a Gap habitat state would develop.

Table 1.8. Probability of transition based on control plots (n = 9)

	probability		elasticity	
	Gap	Canopy	Gap	Canopy
Gap	0.727	0.25	0.4393	0.1399
Canopy	0.273	0.75	0.1399	0.2811

Table 1.9. Probability of transition based on clearance plots (n = 27)

	probability			elasticity	
	Clearance	Gap	Canopy	Gap	Canopy
Gap	0.407	0.917	0.433	0.7689	0.0698
Canopy	0.593	0.0833	0.567	0.0698	0.0913

Table 1.10. Probability of transition based on clearance plots (n = 27)

	probability				elasticity		
	Clearance	Gap	*Sargassum*	*Ecklonia*	Gap	*Sargassum*	*Ecklonia*
Gap	0.407	0.917	0.5	0.167	0.744	0.0539	0.0135
Sargassum	0.482	0.083	0.375	0	0.067	0.0404	0
Ecklonia	0.111	0	0.125	0.833	0	0.0135	0.0672

Canopy	Pre	0	4	10	13	18	22	26	31	34	38
1		100	37	53	46	29	25	48	29	46	40
2		100		59	73	60	68	53	64	46	34
3		100	96	45	60	75	78	51	95	96	90
4		100	64	54		60	73	100	95	100	98
5		100	50	76	78	51	59	64	64	48	85
6		100	42	65	85	52	64	46	60	89	75
7		100	60	87	35	84	60	53	90	82	98
8		100	41	34	90	97	98	69	100	84	90
9		100	64	53	48	85	59	48	95	78	84
Gap	Pre	0	4	10	13	18	22	26	31	34	38
1		100	40	45	48	35	54	50	76	93	93
2		100	50	75	70	31	84	73	81	78	100
3		100	40	37	40	87	87	68	100	98	93
4		100	28	100	54	48	29	60	59	70	90
5		100	39	92	56	54	37	62	48	68	89
6		100	31	93	31	18	45	43	53	53	73
7		100	34	53	73	96	68	48	96	64	79
8		100	42	45	73	93	85	79	92	87	89
9		100	62	85	90	90	100	79	89	100	100
50/50	Pre	0	4	10	13	18	22	26	31	34	38
1		100	48	46	32	32	22	40	40	46	53
2		100	85	60	67	56	79	46	80	84	70
3		100	53	57	56	70	56	50	84	50	81
4		100	37	53	40	79	76	75	78	100	98
5		100	42		67	68	51	53	65	54	84
6		100	62		59	32	43	43	34	35	68
7		100	54	34	34	98	68	54	87	87	93
8		100	65	45	45	75	68	53	96	100	93
9		100	60		76	73	56	51	80	51	70
Controls	Pre	0	4	10	13	18	22	26	31	34	38
Gap		98	73	87	87	89	95	95	93	100	87
Gap		99	73	90	40	37	36	39	40	67	76
Gap		76	84	78	89	93	100	96	100	96	96
Canopy		100	85	93	92	57	59	54	79	100	92
Canopy		100	42	71	45	46	59	51	45	68	56
Canopy		100	73	81	87	67	78	84	76	84	82
50/50		60	53	67	73	48	60	62	70	53	51
50/50		60	58		40	46	68	64	56	84	73
50/50		62	53	46	51	62	48	31	76	73	53

Figure 1.15. Dominant algal groups within clearance (n = 27) and control (n = 9) treatments over the 26 months. Dominant algal types represented are *Ecklonia* sp (brown), turf and low algae (yellow), *Sargassum* spp (orange) and Green algae (green). Minimum cover = 25%

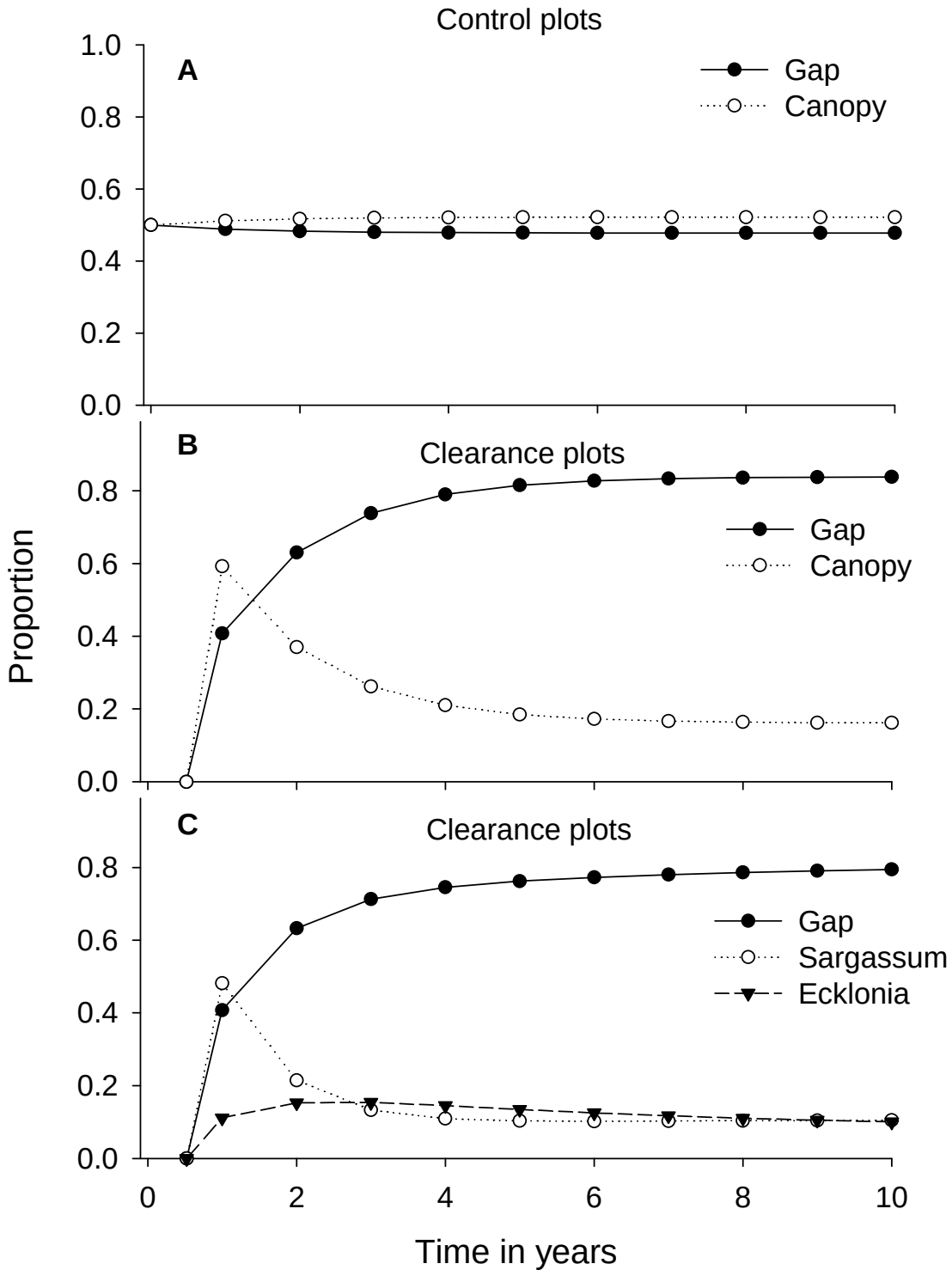

Figure 1.16. Modelled changes in the proportion of: (A) gap and canopy habitats without clearance (B) gap and canopy habitats with clearance, (C) gap, Sargassum and Ecklonia habitats with clearance

1.3.5 Discussion

Broadly similar sequential patterns of colonization were observed among cleared plots, with green algae were characteristically followed by *Sargassum* canopy within the first year. This is similar to the trend and timing of algal assemblages following other experimental clearances of *Ecklonia* habitats on the Australian west coast (Toohey & Kendrick 2007). It did differ in one significant respect, namely the transition through an *Ulva* dominated initial phase. This may be due to differences in the severity of the experimental clearances. In the case of Toohey *et al.,* and other such experiments clearances involved removing canopy only by severing the stipes of *Ecklonia* sporophytes. Our clearances, which included Gap habitats, were necessarily more severe and involved denuding the substratum of all macroalgae thru scouring with a wire brush . However despite these qualitative similarities the strength of these trends varied among treatments, and the habitats established following clearances varied depending on the surrounding habitat type.

Subsequent to the first year after clearance, there was clearly not a simple directional succession toward canopy habitat. Habitat transitions were bi-directional, from Gap to Canopy and vice versa. These bi-directional transitions indicated that there were deterministic components to the likelihood of habitat transitions, and that these depended on the surrounding habitat types. Clearances surrounded by gap habitats were far more likely to remain as gap habitats than to transition to *Sargassum* canopy, and no Gap clearances transitioned to *Ecklonia*. The only plots to transition to Canopy after three years were either surrounded by or adjacent to *Ecklonia* habitat, and interesting all passed through an initial phase of green algal domination. The patterns within these habitats were more variable than in Gap habitats, with only some of the cleared plots transitioning to *Ecklonia* canopy, while the remainder transitioned to Gap habitat. These results are similar to previous experiments where clearances in canopy habitats persisted for periods of several years (Wernberg *et al.*, 2005, Toohey *et al.*, 2007). Symmetrical clearance experiments involving both Gap and Canopy habitats were consistent with the hypothesis that these two broad habitat types represent alternate habitat states, each of which tends to revert to their previous state, or at least to the same state as adjacent habitats.

The nature of the deterministic processes that maintain the mosaic of Canopy and Gap habitats on temperate reefs in south-western Australia is not clear. Deterministic processes may be physical, for example small scale variations in extreme wave forces. We did not measure extreme wave forces in our experimental clearance plots, therefore we cannot exclude this possibility. Our results suggest that such measurements need to be conducted in order to assess this hypothesis. Gap and Canopy habitat patches are frequently found on adjacent apparently similar substrata (Thomson *et al.*, in review) and if present such differences may be subtle. Therefore other deterministic processes are also likely to exist, and biological processes such as species interactions and algal recruitment processes may also play a role in determining habitat transition probabilities. This is clear from clearances within Canopy habitats, where transition to Gap habitat was a likely outcome in the majority of plots. Mechanisms including recruitment limitation and topographic variation have been suggested as explanations for this slow recolonisation (Toohey *et al.*, 2007). The variability in these results probably reflects the stochastic nature of the processes influencing the transitions within Canopy habitat clearances.

Our clearances on the boundaries of Canopy habitat patches all transitioned (with the exception of one plot) to Gap habitats however after three years. Availability of spores is unlikely to have been a major constraining factor on the transition to *Ecklonia* habitat in these plots, suggesting that Gap habitat is able to establish and monopolise space very effectively despite the greater ability of canopy

species to compete for space through processes such as overtopping, shading and abrasion. This suggests that in addition to stochastic processes such as variability in spore supply which may affect transitions in a lottery type process, there are other biologically determined processes that affect these out comes. It is not clear how Gap habitat algal communities suppress the recruitment of canopy species, particularly *Ecklonia*, but potential explanations include the suppression of gametophytes or recruits by low profile but dense assemblages of Gap algae, and even predation of phaeophyte spores by Gap habitat epifauna (Taylor and Cole 1994).

The mosaic of Gap and Canopy habitats in south-western Australian is clearly a ubiquitous and persistent feature of coastal temperate reef ecosystems. Habitat transition models based on our observations of unmanipulated habitats indicate that these mosaics can persist without high levels of disturbance to canopy habitats. The proportions of canopy and gap habitats predicted by these models is roughly similar in magnitude and proportion to the observed proportion of Gap and Canopy habitats on these reefs (40:60%, Thomson *et al.*, in review). Modelling also suggests that even over long periods, reefs in Western Australia will not develop into a state dominated by a single habitat type. Instead, they will be composed of a mosaic of alternate habitat patches. While these patches may be dynamic on time scales of several yrs the proportions of habitat on the reefs will remain relatively constant.

Higher frequency disturbance regimes in southwest Australian reefs are likely to shift the balance of habitat cover from majority Canopy algal assemblages to Gap assemblages. The relative proportion of Gap and Canopy habitat types may be quite different under such regimes, with over 80% Gap habitat. The nature of temperate reef algal assemblages would be strikingly different, with long lived gaps and only occasional patches of Canopy algae. Such habitats occur in areas of coast affected by urbanization (Gorman and Connell 2009) and along a latitudinal gradient as temperate habitats transition through to subtropical reefs that are characterised by assemblages of turfing and foliose algae. Combinations of disturbance and temperature effects can reduce the rate at which *Ecklonia* recruit and re-establish after clearances (Wernberg *et al.*, 2005). Although our observations are relatively short term, only three years, our modelling provides strong evidence that Gap habitat patches created by such disturbance processes may indeed be long lived, with an average turnover time of 12 years. The magnitude of this estimate of gap longevity is consistent with the average estimated age (between 3 and 13 yrs) of colonial corals (*Plesiastrea versipora*) which occur almost exclusively in Gap habitat (Thomson et al in review). Long-lived patches in other temperate algal forests have been reported elsewhere, for example clearances of Ascophyllum in the North Atlantic have taken up to 20 years to infill (Ingolfsson and Hawkins 2008).

Given the potential for increasing levels of disturbance from urbanization (Bennedetti-Cecchi *et al.*, 2001) and climatic factors such as increasing sea temperatures and changing wave intensity regimes (Young *et al.*, 2011), it may be predicted that the relative balance of habitat types on southwest Australian temperate reef ecosystems will change in the future. While this may not necessarily have dire immediate consequences for biodiversity (England *et al.*, 2008) there may be negative implications for secondary production on temperate reefs, where food webs appear to be disproportionately reliant on brown algae as a food source (Vanderklift and Wernberg 2008, Crawley et al 2009). The ability of Gap habitat to occupy space indicates that such changes may be very difficult to reverse, and that we should ensure that we make efforts to manage any processes that may exacerbate the transitions from Kelp to Gap habitats.

1.3.6 References

Airoldi L (2003) The effects of sedimentation on rocky coast assemblages. Oceanography and Marine Biology, Vol 41 41:161-236

Anderson MJ (2001) A new method for non-parametric multivariate analysis of variance. Austral Ecology 26:32-46

Andrew NL, Jones GP (1990) Patch formation by herbivorous fish in a temperate australian kelp forest. Oecologia 85:57-68

Andrew NL, O'Neill AL (2000) Large-scale patterns in habitat structure on subtidal rocky reefs in new south wales. Marine and Freshwater Research 51:255-263

Babcock RC, Kelly S, Shears NT, Walker JW, Willis TJ (1999) Changes in community structure in temperate marine reserves. Marine Ecology-Progress Series 189:125-134

Benedetti-Cecchi L, Pannacciulli F, Bulleri F, Moschella PS, Airoldi L, Relini G, Cinelli F (2001) Predicting the consequences of anthropogenic disturbance: Large-scale effects of loss of canopy algae on rocky shores. Marine Ecology-Progress Series 214:137-150

Booij N, Ris RC, Holthuijsen LH (1999) A third-generation wave model for coastal regions - 1. Model description and validation. Journal of Geophysical Research-Oceans 104:7649-7666

Breen PA, Mann KH (1976) Changing lobster abundance and destruction of kelp beds by sea-urchins. Marine Biology 34:137-142

Burgess SN, McCulloch MT, Mortimer GE, Ward TM (2009) Structure and growth rates of the high-latitude coral: Plesiastrea versipora. Coral Reefs 28:1005-1015

Connell JH, Slatyer RO (1977) Mechanisms of succession in natural communities and their role in community stability and organization. American Naturalist 111:1119-1144

Connell SD, Irving AD (2008) Integrating ecology with biogeography using landscape characteristics: A case study of subtidal habitat across continental australia. Journal of Biogeography 35:1608-1621

Connell SD, Vanderklift MA, Gillanders BM (2007) Negative interactions: The influence of predators and herbivores on prey and ecological systems. In: Marine ecology. Oxford University Press, South Melbourne, p 72-100

Coyer JA, Ambrose RF, Engle JM, Carroll JC (1993) Interactions between corals and algae on a temperate zone rocky reef - mediation by sea-urchins. Journal of Experimental Marine Biology and Ecology 167:21-37

Dayton PK (1975) Experimental studies of algal canopy interactions in a sea otter dominated kelp community at amchitka-island, alaska. Fishery Bulletin 73:230-237

Dayton PK (1985) Ecology of kelp communities. Annual Review of Ecology and Systematics 16:215-245

Dayton PK, Currie V, Gerrodette T, Keller BD, Rosenthal R, Ventresca D (1984) Patch dynamics and stability of some california kelp communities. Ecological Monographs 54:253-289

Dayton PK, Tegner MJ (1984) Catastrophic storms, el-nino, and patch stability in a southern california kelp community. Science 224:283-285

Dayton PK, Tegner MJ, Parnell PE, Edwards PB (1992) Temporal and spatial patterns of disturbance and recovery in a kelp forest community. Ecological Monographs 62:421-445

Denny MW (1988) Biology and the mechanics of the wave-swept environment. Biology and the mechanics of the wave-swept environment:i-xiii, 1-329

Drake JA (1990) Communities as assembled structures - do rules govern pattern. Trends in Ecology & Evolution 5:159-164

England PR, Phillips J, Waring JR, Symonds G, Babcock R (2008) Modelling wave-induced disturbance in highly biodiverse marine macroalgal communities: Support for the intermediate disturbance hypothesis. Marine and Freshwater Research 59:515-520

Fowler-Walker MJ, Wernberg T, Connell SD (2006) Differences in kelp morphology between wave sheltered and exposed localities: Morphologically plastic or fixed traits? Marine Biology 148:755-767

Gorman D, Connell SD (2009) Recovering subtidal forests in human-dominated landscapes. Journal of Applied Ecology 46:1258-1265

Graham MH, Harrold C, Lisin S, Light K, Watanabe JM, Foster MS (1997) Population dynamics of giant kelp macrocystis pyrifera along a wave exposure gradient. Marine Ecology-Progress Series 148:269-279

Harrold C, Watanabe J, Lisin S (1988) Spatial variation in the structure of kelp forest communities along a wave exposure gradient. Marine Ecology-Pubblicazioni Della Stazione Zoologica Di Napoli I 9:131-156

Hatcher A (1989) Variation in the components of benthic community structure in a coastal lagoon as a function of spatial scale. Marine and Freshwater Research 40:79-96

Holthuijsen L (1997) Waves in oceanic and coastal waters, Vol. Cambridge University Press, Cambridge

Hosmer DW, Lemeshow S, Klar J (1988) Goodness-of-fit testing for the logistic-regression model when the estimated probabilities are small. Biometrical Journal 30:911-924

Hughes TP, Reed DC, Boyle MJ (1987) Herbivory on coral reefs - community structure following mass mortalities of sea-urchins. Journal of Experimental Marine Biology and Ecology 113:39-59

Irving AD, Connell SD (2006) Predicting understorey structure from the presence and composition of canopies: An assembly rule for marine algae. Oecologia 148:491-502

Irving AD, Connell SD, Gillanders BM (2004) Local complexity in patterns of canopy-benthos associations produces regional patterns across temperate australasia. Marine Biology 144:361-368

Johnson CR, Mann KH (1988) Diversity, patterns of adaptation, and stability of nova-scotian kelp beds. Ecological Monographs 58:129-154

Jompa J, McCook LJ (2002) Effects of competition and herbivory on interactions between a hard coral and a brown alga. Journal of Experimental Marine Biology and Ecology 271:25-39

Jones GP (1992) Interactions between herbivorous fishes and macroalgae on a temperate rocky reef. Journal of Experimental Marine Biology and Ecology 159:217-235

Jones GP, Andrew NL (1990) Herbivory and patch dynamics on rocky reefs in temperate australasia - the roles of fish and sea-urchins. Australian Journal of Ecology 15:505-520

Keddy PA (1992) Assembly and response rules - 2 goals for predictive community ecology. Journal of Vegetation Science 3:157-164

Kennelly SJ (1987a) Inhibition of kelp recruitment by turfing algae and consequences for an australian kelp community. Journal of Experimental Marine Biology and Ecology 112:49-60

Kennelly SJ (1987b) Physical disturbances in an australian kelp community .1. Temporal effects. Marine Ecology-Progress Series 40:145-153

Konar B, Estes JA (2003) The stability of boundary regions between kelp beds and deforested areas. Ecology 84:174-185

Lauzon-Guay JS, Scheibling RE (2010) Spatial dynamics, ecological thresholds and phase shifts: Modelling grazer aggregation and gap formation in kelp beds. Marine Ecology-Progress Series 403:29-41

Leliaert F, Anderson RJ, Bolton JJ, Coppejans E (2000) Subtidal understorey algal community structure in kelp beds around the cape peninsula (western cape, south africa). Botanica Marina 43:359-366

Lindegarth M, Gamfeldt L (2005) Comparing categorical and continuous ecological analyses: Effects of "Wave exposure" On rocky shores. Ecology 86:1346-1357

Littler MM, Littler DS (1997) Epizoic red alga allelopathic (?) to a caribbean coral. Coral Reefs 16:168-168

McCook LJ, Jompa J, Diaz-Pulido G (2001) Competition between corals and algae on coral reefs: A review of evidence and mechanisms. Coral Reefs 19:400-417

McCormick MI (1994) Comparison of field methods for measuring surface-topography and their associations with a tropical reef fish assemblage. Marine Ecology-Progress Series 112:87-96

Menge BA, Allison GW, Blanchette CA, Farrell TM, Olson AM, Turner TA, van Tamelen P (2005) Stasis or kinesis? Hidden dynamics of a rocky intertidal macrophyte mosaic revealed by a spatially explicit approach. Journal of Experimental Marine Biology and Ecology 314:3-39

Menge BA, Farrell TM, Olson AM, Vantamelen P, Turner T (1993) Algal recruitment and the maintenance of a plant mosaic in the low intertidal region on the oregon coast. Journal of Experimental Marine Biology and Ecology 170:91-116

Miller MW, Hay ME (1996) Coral-seaweed-grazer-nutrient interactions on temperate reefs. Ecological Monographs 66:323-344

Petraitis PS, Dudgeon SR (2005) Divergent succession and implications for alternative states on rocky intertidal shores. Journal of Experimental Marine Biology and Ecology 326:14-26

Rasher DB, Hay ME (2010) Chemically rich seaweeds poison corals when not controlled by herbivores. Proceedings of the National Academy of Sciences of the United States of America 107:9683-9688

Ris RC, Holthuijsen LH, Booij N (1999) A third-generation wave model for coastal regions - 2. Verification. Journal of Geophysical Research-Oceans 104:7667-7681

Scheibling RE, Hennigar AW, Balch T (1999) Destructive grazing, epiphytism, and disease: The dynamics of sea urchin - kelp interactions in nova scotia. Canadian Journal of Fisheries and Aquatic Sciences 56:2300-2314

Scheibling RE, Raymond BG (1990) Community dynamics on a subtidal cobble bed following mass mortalities of sea-urchins. Marine Ecology-Progress Series 63:127-145

Schiel DR (1988) Algal interactions on shallow subtidal reefs in northern new zealand - a review. New Zealand Journal of Marine and Freshwater Research 22:481-489

Siddon CE, Witman JD (2003) Influence of chronic, low-level hydrodynamic forces on subtidal community structure. Marine Ecology-Progress Series 261:99-110

Sousa-Dias A, Melo RA (2008) Long-term abundance patterns of macroalgae in relation to environmental variables in the tagus estuary (portugal). Estuarine Coastal and Shelf Science 76:21-28

Sutherland JP (1990) Perturbations, resistance, and alternative views of the existence of multiple stable points in nature. American Naturalist 136:270-275

Tegner MJ, Dayton PK, Edwards PB, Riser KL (1997) Large-scale, low-frequency oceanographic effects on kelp forest succession: A tale of two cohorts. Marine Ecology-Progress Series 146:117-134

Thomsen MS, Wernberg T, Kendrick GA (2004) The effect of thallus size, life stage, aggregation, wave exposure and substratum conditions on the forces required to break or dislodge the small kelp *ecklonia radiata*. Botanica Marina 47:454-460

Toohey B, Kendrick GA, Wernberg T, Phillips JC, Malkin S, Prince J (2004) The effects of light and thallus scour from *ecklonia radiata* canopy on an associated foliose algal assemblage: The importance of photoacclimation. Marine Biology 144:1019-1027

Toohey BD (2007) The relationship between physical variables on topographically simple and complex reefs and algal assemblage structure beneath an ecklonia radiata canopy. Estuarine Coastal and Shelf Science 71:232-240

Toohey BD, Kendrick GA (2007) Survival of juvenile eeklonia radiata sporophytes after canopy loss. Journal of Experimental Marine Biology and Ecology 349:170-182

Toohey BD, Kendrick GA (2008) Canopy-understorey relationships are mediated by reef topography in ecklonia radiata kelp beds. European Journal of Phycology 43:133-142

Toohey BD, Kendrick GA, Harvey ES (2007) Disturbance and reef topography maintain high local diversity in ecklonia radiata kelp forests. Oikos 116:1618-1630

Underwood AJ, Chapman MG (2000) Variation in abundances of intertidal populations: Consequences of extremities of environment. Hydrobiologia 426:25-36

Vadas RL, Elner RW, Garwood PE, Babb IG (1986) Experimental evaluation of aggregation behaviour in the sea-urchin *strongylocentrotus-droebachiensis* - a reinterpretation. Marine Biology 90:433-448

Vanderklift MA, Kendrick GA (2004) Variation in abundances of herbivorous invertebrates in temperate subtidal rocky reef habitats. Marine and Freshwater Research 55:93-103

Vanderklift MA, Kendrick GA (2005) Contrasting influence of sea urchins on attached and drift macroalgae. Marine Ecology-Progress Series 299:101-110

Vanderklift MA, Wernberg T (2008) Detached kelps from distant sources are a food subsidy for sea urchins. Oecologia 157:327-335

Wernberg T (2005) Holdfast aggregation in relation to morphology, age, attachment and drag for the kelp ecklonia radiata. Aquatic Botany 82:168-180

Wernberg T, Connell SD (2008) Physical disturbance and subtidal habitat structure on open rocky coasts: Effects of wave exposure, extent and intensity. Journal of Sea Research 59:237-248

Wernberg T, Goldberg N (2008) Short-term temporal dynamics of algal species in a subtidal kelp bed in relation to changes in environmental conditions and canopy biomass. Estuarine Coastal and Shelf Science 76:265-272

Wernberg T, Kendrick GA, Phillips JC (2003) Regional differences in kelp-associated algal assemblages on temperate limestone reefs in south-western australia. Diversity and Distributions 9:427-441

Wernberg T, Kendrick GA, Toohey BD (2005) Modification of the physical environment by an ecklonia radiata (laminariales) canopy and implications for associated foliose algae. Aquatic Ecology 39:419-430

1.4 Imposed and inherent scales in cellular automata models of habitat

Published as: Craig PD. (2010) Imposed and inherent scales in cellular automata models of habitat.

Ecological Modelling 221:2425–2434

Peter D. Craig

CSIRO Marine & Atmospheric Research, GPO Box 1538, Hobart, Tasmania, 7001,

1.4.1 Abstract

Both observational and modelling studies of the natural environment are characterised by their 'grain' and 'extent', the smallest and largest scales resolved in time and space. These are imposed scales that should be chosen to ensure that the natural scales of the system are captured in the study. A simple cellular automata model of habitat represents only the presence or absence of vegetation, with global and local interactions described by four empirical parameters. Such a model can be formulated as a nonlinear Markov equation for the habitat probability. The equation produces inherent space and time scales that may be considered as transition scales or the scales for recovery from disturbance. However, if the resolution of the model is changed, the empirical parameters must be changed to preserve the properties of the system. Further, changes in the spatial resolution lead to different interpretation of the spatial structure. In particular, as the resolution is reduced, the apparent dominance of one habitat type over the other increases. The model provides an ability to compare both field and model investigations conducted at different resolution in time and space.

Keywords: habitat model; kelp beds; cellular automata; Markov model; space scales; time scales; model resolution

1.4.2 Introduction

An appreciation of scale is fundamental to observation and understanding of the natural world. A measurement program that does not resolve significant fine-scale variability in either space or time is doomed to be aliased. Similarly, a program that does not resolve the larger scales will be unable to distinguish between variability and trend.

The scales that govern ecological dynamics appear often to be quite different from those chosen for field investigations. In a review of 14 years of literature, Wheatley and Johnson (2009) concluded that only 29% of studies provided a 'biological rationale' for the scale of the measurements. Their review was focused on spatial observations and, in particular, on 'grain' and 'extent', the smallest and largest spatial scales represented in an experimental design. They highlight the need to understand the implications of scale. If measurements are made in similar, or the same, systems but at different scale, then how are the results to be compared? Further, if management or conservation priorities require conclusions to be scaled up or down, then how is this scaling to be done?

Wheatley and Johnson's comment applies equally to temporal, as well as to spatial, scaling. They reviewed only studies of mobile animals, and acknowledged the difficulty of observing and identifying scales of behaviour in such studies. For stationary organisms, that is, sessile animals and plants, observation is clearly likely to be more straightforward. However, the same design criteria apply. The spatial and temporal grain and extent must be chosen to resolve the dominant scales of the organisms' dynamics.

Observations and models are symbiotic. An observation program will usually be based on some form of conceptual model of the system dynamics. The observations will then be used to refine or reformulate this model, and may be the basis for design or calibration of a numerical model. While a numerical model is only a caricature of a real system, it provides the user with the luxury of exploring issues of scale, and various what-if scenarios.

This article concentrates on habitat models, with an emphasis toward marine benthic habitat. Habitat models are established to describe the dynamics of plants in space and time, with the same methodology also applicable to sessile animals. The models may represent time and space continuously or discretely, and may eliminate a dimension by assuming mean conditions in space or equilibrium conditions in time (e.g. Berec, 2002). Probably the most common and most versatile models are cellular automata (e.g. Balzter *et al.*, 1998).

In a cellular automata model, the spatial structure of the habitat is described on a horizontal grid or lattice. The state of the habitat is defined at each grid point, and there are rules, specified as probabilities, for the way neighbours have impact on one another. There may also be global rules for phenomena like recruitment and disturbance. The system is stepped forward in time on the basis of these rules (Baltzer *et al.*, 1998). One of the more familiar applications is the forest-gap model (e.g. Pascual and Guichard, 2005), in which a grid point is occupied by either a tree or a gap. Gaps are caused by storms, which are a global (that is, domain-wide) disturbance. The probability of gap creation, in a model time step, is increased adjacent to a gap, because the surrounding trees are more exposed. Likewise, the more trees adjacent to a gap, the more likely the gap are to be colonised, by local seeding, in a time step. Depending on the complexity of the model, it may include multiple vegetation species or functional types (e.g. Sole *et al.*, 2004; Colasanti *et al.*, 2007).

The simplest cellular automata models have only two states, defined by the presence or absence of organisms at any location on the grid (e.g. Berec, 2002). In such a two-state system, the interaction between occupancy and absence is formulated in exactly the same way as a spatial competition between two species. In this sense, the approach is very similar to the spatial extension of the Lotka-Volterra predator-prey model, that has also been applied to pairs of competing species (e.g. Durrett and Levin, 1994; Bolker *et al.*, 2003; Neuhauser *et al.*, 1999; see also Pascual *et al.*, 2002). The equivalent models are often described as 'interacting particle systems' (Durrett and Levin, 1994), with somewhat more complicated and formalised interactions than in the gap models (Neuhauser *et al.*, 1999). They are backed by the wealth of experience derived from many years of application of the Lotka-Volterra equations (see Durrett and Levin, 1994, for earlier references).

In the context of predator-prey models, there is a set of studies (Rand and Wilson, 1995; Keeling *et al.*, 1997; Pascual and Levin, 1999; see also Durrett and Levin, 1998, and Pascual *et al.*, 2002) devoted to establishing a spatial scale over which model results can be averaged to effectively separate a temporal signal from stochastic noise. This scale is variously called an 'intermediate scale', a 'characteristic scale', or a 'correlation length'. In each of these studies, the grain is defined to be the space occupied by a single organism. The intermediate scale in effect defines a minimum spatial extent for the model domain.

The rules governing a cellular automata model can be written as difference equations for the probability of occurrence of the different states of the system (see Section 2). If the spatial terms in these equations are removed, either as an approximation or by averaging over the domain, to form the 'mean-field' equation (e.g. Berec, 2002), then the model becomes a Markov chain. For a strict Markov chain, the system state at one time step is dependent only on the single previous time step, and not time steps prior to that. Spatial variability can be incorporated into the Markov formalism (Balzer *et al.*, 1998), but requires single-step backward and forward dependency in the space dimensions, to encompass neighbours on all sides. While it may seem a contradiction in terms, the Markov equations for the habitat probabilities are actually deterministic (see Section 2). The present study concentrates on the Markov form of the cellular automata model, which is more amenable to analysis than the stochastic form. However, as we shall see, the stochastic model may be required to calibrate the Markov model.

The parameters in a cellular automata model are empirical. Observation may be able to suggest the probability with which a certain species will recruit to a certain sized vegetation gap, surrounded by particular neighbours, under specified conditions, within a given time. However, such observation is usually not easy or definitive, especially at the level of repetition required to account for the stochasticity of the processes. This is particularly true for the marine environment, where observations are usually labour intensive. Langmead and Sheppard (2004) calibrated a model of 10 different coral species in the Caribbean from 40 years of data, while Dunstan and Johnson (2005) worked with an epibenthic community of 13 dominant species on a jetty wall that was small enough to be captured in single camera frames. However, such detailed observation and experience is atypical.

There are many decisions to be made in setting up a cellular automata model. The technical questions are concisely enunciated by Berec (2002). They include the choice of space and time scales, the spatial template (that is, how many 'nearest neighbours'), and the initial and boundary conditions. The more philosophical questions, posed as 'rules', are discussed by Grimm (1999). These include the level of simplicity of the model, the approach to analysing the results, and the reason for modelling.

The reason for modelling is not always as obvious as might be expected. The models cannot hope to have the predictive accuracy of, say, a numerical weather-forecasting model that is based on well-established physical laws and a large network of (assimilated) observations. In many reported cellular automata exercises, the object seems to be the development of the model itself. However, it is hard to argue with Grimm's (1999) third rule: 'the most important purpose of modelling is understanding'. What understanding comes from applying, to a stochastic ecosystem, a stochastic model that has been empirically calibrated against the ecosystem itself? Even the most complicated of these models are still gross over-simplifications of the true ecosystem. However, satisfactory performance (in some defined sense) from the model will suggest that the model is capturing significant features of the ecosystem behaviour.

In the terminology of Schroder and Seppelt (2006), by representing a small number of *processes* in the model, we hope to be able to reproduce *patterns* of behaviour in the ecosystem. Others refer to the *bottom-up* description in the model reproducing the *top-down* style of 'classical theoretical ecology' (Grimm, 1999; see also Pascual *et al.*, 2002). In recent years, there has been considerable comment on the ability of simple spatial models to reproduce self-similarity, or scale-invariance, in simulated ecosystems (e.g. Sole *et al.*, 1999; Wootton, 2001a; Pascual and Guichard, 2005; Reitkerk *et al.*, 2004; Grimm *et al.*, 2005). In a scale-invariant system, the frequency of occurrence of patch sizes varies as a power of the patch size itself. Scale-invariance occurs in ecosystems that are at criticality, that is, at the point of transition between two different system states, so that a small change in the

system forcing, represented by the model parameters, can cause a dramatic change in the structure of the system (see references above).

Beyond their role in providing understanding, cellular automata models can be used for scenario-testing, and in this context are proposed as management tools, for example in forestry (e.g. Mathey *et al.*, 2008) and land-use planning (e.g. Syphard *et al.*, 2005). Clearly, however, predictions from empirical models need to be treated with caution. This is particularly so should the system go beyond criticality to an actual change of state, that would take the model to a situation for which it has not been calibrated. However, a warning from a model that a system is on the verge of transition is likely to be important management information.

A priority of management is to establish the ability of a system to cope, or recover from, disturbance. The obverse of criticality is stability, around which there has grown a 'virtual Babel' of terminology (Pawlowski and McCord, 2009). Many cellular automata models are set up specifically to look at the consequences of disturbance. Disturbance can be in the form of natural events, such as winds and waves (e.g. Guichard *et al.*, 2003; Langmead and Sheppard, 2004; Wootton, 2001a), deliberate (Sole *et al.*, 2004) or accidental (Fonseca *et al.*, 2004) clearance, and can also include 'infective' events such as fire and disease (Pascual and Guichard, 2005). Sole *et al.*, (2004) quote studies that show 10% habitat clearance causing species' decline from 5% (in forests) to 50% (in coral).

The present study, although generic, was motivated by a management issue: the imperative to protect reef habitat adjacent to a rapidly growing city. The coastline of the city of Perth (at 32 °S) in Western Australia is fringed by a limestone reef system, approximately 1600 km long, and typically between 1 and 5 km offshore (Wernberg *et al.*, 2003). The reefs are mostly in water less than 20 m deep, and are densely populated by macroalgae. The southern Australian region 'has the highest levels of species richness and endemism of any regional macroalgal flora in the world' (Phillips, 2001). While 150 species of macroalgae have been identified in the coastal waters around Perth, the habitat is dominated by a kelp, *Ecklonia radiata*, that grows to a length of 1-2 m, and a weight per plant of 1-2 kg (Wernberg *et al.*, 2003).

Our conceptual model of the kelp dynamics is similar to that for terrestrial forests, with gaps created by waves, and recolonised predominantly by propagules from nearby plants (e.g. Toohey *et al.*, 2007). The west Australian coastline is exposed to the Indian Ocean, and large waves are primarily a consequence of swell generated by winter storms propagating eastward in the Southern Ocean (Hemer *et al.*, 2010). Waves dislodge individual kelp plants at the holdfast (Toohey *et al.*, 2007) so that, after storms, large amounts of macroalgal wrack are washed into the surf zone and onto the beach (Wernberg *et al.*, 2006). The recovery time is much longer than the gap-creation time. After artficial clearance of *E. radiata*, to simulate the impact of waves, the biomass took 34 months to reach 75% of that at control sites (Toohey *et al.*, 2007).

In a model, the 'grain' is set by the space and time steps, and the 'extent' is the duration of the model run and the size of the model's spatial domain. In addition, there are inherent scales (sometimes seen as patterns, as noted above) that emerge in the model results. These scales can serve as indicators of the temporal or spatial influence of a localised (in time or space) disturbance. The model grain size must be chosen to resolve these 'natural' scales of the system. The scales must also remain constant if the model resolution, that is, the grain size, is changed. However, if the resolution of a model is changed, then the parameters of the model must also change, to preserve the dynamical properties of the system. Similarly when the model is calibrated against data, the data must either have been collected at the same (spatial and temporal) resolution, or modified in a manner consistent with the change in scale.

The dependence of model parameters and results on the resolution of the model will be demonstrated in the following sections with a simple model that represents both spatial and temporal variability. This is a gap (presence-absence) model, with nearest-neighbour and global interactions. After initial discussion, and without any real loss of generality, the model will be reduced from two space dimensions to one. In this form, the model is expressed by a pair of nonlinear, two-dimensional (time and space), second-order difference equations. Solution of the equations is straightforward, and demonstrates, relatively simply, some of the subtleties of scale that are relevant to both the observation and model representation of natural systems.

1.4.3 A cellular automata model

In the cellular automata model, habitat is defined by the variable $H(x,y,t)$, where x and y are rectangular, horizontal space coordinates, and t is time. In the present study, H takes only two values, 1 for an empty location, and 2 for an occupied location. An empty location is also referred to as a gap. The coordinate system is discretised into individual square cells of size Δx, and the total domain is a rectangle, given by

$$x = 0, \Delta x, 2\Delta x, \ldots, M\Delta x; \quad y = 0, \Delta x, 2\Delta x, \ldots, N\Delta x.$$

Even at this early stage, we have already imposed 3 spatial scales on the system: the discretisation scale, or grain-size, Δx, and the domain extent in each of 2 dimensions, $M\Delta x$ and $N\Delta x$. For the marine system, the domain extent may be envisaged as an idealised (rectangular) representation of an individual reef, which might be hundreds or thousands of metres long and wide. The discretisation scale, Δx, will be discussed in the following.

The probability that $H(x,y,t)$ equals 1 or 2 is designated by $P_1(x,y,t)$ and $P_2(x,y,t)$, respectively. Because there are only 2 states,

$$P_1(x,y,t) + P_2(x,y,t) = 1, \text{ for all } x, y \text{ and } t. \qquad (1)$$

Given the state of the system at time t, the model describes its state at time $t+\Delta t$, where Δt is a defined time increment. The model has four specified, non-negative parameters, N_{12}, N_{21}, S_{12} and S_{21}, that define the probabilities that an individual grid point will change its state in time step Δt. The N_{ij} give the neighbour replacement rules: that is, N_{ij}, $i \neq j$, is the probability that state i (at x,y) will be replaced by the state j that a neighbour is in. Thus, if 4 neighbours are in state j, the probability that the point x,y will transition from state i to state j, because of its neighbours, is $4N_{ij}$. The parameters S_{ij} allow for the possibility of 'succession', beyond the mechanism of neighbour replacement. Thus, S_{ij} is the probability that, regardless of the state of its neighbours, a point in state i at time t will change to state j at $t+\Delta t$. Therefore, if S_{12} is nonzero, there is a possibility of background seeding, so that an empty point may still transition to an occupied state, even if its neighbours were also empty. Similarly, nonzero S_{21} allows the possibility that a gap may be created at a point, even if it is protected by occupied neighbours.

Expressed in its Markov form, the model is described by 2 equations:

$$P_1(x,y,t+\Delta t) = P_1(x,y,t) \left(1 - S_{12} - N_{12}\left(P_2(x-\Delta x,y,t) + P_2(x+\Delta x,y,t) + P_2(x,y-\Delta x,t) + P_2(x,y+\Delta x,t)\right)\right) + P_2(x,y,t)\left(S_{21} + N_{21}\left(P_1(x-\Delta x,y,t) + P_1(x+\Delta x,y,t) + P_1(x,y-\Delta x,t) + P_1(x,y+\Delta x,t)\right)\right) \quad (2)$$

And

$$P_2(x,y,t+\Delta t) = P_1(x,y,t) \left(S_{12} + N_{12}\left(P_2(x-\Delta x,y,t) + P_2(x+\Delta x,y,t) + P_2(x,y-\Delta x,t) + P_2(x,y+\Delta x,t)\right)\right) + P_2(x,y,t)\left(1 - S_{21} - N_{21}\left(P_1(x-\Delta x,y,t) + P_1(x+\Delta x,y,t) + P_1(x,y-\Delta x,t) + P_1(x,y+\Delta x,t)\right)\right) \quad (3)$$

A simple representation of the model, with only 5 space steps in one dimension, is shown over 4 time steps in Figure 1.17.

There are a number of immediate observations about equations (2) and (3).

- The equations are consistent, in the sense that

  $$P1(x,y,t+\Delta t) + P2(x,y,t+\Delta t) = P1(x,y,t) + P2(x,y,t) = P1(x,y,0) + P2(x,y,0).$$

  Thus, so long as the initial state (i.e. at $t = 0$) satisfies (1), one of equations (2) and (3) is redundant.

- To ensure that the probability of transition from one habitat state to the other is at most 1,

  $$nN_{12} + S_{12} \leq 1 \text{ and } nN_{21} + S_{21} \leq 1, \quad (4)$$

  where n is the number of neighbours for each point.

- The parameters N_{ij} and S_{ij} do not need to be constant in space or time. However, they are assumed to be so in the present analysis. This assumption leads to limitations both in the range of the parameters, and in the scenarios that can be assessed, as will be discussed in the following section.
- In (2) and (3), the space step Δx defines not only the spatial scale represented by each individual element in the model, but also the spatial scale that each element can influence in a

single time step. In this sense it is equivalent to a first or second-order finite-difference approximation of a spatial derivative.

- Equations (2) and (3) contain the assumption that an individual point (x,y) is influenced by four neighbours on a cross pattern. It is also straightforward to incorporate neighbours on triangular (3 neighbours), square (8 neighbours) or hexagonal (6 neighbours) templates (see Berec, 2002).

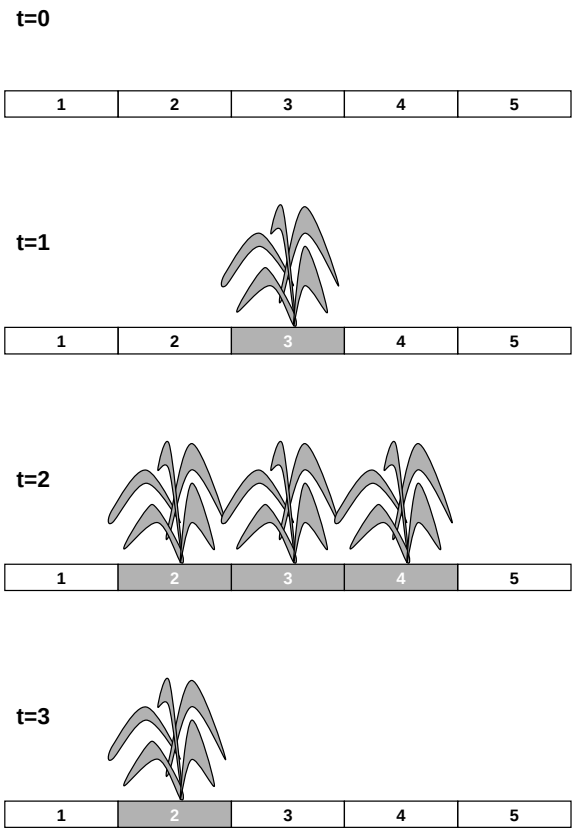

Figure 1.17. A simple representation of the cellular automata model with 5 space steps. At t=0, H=0 at all locations. At t=1, space-step 3 becomes occupied, with probability S_{12}. At t=2, space-steps 2 and 4 also become occupied, with probability $S_{12}+N_{12}$. At t=3, space-step 3 is emptied, with probability S_{21}, and space-step 4 is emptied with probability $S_{21}+N_{21}$.

For the present study, we will simplify the geometry even further, and assume only a single space dimension, designated by x. The one-dimensional system may be envisioned physically as a long, thin reef, or as a single transect along a reef, although neither of these representations is strictly correct, because of boundary influences. One-dimensionality is assumed because it makes explanation simpler. The conclusions all carry over to two dimensions. In one-dimension, (2) and (3) become:

$$P_1(x,t+1) = P_1(x,t)\left(1 - S_{12} - N_{12}\left(P_2(x-1,t) + P_2(x+1,t)\right)\right) + P_2(x,t)\left(S_{21} + N_{21}\left(P_1(x-1,t) + P_1(x+1,t)\right)\right) \quad (5)$$

and

$$P_2(x,t+1) = P_1(x,t)\left(S_{12} + N_{12}\left(P_2(x-1,t) + P_2(x+1,t)\right)\right) + P_2(x,t)\left(1 - S_{21} - N_{21}\left(P_1(x-1,t) + P_1(x+1,t)\right)\right) \quad (6)$$

in which the Δx and Δt notation has been simplified, so that $t+1$ represents a time step of Δt beyond t, while $x+1$ and $x-1$ are the neighbours a distance Δx from point x.

It is obvious how (5) and (6) are stepped forward in time. If P_1 and P_2 are known for all x values at time t, then (5) and (6) are simply the rules for creating the new values at time $t+1$. This time-stepping is described as 'synchronous', in the sense that both variables are simultaneously updated at all spatial locations (e.g. Rand and Wilson, 1995; Dunstan and Johnson, 2005; see also discussion on 'process ordering' in Berec 2002).

At this stage, we can easily describe how the stochastic version of the model is established. At a given time step, including the initial time $t=0$, $H(x,t)$ is specified as 1 or 2 at every x location on the grid. For each location, time-stepping requires the generation of a random number, r, chosen on the closed interval [0,1]. If, say, for a particular x, $H(x,t)=1$, then $H(x,t+1)=2$ if the following condition is satisfied:

$$r < S_{12} + n\,N_{12}$$

where n is the number of neighbours (i.e. the points $x+1$ and $x-1$) for which

$H = 2$ at time t. Otherwise, $H(x,t+1)$ retains the value 1.

Aside from the selection of Δx and Δt, two other issues have been ignored to this point: the specification of initial conditions and boundary conditions. Initial conditions require that, for the stochastic form of the model, $H(x,0)$ must be set for all x. Equivalently, in the Markov form, $P_1(x,0)$ and $P_2(x,0)$ have to be specified. How are these initial values chosen? Common choices are: a random allocation, an allocation to represent an observed state of an actual ecosystem, or choice of a particular state. We will choose the third option, and begin with a totally cleared habitat: that is $H(x,0)=1$ for all x, or, equivalently, $P_1(x,0)=1$, $P_2(x,0)=0$. This state represents the aftermath of a severe disturbance, and will allow investigation of the system recovery (e.g. Wootton, 2001b). It should be noted that there will be recovery only if $S_{12}\neq 0$.

An important question here is whether the ultimate state of the system depends on its initial conditions. In Markovian terminology, a system that achieves independence from its initial state is ergodic (e.g. Balzer *et al.*, 1998). In such a case, it is important to identify the time-scale over which recovery takes place, and the system is able to 'forget' its initial (or disturbed) state.

The boundary points $x=0$ and $x=M\Delta x$ require special treatment because they do not have $x-1$ or $x+1$ neighbours, respectively. A common treatment is to 'wrap' the boundary points, by setting $H(0,t)=H(M\Delta x,t)$ (e.g. Guichard *et al.*, 2003; Sole *et al.*, 2004; Langmead and Sheppard, 2004). In the 1-dimensional case, this effectively creates a circular domain. The approach is viewed as a way of representing an effectively infinite domain, but such a domain obviously has a periodicity (and a

possibly artificial length scale) imposed on it. As already noted, in this study, we take $M\Delta x$ to be the length of the reef (or other habitat element). Thus, we can assume that the end elements are permanently empty. That is,

$$H(0,t) = H(M\Delta x,t) = 1, \text{ and } P_1(0,t) = P_1(M\Delta x,t), \text{ for all } t.$$

Formally, the domain length is $M\Delta x$, while the actual reef length is $(M\text{-}2)\Delta x$. This domain structure allows for the investigation of edge effects, that is, of the transition zone from the boundary into the domain interior. Again, the end-points of the domain may be imagined as locations of disturbance, such as dredging. In such a case, the end zone indicates the spatial impact of the disturbance.

1.4.4 Time-dependence

Figure 1.18 shows a solution for P_2. The run was initialised with $P_2(x,0)=0$ for all x, with transition probabilities arbitrarily set to

$$[N_{12}\ \ N_{21}\ S_{12}\ \ S_{21}] = [0.2\ 0.15\ 0.2\ 0.15] .$$

The domain length is defined by M=20, and the model has been run for 25 time steps. Figure 1.18a shows the spatial distribution of P_2 after the 25 time steps, and Figure 1.18b shows the evolution of P_2 at the midpoint of the domain. Immediately obvious properties of the solution for P_2 are: (i) that it reaches a steady value (of 0.64) in about 10 time steps (Figure 1.18b); and (ii) that it is uniform across most of the domain, but with edge zones about 4 units wide at each end of the 'reef'.

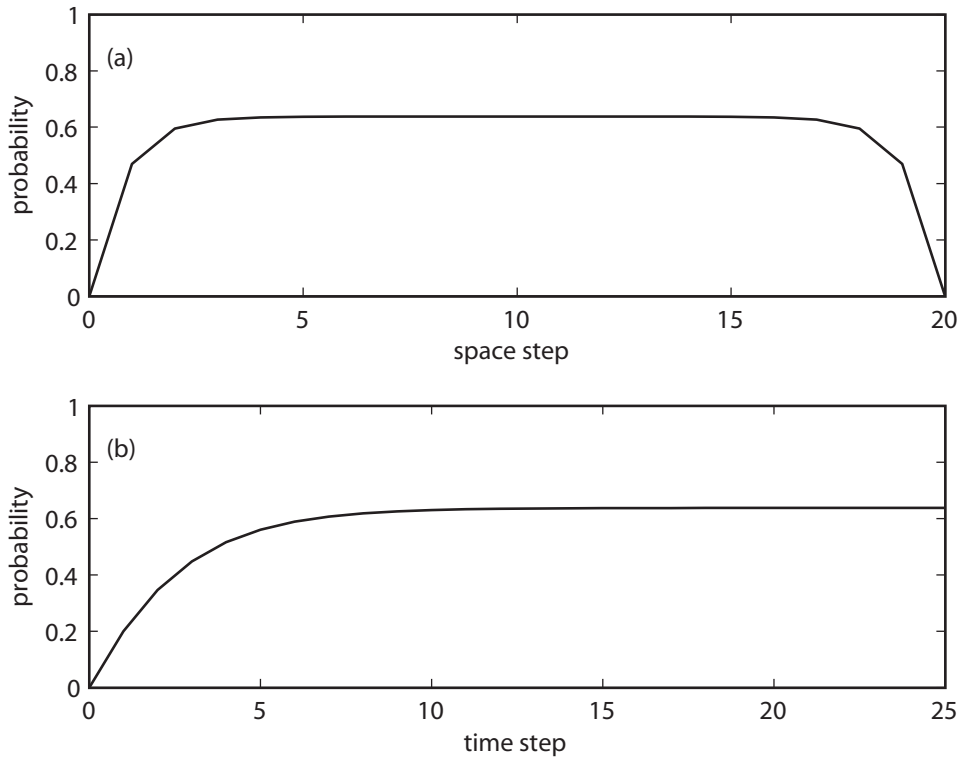

Figure 1.18. The probability P2 calculated from the Markov model on a domain 20 steps wide. (a) Spatial structure after running the model for 25 time steps. (b) Time evolution at space step 10 over 25 time steps.

The steady value of P_2 can be calculated without time-stepping the model. In the internal domain, away from the edge-zones, the solution is spatially uniform, that is, independent of x. Thus, if P represents the steady solution for P_2 then, in (6), each term in P_2 in can be replaced by P, while each P_1 term can be replaced by 1-P. The equation then becomes a simple algebraic quadratic in P:

$$P^2 + bP + c = 0 \text{ with } b = -1 - \frac{S_{12} + S_{21}}{2(N_{21} - N_{12})} \text{ and } c = \frac{S_{12}}{2(N_{21} - N_{12})} \ . \qquad (7)$$

Although (7) is a quadratic, it is relatively straightforward to show that, if S_{12}, $S_{21} \neq 0$, there is only one solution that satisfies $0 \leq P \leq 1$. The special case $N_{12}=N_{21}$ will be discussed in Section 4.
It is important to note that we have been able to derive the solutions in Figure 1.18 without specifying Δx or Δt, neither of which occurs explicitly in (7). Thus, the domain width and the model run-time, and therefore the edge-zones (Figure 1.18a) and set-up time (Figure 1.18b), appear to be arbitrary. However, Δx and Δt are implicit in the specification of the transition probabilities, in ways that will be explored in this and the following section. This section will focus on time, with space examined in Section 4.

The temporal behaviour implied by (6) is relatively easy to understand, because the equation can be readily expressed in finite-difference form in time (e.g. Berec, 2002), that is:

$$\begin{aligned} \frac{P_2(x,t+1) - P_2(x,t)}{\Delta t} = {} & P_1(x,t)\left(\frac{S_{12}}{\Delta t} + \frac{N_{12}}{\Delta t}\left(P_2(x-1,t) + P_2(x+1,t)\right)\right) \\ & - P_2(x,t)\left(\frac{S_{21}}{\Delta t} + \frac{N_{21}}{\Delta t}\left(P_1(x-1,t) + P_1(x+1,t)\right)\right) \end{aligned} \qquad (8)$$

To convert the equation to differential form, the transition probabilities must be re-expressed as transition rates, according to

$$s_{ij} = S_{ij}/\Delta t \quad \text{and} \quad n_{ij} = N_{ij}/\Delta t \ , \qquad (9)$$

in which case, in the limit $\Delta t \rightarrow 0$, (8) becomes

$$\begin{aligned} \frac{\partial P_2}{\partial t}(x,t) = {} & P_1(x,t)\left(s_{12} + n_{12}\left(P_2(x-1,t) + P_2(x+1,t)\right)\right) \\ & - P_2(x,t)\left(s_{21} + n_{21}\left(P_1(x-1,t) + P_1(x+1,t)\right)\right) \end{aligned} \qquad (10)$$

In the form (10), it is clear that the rates s_{ij} and n_{ij} express the fundamental properties of the system, while the probabilities S_{ij} and N_{ij} are dependent on the time step (or discretisation step, or temporal granularity) of the solution scheme, according to (9).

From (10), and using the steady value P of P_2 from (7), it is straightforward to provide a first-order estimate of the initial transition time (from 0 to P) in Figure 1.18b. If the transition time is represented by τ, then the left-hand side of (10) is approximated by the difference $(P\text{-}0)/\tau$ while, on the right-hand side, P_1 is replaced by (1-P_2), and P_2 is estimated by the central value in the transition, 0.5P. The formula for τ is then:

$$\tau = 2P/\left((2-P)(s_{12} + n_{12}P) - P(s_{21} + n_{21}(2-P)\right) \ . \qquad (11)$$

Inserting the appropriate values into (11), with Δt=1, gives τ=6.

There are two apparent paradoxes in (8) that imply a minimum on the observational value of Δt, and a maximum on the value used in the solution scheme. The lower limit on Δt arises because of the assumption that S_{ij} and N_{ij}, or equivalently s_{ij} and n_{ij}, are constants. For many natural systems, this assumption will be approximately correct over a year, which is the time-scale of both the reproductive cycle, that fills habitat gaps, and the weather or storm cycle, that creates them. Observations taken on a shorter time interval will vary on seasonal and shorter time-scales, while those separated by multiple years will be aliased. However, once s_{ij} and n_{ij} are determined, the time-stepping model (8) can be run with an arbitrarily small time step, provided the values of S_{ij} and N_{ij} are appropriately adjusted. Shorter time steps may make the model performance smoother, but will not allow resolution of behaviour at time-scales shorter than that on which S_{ij} and N_{ij} were determined.

In a real application, this restriction to constant transition rates in the model may be artificial and undesirable, and not good *a priori* modelling practice. Fundamentally, the model does not resolve a primary source of variability in the system, that is, the time-scale of storm events. A model that represents individual storms and recolonisation events is not conceptually difficult, but would be considerably more difficult to parameterise than a representation of the annual cycle. Its results would also be harder to characterise. The constant transition rates provide a simpler demonstration of the principles of scaling.

The maximum value on Δt arises because S_{ij} and N_{ij} are probabilities. Not only must each probability be less than 1, but the elements must also satisfy the inequality (4), which may be restated as:

$$\Delta t \le \min\left\{\left(2n_{12} + s_{12}\right)^{-1}, \left(2n_{21} + s_{21}\right)^{-1}\right\} \qquad (12)$$

Thus, although (8) seems to imply that we can choose a large time step to reduce model run-times, a Δt that does not satisfy (12) violates the assumptions of the model. In fact, the model goes numerically unstable for such large time steps.

To summarise the discussion thus far, the transition probabilities are determined from appropriate field observation. (A calibration technique is described in Section 5.) The probabilities and time step allow the transition rates to be determined via (9). Thereafter, the model can be run with a different time step, if desired, so long as new values of S_{ij} and N_{ij} are calculated by (9), and the time step satisfies (12). However, S_{ij} and N_{ij} also have a dependence on the space step that has been ignored in this section by limiting consideration to the central domain away from the end zones. The spatial dependence will be considered in the following section.

1.4.5 Spatial structure

Properties of the difference equation

As we have already noted, there are two spatial scales imposed on the model. The first is the size of the domain, which has physical manifestation in the spatial extent of the habitat being studied. The second scale is the space step, which represents both the spatial resolvability of the domain and, by assumption in (5) and (6), the extent of influence of a single point in a single time step. At this stage, the space step appears to be arbitrary. Finally, there is an inherent scale in the model, which appeared in the form of the edge-zone seen in Figure 1.18a. In this section, we will concentrate on the steady solution, where P_1 and P_2 are not functions of time (Figure 1.18b).

In a real habitat survey, the finest scale of observation is an individual plant or gap. Unfortunately, from a mathematical perspective, plants are not uniform in size, especially when, as in a presence-absence model, all species are classified into a single category. Further, in many systems, individual plants are too small, relative to the size of the domain, to be counted discretely. Thus, a habitat survey usually involves gridding up the habitat into elements that may be classified according to the dominant occupancy. Consistent with the one-dimensional approach taken in this paper, we will envisage the survey as a swath along the domain. For marine habitat, such a survey would normally be conducted by a diver or video camera (e.g. Goodsell *et al.*, 2004; Wernberg and Connell, 2008).

A single survey will return estimates of the probability of occurrence of the different types of habitat. For habitat that can be reasonably represented by equations (5) and (6), we know that, in an undisturbed state or long enough after disturbance, the occurrence probabilities are constant away from the edge zones. Thus, single-value estimates of probabilities (that is, with no spatial or temporal variability) are useful and valid for such habitat. However, these estimates, by themselves, are of no use in predicting the space- or time-scales of the response to, or recovery from, disturbance.

The spatially-dependent, steady equation can be expressed in differential form by invoking the relationship:

$$\frac{d^2P_2}{dx^2} \approx \frac{P_2(x-1) - 2P_2(x) + P_2(x+1)}{\Delta x^2} ,$$

to give

$$\begin{aligned} &\left(N_{12} + (N_{21} - N_{12})P_2\right)\Delta x^2 \frac{d^2P_2}{dx^2} \\ &\qquad = \left(S_{12} + S_{21} + 2(N_{21} - N_{12})(1 - P_2)\right)P_2 - S_{12} \end{aligned} \tag{13}$$

However, unlike Δt in the time-dependent, space-independent equation (8), Δx in (13) cannot be easily scaled into the S_{ij} and N_{ij} terms, a consequence of the more complicated relationship between the space step and the transition probabilities.

There is a special case that illustrates the consistency we would be hoping to see in the model formulation. If $N_{12} = N_{21}$, then (13) reduces to

$$N_{12}\Delta x^2 \frac{d^2P_2}{dx^2} = \left(S_{12} + S_{21}\right)P_2 - S_{12} . \tag{14}$$

In this situation, it is apparent that the N_{ij} scale with Δx^2, while the S_{ij} have no dependence on Δx. For example, if Δx is doubled, N_{12} and N_{21} would be quartered (to keep the coefficient of d^2P_2/dx^2 constant), while S_{12} and S_{21} are unchanged. With equality of N_{12} and N_{21}, the full differential equation for P_2, including both time and space dependence, is

$$\frac{\partial P_2}{\partial t} = (1 - P_2)s_{12} - P_2 s_{21} + k\frac{\partial^2 P_2}{\partial x^2} , \tag{15}$$

where

$$k = \Delta x^2 N_{12} / \Delta t , \tag{16}$$

and s_{12}, s_{21} and k are determining parameters for the system, each independent of Δx and Δt.

Thus, away from the edge-zones, in the central region where $\partial P_2/\partial x=0$ (Figure 1.18a), the time-dependence is unaffected by the N_{ij} terms, and therefore by any scaling of these terms with Δx. The steady solution in this case is given by

$$P = \frac{s_{12}}{s_{12} + s_{21}} = \frac{S_{12}}{S_{12} + S_{21}}, \qquad (17)$$

which is independent of both Δx and Δt, and is the same as the spatially uniform solution to (14). Finally, ignoring the constant S_{12} term, (14) indicates an exponential spatial scale given by

$$L = \Delta x \left(\frac{N_{12}}{S_{12} + S_{21}} \right)^{1/2} = \left(\frac{k}{s_{12} + s_{21}} \right)^{1/2},$$

which is is the scale of the transition zones at the edge of the domain (Figure 1.18a), valid when $N_{12} = N_{21}$.

As an aside, we may note here that k defined in (16) is a diffusion coefficient and (15), the differential form of the linearised equation for P_2, is effectively a reaction-diffusion equation, reminiscent of the form used to represent animal movement in spatial extensions of the predator-prey model (e.g. Durrett and Levin, 1994). While it is tempting to view the spread of propagules, for instance, as a diffusive process, this would need to be developed through equations for the population numbers (as in the predator-prey models), not the equations for probability.

The special case of $N_{12} = N_{21}$ illustrates several desirable features of a model:

1. the relationship of the model parameters to the spatial and temporal discretisation is explicitly defined;

2. the inherent spatial and temporal scales of the system dynamics (in this case represented by the recovery time scale and the edge-zone space scale) are preserved when the model discretisation is changed;

3. the overall structure of the solution (for example, as represented in space and time in Figure 1.18) is maintained when the discretisation is changed.

In the fully nonlinear model (with $N_{12} \neq N_{21}$), it is difficult to maintain all of these properties. For example, if the N_{ij} are scaled differently from the S_{ij}, then the solution for the steady value of P_2 is likely to change – see (7). This apparent contradiction raises fundamental issues about the formulation of the models that will be pursued below.

Point vs cell probabilities

In the stochastic form of a cellular automata model, the state of the habitat is usually assumed to be uniform across a grid cell (e.g. Balzer *et al.*, 1998; Berec, 2002). In other words, the habitat, or habitat probability, at a central point of the cell can be considered representative of the habitat out to $0.5\Delta x$ on either side of the point. However, this is not strictly compatible with the Markov form of the model, which represents the probability at a point.

In observational terms, a point is defined by the resolution or pixel scale, that is, the minimum size of an element (plant or gap) that is resolved by the observation technique. In a sense, this is a third spatial scale imposed on the system, in addition to the domain size and the space step. Thus, an observation made at a point should give the habitat state at that point, at the resolution of the observations. For compatibility with the Markov form of the model, it should not be an average of the state across the grid scale, unless the grid spacing and the observation resolution are the same.

The issue can be demonstrated with a very simplified model. We may imagine that each unit of habitat (a plant or a gap) occupies the same space, Δx, and that the set of observations is initially made in the centre of each unit. The observations will return an unambiguous habitat type 1 or 2 for each cell, and a stochastic or Markov model may be established at this spatial resolution. Now, we can reduce the model resolution by clustering the cells into groups of 3, so that each grid point is now at the centre of a cell of size $3\Delta x$. On this new grid, the probability of habitat type 2 at the original grid point is still P_2, but the probability that the $3\Delta x$ cell, is dominated by, and would therefore be classified as, type 2 habitat is $(3P_2^2-2P_2^3)$. Simple algebra shows that $(3P_2^2-2P_2^3)>P_2$ if $P_2>0.5$.

This pattern continues as the aggregation is increased. That is, the larger the number of original cells that are aggregated to make the new cell, the higher the probability that the cell will be classified as the dominant habitat type. Formally, the cell will be classified as type-2 habitat if more than half of the original cells are of type 2. Thus, the probability that an aggregation of n cells is classified as habitat 2 is given by

$$\text{prob}\{n \text{ cells classified as habitat 2}\} = \sum_{n/2<i\le n} \frac{n!}{(n-i)!i!} P_2^{\,i} (1-P_2)^{n-i} \quad .$$

This effect of reduced resolution, or increased space step, on the probability is illustrated very simply in Figure 1.19, and then more comprehensively in Figure 1.20. Figure 1.19 shows a small segment of habitat with 15 cells, 9 of which are occupied, giving an occupancy frequency of 0.6. Aggregating to 3 cells increases the occupancy frequency to 0.8, while an aggregation to 5 cells results in a frequency of 1.

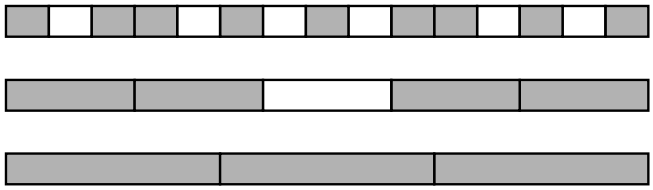

Figure 1.19. A simple demonstration of the effect of aggregation on the occupancy frequency. The top row is a habitat segment of 15 cells, 9 (i.e. 60%) of which are occupied (shaded). In the middle line, the cells are aggregated into triplets, and each triplet classified according to the dominant state. Now, 4 of 5 large cells (i.e. 80%) are occupied. In the third row, the aggregation is to 5 cells, resulting in 100% occupancy.

In Figure 1.20, P_2=0.6, and cells are incremented two at a time (i.e. symmetrically about the central point) to create larger aggregations. The probability asymptotes to 1 as the size increases. For the example in Figure 1.20, an aggregation of 99 elements leads to a probability for type 2 of 0.978, and at 199 elements it is 0.998. Thus, in situations where there are large numbers of elements per cell (typically, areas of habitat made up of elements that are much smaller than the domain size), the model, or the observations, lose their discriminatory ability and return a probability for the dominant habitat type that is effectively 1 in each cell.

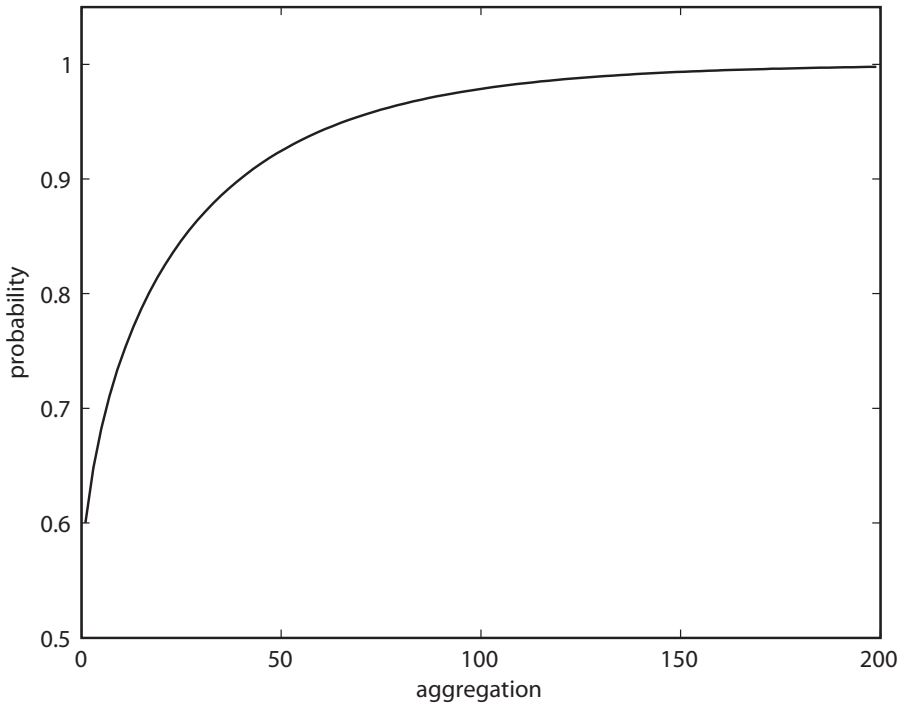

Figure 1.20. The effect of cell aggregation on the probability of occurrence P_2 of habitat type 2. The probability is set at 0.6 for a single cell.

It is important to reiterate that the habitat probability at the central point remains defined by the single element in which it sits. This is the situation described by the Markov model. The simplest demonstration of this is the special case with $N_{12}=N_{21}$, described by (14) and (15). Here, the steady probability (17) is independent of the space step, consistent with the point description, but not a cell description, of the domain.

Of course, a new version of the model may be set up, in which an aggregation of the cells becomes the new spatial element. We would expect such a model, if it properly represents the system, to have the same recovery time-scale, and end-zone size, as the original model. However, the steady probability would be different. Such a model would obviously need all of its transition rates recalibrated. The recalibration is required because, as cells are aggregated, the definition of neighbours, and neighbour interactions, changes. Cells that were previously neighbours may be aggregated into a larger single cell, and interactions that were previously between neighbours become internalised to the larger cell. With aggregation, the N_{ij} terms decrease in magnitude, while the S_{ij} values increase.

From the perspective of the modeller, if the spatial resolution (Δx) changes, then the model must be distinguished either as a point model or a cell model. In the former case, the specified transition probabilities, N_{ij} and S_{ij}, change with the resolution while, in the latter, the occupancy probabilities (P_1 and P_2) must change as well. The technique for recalibrating the model will be described in Section 5.

Patch scales

Patch scale is one of the more easily observable and frequently reported parameters from field studies of habitat. The size of an individual patch is defined by the number of contiguous elements that have the same habitat type. Patch sizes derived from observation are routinely plotted against frequency of occurrence (e.g. Wootton, 2001a; Pascual and Guichard, 2005). As noted in Section 1, patch-size distribution is regarded as a definitive feature of a habitat. It is an observation that models ought to reproduce.

In the present model, where the probability of occurrence of a particular habitat becomes constant away from the habitat edges, the probability that a single patch has size $n\Delta x$ is given by:

$$\text{prob}\{\text{ patch size}=n\Delta x\} = (1-P_2)^2 P_2^{\,n} \quad .$$

While this relationship is obviously a power-law, it is different from the 'critical' power-law distribution described in Section 1 (e.g. Pascual and Guichard, 2005), in which the probability varies as a power of the patch size (that is, $n\Delta x$) itself.

Figure 1.21 shows a frequency distribution plot for patch sizes, plotted on log-linear axes. The curves were derived using a Monte Carlo approach. That is, a habitat domain of 900 elements was randomly generated 1000 times with P_2=0.6. The patch sizes were counted, and averaged over the 1000 repetitions. The left-hand curve on Figure 1.21 shows the number of occurrences of patches of different length, ranging from an average 130 occurrences of single-element patches to 1.3 occurrences for a patch of length 10 cells. The distribution has a power-law distribution described by

$$\text{frequency}\{\text{patches of length } n\Delta x\} = ab^n \qquad (18)$$

where, empirically, a=0.24, and b=0.60.

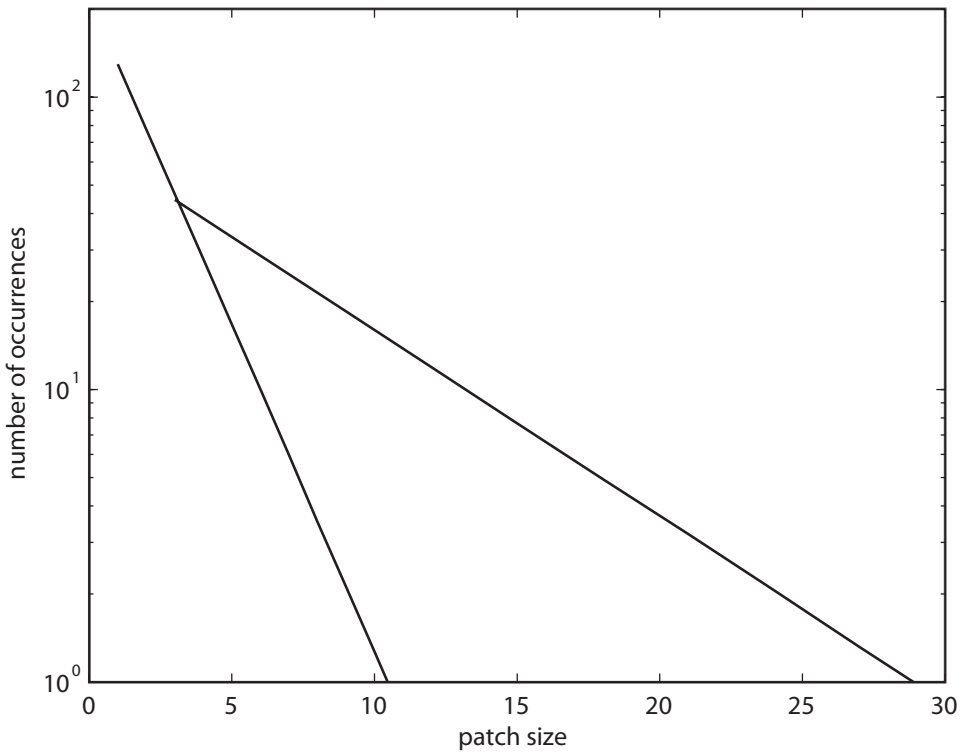

Figure 1.21. The number of occurrences of patches of increasing size for type-2 habitat. The left-hand curve is for a domain 900 cells wide, with P_2=0.6. The patch size is expressed in numbers of cells. The right-hand curve shows the effect of reduction in resolution caused by aggregating into 3-cell elements.

The right-hand curve in Figure 1.21 shows the effect of aggregating into 3 cells. In this case, the new probability for type-2 habitat is ($3P_2^2$-$2P_2^3$), which, for P_2=0.6, takes a value 0.68. The horizontal axis in Figure 1.19 is expressed in original cell units so that, for the second curve, the first value is at 3, and subsequent points are plotted at increments of 3. That is, the length unit for the two curves on the plot is the same. It is immediately obvious that, even though the new curve obeys a power-law of the form (18), it predicts patch sizes considerably larger than in the case of the single-cell increments. The expected value of the patch length is 2.5 cells for the single-cell case, and 8.5 for the triple cells. Clearly, the patch-size distribution is dependent on the sampling scale.

1.4.6 Discussion

The standard cellular automata formulation reduces habitat interactions to just two levels: global, represented by the S_{ij} terms, and nearest neighbour, represented by the N_{ij} terms (Balzer *et al.*, 1998). There are many conceptual complications with such an approach, and these begin to become apparent when discretisation scales are changed, as discussed in the previous two sections. The role and robustness of the interactions, and their implications for scale, will be further discussed in the present section.

The present study has considered the model domain to be an isolated stand of habitat, envisaged in the marine context as an individual reef. As discussed in Section 2, the imposition of 'open' boundaries

appears less common in cellular automata modelling than the use of 'wrapped' boundaries, that are considered to represent effectively infinite domains. Wrapped boundary conditions may be appropriate for very large stands of habitat, but must be approached with caution for two reasons. Firstly, the wrapped domain is not in fact infinite, but periodic. In this case, the domain size is an artificially imposed length scale that may cause the system to be misrepresented in the model. Secondly, wrapped boundary conditions will exclude the presence of end zones (Figure 1.18a), which may be significant both as real habitat transitions and, as discussed throughout this study, as indicators of inherent system properties.

The discretisation (or granularity) of the spatial and temporal domain are imposed scales, usually determined by the pragmatics of an observational program. For example, in a diver survey of the kelp forests described in Section 1, the diver will swim a defined transect, recording the habitat type. The temporal discretisation will be defined by the frequency of surveys, which may change over the course of an experiment. The spatial discretisation will be decided in the survey planning. Typically, a 1m-wide transect will be divided into observational units of order 1 m in length (e.g. Goodsell *et al.*, 2004; Wernberg and Connell, 2008). The diver could record a point observation, such as the habitat type at the centre of each observation square, but more often assesses the dominant habitat structure or type across the whole square.

The spatial and temporal transition scales evident in the model results of Figure 1.18a and b are inherent, or natural, scales of the system. In Figure 1.18b, the temporal transition is well resolved by the discretisation, and the curve progresses smoothly from 0 to the steady value of just over 0.6. In Figure 1.18a, the spatial transition is less-well resolved, and the curve is distinguishable as a set of straight-line segments. Clearly, if the space step had been chosen as, say, 5 units instead of 1, the transition would be poorly represented. The same conclusion also applies to observations: if the resolution of the measurements is too coarse, the natural scales will be distorted or obscured.

The straight-line segments in Figure 1.18a are interpolations between point values, which is appropriate for a continuous function like the probability. By contrast, Figure 1.22 shows instantaneous output from the stochastic model on the same domain, interpreted in the two ways discussed in Section 4. Figure 1.22a shows values of the habitat type, H, at each of the model points. The plot could equally represent results from an observation program. The dotted line on Figure 1.22a is a linear interpolation between data points, drawn for the sake of demonstration. However, since H is discrete, taking values of only 1 or 2 in both model and observations, the interpolation has no real meaning. It is important to reiterate that, if Figure 1.22a were based on observations, each individual data value is representative of the observation window, which may range from a single point up to the whole data interval (Δx), as discussed above. Figure 1.22b is the 'usual' interpretation of habitat data (e.g. Balzer *et al.*, 1998; Berec, 2002; Goodsell *et al.*, 2004; Wernberg and Connell, 2008)), in which the point values in Figure 1.22a are assumed to apply across the data interval, in this case out to $0.5\Delta x$ on either side of the central point.

If the time-interval varies between surveys, or the spatial resolution of the observations is changed from one survey to the next, then this must be accounted for using the theory described in Sections 3 and 4. Similarly, if surveys from different locations are compared, the results must be standardised with respect to temporal and spatial resolution. Further, if a model is to be calibrated from field results, any difference in the resolution of the model and measurements must be accounted for. Model calibration, or recalibration to adjust to new resolution, is done with the stochastic (as opposed to the Markov) model, and is described below.

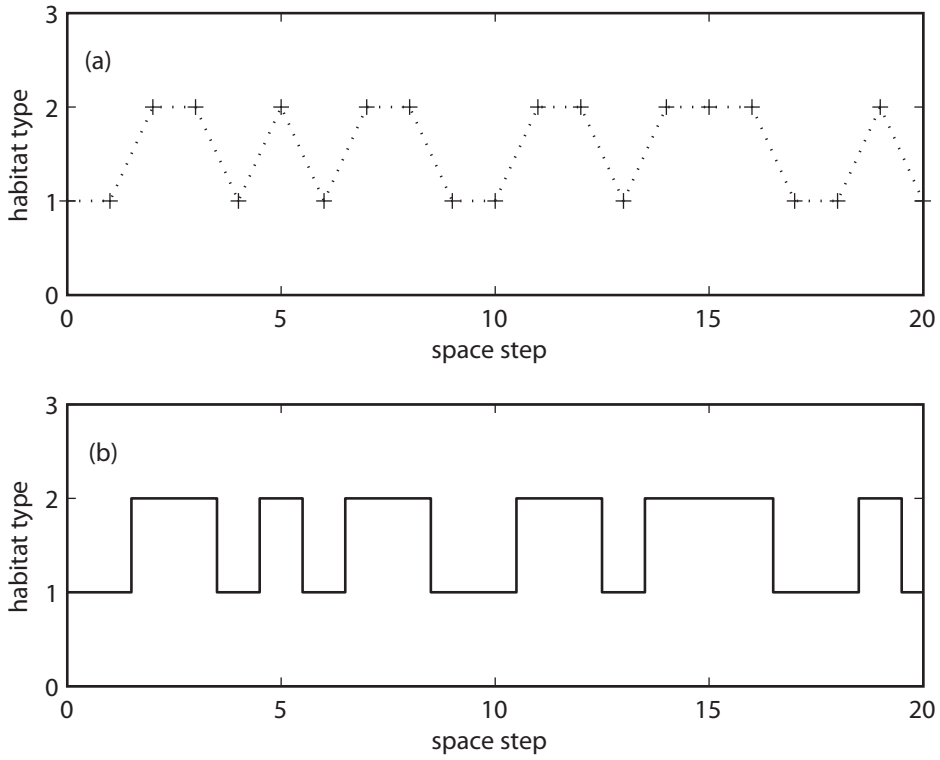

Figure 1.22.: Instantaneous output from the stochastic model: (a) values of the habitat function *H* across the domain, with the dotted line a linear interpolation between the point values; (b) the same data, but with each point value of *H* taken to be representative over a full Δx interval.

The frequency distribution of patch scale is a high-level descriptor of habitat. We have seen (Figure 1.21) that even this measure is a function of the spatial resolution. It must be adjusted if results from different surveys, or models, are compared. However, the frequency distribution is a function only of the probability P_2, and not of the specific values of the transition probabilities. Similarity of frequency distributions across sites does not mean that the system dynamics (as represented by the S_{ij} and N_{ij}) are the same. By contrast, the 'recovery scales' of the habitat depend critically on the S_{ij} and N_{ij} values. These are the inherent scales of the system, that should be preserved when the resolution is changed. They are the scales with which environmental managers are most likely to be concerned.

Recalibration of the model, that is, calculation of the new S_{ij} and N_{ij} values for changed spatial resolution, is relatively straightforward. For example, for a 3-cell aggregation, that is, a 3-fold increase in Δx, the original 1-cell stochastic model is run for many time steps. After the run, the cells are aggregated into triplets at each time step. For the new S_{12}, all of the (aggregated) type-1 cells that have only type-1 neighbours are counted at a given time step. The proportion of these that become type 2 over the subsequent time step is an estimator for S_{12}. N_{12} is then estimated by looking at the type-1 points that have type-2 neighbours, taking into account that some of these will change through global influence, at a rate that has already been determined. S_{21} and N_{21} are estimated in the same way.

This same approach may be adopted to provide estimates of the transition probabilities from a field investigation. Success of the technique requires sufficient numbers of spatial elements and sufficient time steps to ensure that the transition probabilities are statistically meaningful. Historical, or specifically designed, field programs with large numbers of observations of individual transitions are

rare, with exceptions such as Dunstan and Johnson (2004) and Langmead and Sheppard (2004) noted in Section 1. Alternatively, the parameters can be specified by educated guesswork, and tested in the model to see if it reproduces observations (e.g. Hilker *et al.*, 2006).

The present model is a system of effectively one variable (P_2), and four constant parameters. It is not at all obvious that such a simple model has the capacity to accurately reproduce the recovery scales for a real habitat system. From both practical and theoretical perspectives, the constant-coefficient model is limited by its inability to resolve individual disturbance and reseeding events. Further, the representation of habitat as a discrete function is not entirely realistic. Even in the case of only two habitat types, a finite cell or pixel that is larger than an individual plant may obviously contain a proportion of each type.

However, as we have seen, even with the present system there are subtleties of scale and behaviour that result principally from the nonlinearity of the equation. Further complication would remove much of the attraction of the model. Grimm *et al.,* (2005) highlight the representation of processes in a model as another resolution issue (see also Grimm, 1999). Durrett and Levin (1994) open with the sentence: 'One of the fundamental issues in the modeling of any system is the choice of level of detail'. In the context of 'pattern-oriented modelling', Grimm *et al.,* (2005) propose that the model complication should be tailored to the explanations required of the model. In the present context, the constant-coefficient model has served to demonstrate the care that must be taken in assigning and interpreting scales in the simplest of cellular automata models. There is no shortage of refinements that can be added to take the approach to another level of difficulty.

1.4.7 Acknowledgements

This study was supported by the Western Australian Marine Science Institute. I thank Russ Babcock and Phillip England for discussion that led to the manuscript, and Russ Babcock and Piers Dunstan for their comments on the manuscript. I also thank two anonymous reviewers, whose comments undoubtedly improved the clarity of the text.

1.4.8 References

Balzter H, Braun PW, Kohler W (1998) Cellular automata models for vegetation dynamics. Ecol Model 107:113–125

Berec L (2002) Techniques of spatially explicit individual-based models: construction, simulation, and mean-field analysis. Ecol Model 150:55–81

Bolker BM, Pacala SW, Neuhauser C (2003) Spatial dynamics in model plant communities: what do we really know? Am Nat 162:135–148

Colasanti RL, Hunt R, Watrud L (2007) A simple cellular automaton model for high-level vegetation dynamics. Ecol Model 203:363–374

Dunstan PK, Johnson CR (2005) Predicting global dynamics from local interactions: individual-based models predict complex features of marine epibenthic communities. Ecol Model 186:221–233

Durrett R, Levin SA (1994) The importance of being discrete (and spatial). Theor Popul Biol 46:363–394

Durrett R, Levin SA (1998) Spatial aspects of interspecific competition. Theor Popul Biol 53:30–43

Fonseca MS, Whitfield PE, Kenworthy WJ, Colby DR, Julius BE (2004) Use of two spatially explicit models to determine the effect of injury geometry on natural resource recovery. Aquat Conserv 14:281–298

Goodsell PJ, Fowler-Walker MJ, Gillanders BM, Connell SD (2004) Variations in the configuration of algae in subtidal forests: implications for invertebrate assemblages. Austral Ecol 29:350–7

Grimm V (1999) Ten years of individual-based modelling in ecology: what have we learned, and what could we learn in the future? Ecol Model 115:129–148

Grimm V, Revilla E, Berger U, Jeltsch, F, Mooij WM, Railsback SF, *et al*. (2005) Pattern-oriented modeling of agent-based complex systems: lessons from ecology. Science 310:987–991

Guichard F, Halpin PM, Allison GW, Lubchenco J, Menge BA (2003) Mussel disturbance dynamics: signatures of oceanographic forcing from local interactions. Am Nat 161:889–904

Hemer MA, Church JA, Hunter JR (2010) Variability and trends in the wave climate of the Southern Hemisphere. Int J Climatol 30:475–491

Hilker FM, Hinsch M, Poethke HJ (2006) Parameterizing, evaluating and comparing metapopulation models with data from individual-based simulations. Ecol Model 199:476–485

Keeling M J, Mezic I, Hendry RJ, McGlade J, Rand DA (1997) Characteristic length scales of spatial models in ecology via fluctuation analysis. Philos T R Soc Lon B 352:1589–1601

Langmead O, Sheppard C (2004) Coral reef community dynamics and disturbance:
a simulation model. Ecol Model 175:271–290

Mathey A-H, Krcmar E, Dragicevic S, Vertinsky I (2008) An object-oriented cellular automata model for forest planning problems. Ecol Model 212:359–371

Neuhauser C, Pacala SW (1999) An explicitly spatial version of the Lotka-Volterra model with interspecific competition. Ann Appl Probab 9:1226–1259

Pascual M, Levin SA (1999) From individuals to population densities: searching for the intermediate scale of nontrivial determinism. Ecology 80:2225–2236

Pascual M, Roy M, Franc A (2002) Simple temporal models for ecological systems with complex spatial patterns. Ecol Let 4:412–9.

Pascual M, Guichard F (2005) Criticality and disturbance in spatial ecological systems. Trends Ecol Evol 20:88–95

Pawlowski CW, McCord C (2009) A Markov model for assessing ecological stability properties. Ecol Model 220:86–95

Phillips JC (2001) Marine macroalgal biodiversity hotspots: why is there high species richness and endemism in southern Australian marine benthic flora? Biodiv Conserv 10:1555–7

Rand DA, Wilson HB (1995) Using spatio-temporal chaos and intermediate scale determinism in artificial ecologies to quantify spatially extended systems. P Roy Soc Lond B Bio 259:111–7

Rietkerk M, Dekker SC, Ruiter PC, van de Koppel J (2004) Self-organized patchiness and catastrophic shifts in ecosystems. Science 305:1926–9

Schroder B, Seppelt R (2006) Analysis of pattern–process interactions based on landscape models—overview, general concepts, and methodological issues. Ecol Model 199:505–516

Sole RV, Manrubia SC, Benton M, Kauffman S, Bak P (1999) Criticality and scaling in evolutionary ecology. Trends Ecol Evol 14:156–160

Sole RV, Alonso D, Saldana J (2004) Habitat fragmentation and biodiversity collapse in neutral communities. Ecol Compl 1:65–75

Syphard AD, Clarke KC, Franklin J (2005) Using a cellular automaton model to forecast the effects of urban growth on habitat pattern in southern California. Ecol Compl 2:185–203

Toohey BD, Kendrick GA, Harvey ES (2007) Disturbance and reef topography maintain high local diversity in *Ecklonia radiata* kelp forests. Oikos 116:1618–1630

Wernberg T, Connell SD (2008) Physical disturbance and subtidal habitat structure on open rocky coasts: effects of wave exposure, extent and intensity. J Sea Res 59:237–248

Wernberg T, Kendrick GA, Phillips JC (2003) Regional differences in kelp-associated algal assemblages on temperate limestone reefs in southwestern Australia. Divers Distrib 9:427–441.

Wernberg T, Vanderklift MA, How J, Lavery PS (2006) Export of detached macroalgae from reefs to adjacent seagrass beds. Oecologia 147:692–701

Wheatley M, Johnson C (2009) Factors limiting our understanding of ecological scale. Ecol Compl 6:150–9

Wootton JT (2001) Local interactions predict large-scale pattern in empirically derived cellular automata. Nature 413, 841–4

Wootton JT (2001) Prediction in complex communities: analysis of empirically derived Markov models. Ecol 82:580–598

2. AN ASSESSMENT OF ECOSYSTEM PROCESSES WITH PARTICULAR RELEVANCE TO CONTRASTING FISHED AND NON-FISHED AREAS

Mat A Vanderklift, Russ C Babcock, Fiona Graham, John K Keesing

CSIRO Marine and Atmospheric Research

2.1 Introduction

Spatial management tools – such as sanctuary zones – are increasingly used in conservation and fisheries management to protect species and populations from over-exploitation. However, the utility of these tools relies on information about how well they are achieving their goals (Levin *et al.*, 2009). The ability of reserves to meet the common goal of higher density and biomass of valued fish and invertebrates is likely to rely in part on the size of the area protected from fishing. Small reserves might be less likely to meet these objectives for some species, because there is a greater likelihood of individuals moving beyond the boundaries of the reserve, where they then face greater susceptibility to fishing mortality. Small reserves might therefore be effective only for species that tend to remain within a small home range. However, while some form of positive relationship between reserve effectiveness and reserve size is theoretically likely, there is very little empirical data to test whether this does in fact occur (Halpern 2003).

Research in WAMSI project 1.2 (Output 2) has been directed at contrasting patterns of commonly-used indicators of resource condition between sanctuary zones (SZs) and adjacent fished areas. The method taken has been to contrast six Sanctuary Zones (fully protected from all forms of fishing) with adjacent fished areas on the temperate west coast. The reserves selected for inclusion are all within the same biogeographic region, and so share similar ecosystems, but vary in size. A focus was on contrasting measurements between large and small SZs and adjacent fished areas. We chose to survey three relatively large SZs (>100 ha: Kingston Reef, Fishermans Islands and Boullanger Island) and three relatively small SZs (<30 ha: The Lumps, Boyinaboat, Parker Point). The indicators selected for inclusion are all commonly-used indicators of abundance and biomass.

2.2 Methods

2.2.1 Study Area

Three regions on the temperate west Australian coast were surveyed as part of this study, Marmion, Rottnest Island and Jurien Bay. These regions share similar ecosystem characteristics and are exposed to varying degrees of fishing pressure, both recreational and commercial, which is managed spatially by the implementation of marine parks and sanctuary zones. (Other regulations, such as bag limits and length restrictions also exist, but are the same in each region.)

Marmion Marine Park is situated 20km north of Perth and is characterised by medium to high relief limestone reefs interspersed with bare sand and seagrass. Surveys were conducted at six sites within

the Marmion Marine Park contrasting the Lumps and Boyinaboat Sanctuary Zones with adjacent fished areas (Figure 2.1).

Rottnest Island (Figure 2.2) is approximately 20 km from the mainland metropolitan coast and dominated by complex limestone and diverse macroalgal communities. Study sites located within Kingston Reefs Sanctuary Zone and Parker Point Sanctuary Zone were compared with sites in general use zones.

Similarly Jurien Bay Marine Park encompasses extensive limestone reefs dominated by macroalgal communities and varying in exposure to wave action, and is situated approximately 200 km north of Perth. Surveys were conducted within Fisherman Islands and Boullanger Island sanctuary zones as well as areas adjacent to these that are open to fishing (Figure 2.3).

2.2.2 Survey Design

Within each region, sites were selected based on their management status and habitat types. Sampling was stratified within reef (Table 2.1) and seagrass habitats (Table 2.2) and within fully-protected (Sanctuary Zones) and fished (General Use Zones or Recreation Zones) locations. Sanctuary zones encompassed ages from 5 to 19 years at the time of survey, and sizes from <10 ha to >1,000 ha (Table 2.3).

Figure 2.1. Location of sites at Marmion (Marmion, Western Australia, 20/05/2009, Google Earth Digital Globe)

Figure 2.2. Location of sites at Rottnest Island (Rottnest Island, Western Australia, 20/05/2009, Google Earth Digital Globe)

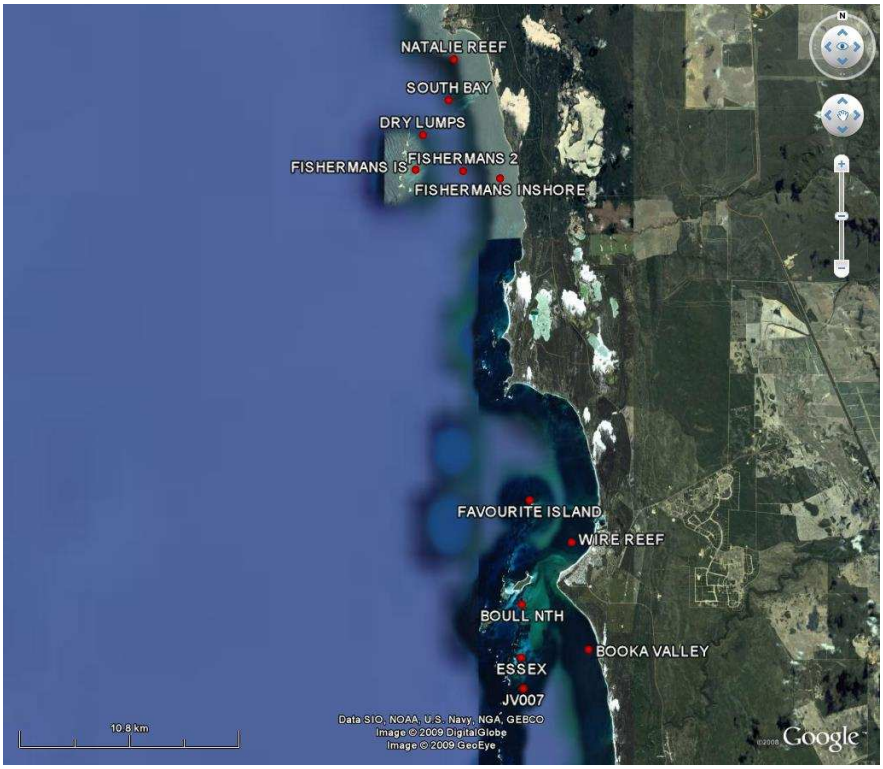

Figure 2.3. Location of sites at Jurien Bay (Jurien Bay, Western Australia, 20/05/2009, Google Earth Digital Globe)

Table 2.1. Reef sites at Jurien Bay, Marmion and Rottnest Island

Region	Site	Zone	Mean Depth	Min Depth	Max Depth	Latitude	Longitude
Jurien Bay	Booka Valley	Boullanger Island Sanctuary Zone	4.5	4.5	4.5	30°20'44.64"S	115° 2'14.46"E
Jurien Bay	Essex Rocks	Boullanger Island Sanctuary Zone	3.5	3.0	4.0	30°20'56.02"S	115° 0'10.93"E
Jurien Bay	Boull Nth	Boullanger Island Sanctuary Zone	4	4	4	30°19'31.68"S	115° 0'12.42"E
Jurien Bay	JV007	General Use Zone	5.5	4.7	7.0	30°21'45.06"S	115° 0'15.13"E
Jurien Bay	Favourite Island	General Use Zone	5.0	5.0	5.0	30°17'0.12"S	115° 0'8.94"E
Jurien Bay	Wire Reef	General Use Zone	8.0	5.0	8.6	30°17'52.92"S	115° 1'44.22"E
Jurien Bay	Fishermans 2	Fisherman Islands Sanctuary Zone	6.7	6.4	7.0	30° 7'58.50"S	114°57'10.32"E
Jurien Bay	Fishermans Inshore	Fisherman Islands Sanctuary Zone	3.6	3.6	3.6	30° 8'16.79"S	114°59'32.36"E
Jurien Bay	Fishermans Island	Fisherman Islands Sanctuary Zone	4.6	4.3	6.0	30° 8'3.00"S	114°56'57.12"E
Jurien Bay	Dry Lumps	General Use Zone	4.5	4.5	4.6	30° 7'7.80"S	114°57'10.74"E
Jurien Bay	Natalie Reef	General Use Zone	5.9	4.7	7.0	30° 5'7.82"S	114°58'7.49"E
Jurien Bay	South Bay	General Use Zone	4.8	3.5	6.0	30° 6'12.60"S	114°57'57.69"E
Marmion	Boyinaboat	Boyinaboat Sanctuary Zone	4.6	4.2	5.0	31°49'33.06"S	115°43'56.49"E
Marmion	Cow Rock	General Use Zone	3.9	2.8	5.0	31°49'10.59"S	115°43'38.80"E
Marmion	North Lumps	The Lumps Sanctuary Zone	6.2	5.9	6.5	S31°47.219'	E115°42.862'
Marmion	South Lumps	The Lumps Sanctuary Zone	5.1	4.6	5.6	31°47'36.48"S	115°42'59.52"E
Marmion	Whitfords Rock	General Use Zone	5.2	4.6	5.8	31°47'56.46"S	115°43'6.60"E
Marmion	Wreck Rock	General Use Zone	5.6	5.3	5.9	31°48'9.15"S	115°43'2.79"E
Rottnest Island	Kingston Reef 03	Kingston Reefs Sanctuary Zone	7.3	7.0	7.5	31°59'9.24"S	115°33'16.32"E
Rottnest Island	Kingston Reef 07	Kingston Reefs Sanctuary Zone	5.5	5.0	6.0	31°59'17.28"S	115°33'11.40"E
Rottnest Island	Kingston Reef 14	Kingston Reefs Sanctuary Zone	4.9	4.9	4.9	31°59'23.70"S	115°33'29.22"E
Rottnest Island	Kingston Reef 08	Kingston Reefs Sanctuary Zone	7.0	7.0	7.0	31°59'15.18"S	115°33'26.34"E
Rottnest Island	Bickley Point	Recreation Zone	6.8	6.5	7.0	32° 0'53.04"S	115°33'26.28"E
Rottnest Island	Monday Rock 2	Recreation Zone	8.0	8.0	8.0	31°59'10.02"S	115°32'13.32"E
Rottnest Island	Parker Point 1	Recreation Zone	6.0	6.0	6.0	32° 1'14.21"S	115°32'2.36"E
Rottnest Island	Phillip Rock	Recreation Zone	5.5	5.0	6.0	31°59'52.50"S	115°33'43.32"E
Rottnest Island	Pocillopora Reef	Parker Point Sanctuary Zone	3.0	2.0	4.0	32° 1'33.57"S	115°31'45.67"E

Table 2.2. Seagrass sites at Jurien Bay, Marmion and Rottnest Island

Region	Site	Zone	Mean Depth	Min Depth	Max Depth	Latitude	Longitude
Jurien Bay	Booka Valley	Boullanger Island Sanctuary Zone	4.5	4.5	4.5	30°20'44.64"S	115° 2'14.46"E
Jurien Bay	Essex Rocks	Boullanger Island Sanctuary Zone	3.5	3.0	4.0	30°20'56.02"S	115° 0'10.93"E
Jurien Bay	Boull Nth	Boullanger Island Sanctuary Zone	4	4	4	30°19'31.68"S	115° 0'12.42"E
Jurien Bay	JV007	General Use Zone	5.5	4.7	7.0	30°21'45.06"S	115° 0'15.13"E
Jurien Bay	Favourite Island	General Use Zone	5.0	5.0	5.0	30°17'0.12"S	115° 0'8.94"E
Jurien Bay	Wire Reef	General Use Zone	8.0	5.0	8.6	30°17'52.92"S	115° 1'44.22"E
Jurien Bay	Fishermans 2	Fisherman Islands Sanctuary Zone	6.7	6.4	7.0	30° 7'58.50"S	114°57'10.32"E
Jurien Bay	Fishermans Inshore	Fisherman Islands Sanctuary Zone	3.6	3.6	3.6	30° 8'16.79"S	114°59'32.36"E
Jurien Bay	Fishermans Island	Fisherman Islands Sanctuary Zone	4.6	4.3	6.0	30° 8'3.00"S	114°56'57.12"E
Jurien Bay	Dry Lumps	General Use Zone	4.5	4.5	4.6	30° 7'7.80"S	114°57'10.74"E
Jurien Bay	Natalie Reef	General Use Zone	5.9	4.7	7.0	30° 5'7.82"S	114°58'7.49"E
Jurien Bay	South Bay	General Use Zone	4.8	3.5	6.0	30° 6'12.60"S	114°57'57.69"E
Marmion	Boyinaboat	Boyinaboat Sanctuary Zone	4.6	4.2	5.0	31°49'33.06"S	115°43'56.49"E
Marmion	Cow Rock	General Use Zone	3.9	2.8	5.0	31°49'10.59"S	115°43'38.80"E
Marmion	North Lumps	The Lumps Sanctuary Zone	6.2	5.9	6.5	S31°47.219'	E115°42.862'
Marmion	South Lumps	The Lumps Sanctuary Zone	5.1	4.6	5.6	31°47'36.48"S	115°42'59.52"E
Marmion	Whitfords Rock	General Use Zone	5.2	4.6	5.8	31°47'56.46"S	115°43'6.60"E
Marmion	Wreck Rock	General Use Zone	5.6	5.3	5.9	31°48'9.15"S	115°43'2.79"E
Rottnest Island	Parker Point 1	Recreation Zone	6.0	6.0	6.0	32° 1'14.21"S	115°32'2.36"E
Rottnest Island	Pocillopora Reef	Parker Point Sanctuary Zone	3.0	2.0	4.0	32° 1'33.57"S	115°31'45.67"E

Table 2.3. Characteristics of Sanctuary Zones

Region	Sanctuary Zone	Year gazetted	Size (ha)	Month and Year surveyed	Age at time of survey (years)	Proportion of Sanctuary Zone (%)*			
						Intertidal Reef	Subtidal Reef	Seagrass	Sand
Jurien Bay	Boullanger Island	2003	1334	April 2008	5	5	15	25	55
	Fisherman Islands	2003	473	April 2008	5	0	26	74	0
Marmion	Boyinaboat	1999	7.4	January 2007	8	0.5	0.5	66	33
	The Lumps	1999	27.9	January 2007	8	0	69	5	26
Rottnest Island	Kingston Reefs	1988	126 (increased to 164 in 2007)	February 2007	19	2	30	11	57
	Parker Point	1988	5 (increased to 89 in 2007)	February 2007	19	48	39	7	6

* Based on habitat maps sourced from by the Department of Environment and Conservation and Rottnest Island Authority.

2.2.3 Fish Surveys

Fishes were surveyed using underwater visual census (UVC). This involved a lone SCUBA diver swimming along a 25m x 5m belt transect, identifying, counting and estimating the total lengths of all fishes observed within the transect. Three replicate transects were completed at each site and surveys were completed in both reef and seagrass habitats. Larger, more solitary fishes (including important target species as well as ecologically important species, such as terminal phase wrasses) were surveyed over a 50 x 10m belt transect. Length estimates were converted to biomass using standard length-weight relationships obtained from literature and FishBase (http://www.fishbase.org). Where length-weight relationships for specific species could not be obtained we used the values from the most similar shaped fish that were available.

2.2.4 Western Rock Lobster Surveys

The abundance of western rock lobsters (*Panulirus cygnus*) was determined at each site by underwater visual census (UVC). Sites at Jurien Bay were surveyed using three replicate transects of 30 x 10m each. Sites at Rottnest Island and Marmion were surveyed using three replicate transects of 30 x 5m each on reef habitat. Where possible the size and sex of the rock lobster was estimated or measured. Biomass was calculated from length weight data published in Babcock *et al* (2007). Where sex of rock lobster had not been recorded, sex was randomly assigned in order to estimate biomass. To account for the different sizes of transect used, all estimates were standardised to $100m^2$.

2.2.5 Data analysis

The primary aim of the surveys was to determine whether there were differences in the biomass or density of key groups of fish, and western rock lobsters, between Sanctuary Zones (SZ) and adjacent fished areas. An extension of this was to determine whether there were consistent patterns of differences according to size of the SZ. To test these questions, we performed two types of analysis.

First, we used mixed effects ANOVA to test for differences between management zones (fixed effect with two levels: SZ and fished), size of sanctuary (fixed effect with two levels: large >100 ha and small <30 ha), locations (random effect with six levels reflecting the six SZs surveyed), and among sites (random effect). The focus for these analyses was on the interaction between Zone and Size – if large SZs are more effective, we should record higher measurements inside large SZs, but not small SZs.

A second set of analyses was focussed on testing for differences separately for each of the six SZs surveyed. Data was analysed using one-way ANOVA with planned contrasts to test a priori hypotheses about differences between SZs and adjacent fished locations. Analyses were done using the statistical software R.

For both sets of analyses, we performed separate analyses for all fish combined, and separately for targeted species and non-targeted species. For fish surveyed using 25-m transects on reef habitat, we also separately analysed three key trophic guilds: piscivores, herbivores and invertivores.

2.3 Results

2.3.1 Fish

A total of 93 species (7,069 individuals) from 34 families were recorded during the visual census over all three regions. Analyses of all fish combined from the 25 m transects on reef habitat did not yield any statistically significant patterns related to Zone for biomass or density (Table 2.4, Table 2.5, Figure 2.4). Surveys using longer transects yielded higher overall density and biomass of fish in large SZs, but this pattern was not statistically significant (Table 2.8, Table 2.9, Figure 2.6). Surveys from seagrass habitat did not yield patterns in combined fish biomass or density that corresponded to management zones (Table 2.6, Table 2.7, Figure 2.5).

Of the 93 species, 13 were classified as 'targeted' – that is, species that fishers are likely to specifically seek to catch. The remainder were classified 'non-targeted' – however, this also includes species that are likely to be captured as bycatch. For targeted species, there was a pattern of higher biomass inside large SZs on reef habitat from the short transects, and this difference approached statistical significance (Table 2.4, Table 2.5, Figure 2.4). There was a statistically significant interaction between Zone and Size for the biomass of targeted species in seagrass habitat, but the pattern did not conform to that expected (Table 2.6, Table 2.7, Figure 2.5).

For non-targeted species, there were no patterns yielded by analyses of measurements from the short transect on reef habitat, but longer transects did yielded a near-significant interaction between Zone and Size, and the pattern was consistent with that expected (Table 2.4, Table 2.5, Table 2.8, Table 2.9, Figure 2.4, Figure 2.5). There was a statistically significant interaction effect of Zone for the biomass of fish recorded in seagrass habitat, with a greater biomass occurring in SZs (Table 2.5, Figure 2.4).

None of the three trophic guilds analysed yielded statistically significant patterns of higher measurements in large SZs (Table 2.4, Table 2.5).

Table 2.4. Results of analyses testing for differences in biomass of fish from reef habitat among sanctuary zones of different sizes, using measurements from 25-m long transects

Source	df	SS	MS	F	Pval
(a) Reef 25 m all fish combined					
Zone	1	225.13	225.13	0.30	0.615
Size	1	0.00	0.00	0.00	0.999
Location (Size)	4	5783.98	1446.00	2.47	0.093
Zone x Size	1	2290.98	2290.98	3.02	0.157
Zone x Location (Size)	4	3038.94	759.73	1.30	0.319
Site (Zone x Location (Size))	14	8206.98	586.21	1.16	0.331
Residual	52	26241.26	504.64		
(b) Reef 25 m piscivore					
Zone	1	6.23	6.23	1.30	0.318
Size	1	3.59	3.59	0.65	0.465
Location (Size)	4	22.04	5.51	0.75	0.573
Zone x Size	1	2.77	2.77	0.58	0.490
Zone x Location (Size)	4	19.19	4.80	0.65	0.633
Site (Zone x Location (Size))	14	102.55	7.33	4.57	**0.000**
Residual					
(c) Reef 25 m herbivores					
Zone	1	360.64	360.64	0.46	0.534
Size	1	173.04	173.04	0.16	0.713
Location (Size)	4	4441.08	1110.27	1.75	0.196
Zone x Size	1	2133.02	2133.02	2.73	0.174
Zone x Location (Size)	4	3122.25	780.56	1.23	0.343
Site (Zone x Location (Size))	14	8902.11	635.86	1.33	0.225
Residual	52	24930.95	479.44		
(d) Reef 25 m invertevores					
Zone	1	2.22	2.22	0.11	0.759
Size	1	127.47	127.47	1.41	0.301
Location (Size)	4	361.62	90.40	1.70	0.206
Zone x Size	1	11.18	11.18	0.54	0.502
Zone x Location (Size)	4	82.13	20.53	0.39	0.815
Site (Zone x Location (Size))	14	744.78	53.20	1.39	0.193
Residual	52	1993.13	38.33		
(e) Reef 25 m targeted species					
Zone	1	4.54	4.54	9.80	**0.035**
Size	1	47.90	47.90	3.58	0.132
Location (Size)	4	53.59	13.40	3.21	**0.046**
Zone x Size	1	2.33	2.33	5.03	0.088
Zone x Location (Size)	4	1.85	0.46	0.11	0.977
Site (Zone x Location (Size))	14	58.35	4.17	2.48	**0.009**
Residual	52	87.30	1.68		

(f) Reef 25 m non-targeted species					
Zone	1	165.74	165.74	0.22	0.666
Size	1	47.47	47.47	0.04	0.855
Location (Size)	4	5014.63	1253.66	2.09	0.137
Zone x Size	1	2147.19	2147.19	2.81	0.169
Zone x Location (Size)	4	3057.96	764.49	1.27	0.327
Site (Zone x Location (Size))	14	8410.20	600.73	1.18	0.318
Residual	52	26473.04	509.10		

Table 2.5. Results of analyses testing for differences in density of fish from reef habitat with size of sanctuary zone, using measurements from 25-m long transects

Source	df	SS	MS	F	Pval
(a) Reef 25 m all fish combined					
Zone	1	108.51	108.51	0.05	0.836
Size	1	11445.00	11445.00	3.75	0.125
Location (Size)	4	12207.05	3051.76	0.69	0.613
Zone x Size	1	3922.99	3922.99	1.76	0.255
Zone x Location (Size)	4	8910.16	2227.54	0.50	0.736
Site (Zone x Location (Size))	14	62233.00	4445.21	2.94	**0.002**
Residual	52	78684.00	1513.15		
(b) Reef 25 m piscivore					
Zone	1	216.67	216.67	1.35	0.309
Size	1	102.31	102.31	0.63	0.472
Location (Size)	4	650.26	162.56	0.60	0.668
Zone x Size	1	96.30	96.30	0.60	0.481
Zone x Location (Size)	4	640.48	160.12	0.59	0.674
Site (Zone x Location (Size))	14	3785.11	270.37	49.74	**0.000**
Residual	52	282.67	5.44		
(c) Reef 25 m herbivores					
Zone	1	492.51	492.51	0.56	0.496
Size	1	79.34	79.34	0.06	0.817
Location (Size)	4	5183.84	1295.96	2.07	0.140
Zone x Size	1	332.32	332.32	0.38	0.572
Zone x Location (Size)	4	3516.86	879.22	1.40	0.284
Site (Zone x Location (Size))	14	8780.61	627.19	1.47	0.155
Residual	52	22162.00	426.19		
(d) Reef 25 m invertevores					
Zone	1	8.67	8.67	0.01	0.927
Size	1	7736.80	7736.80	1.65	0.268
Location (Size)	4	18723.63	4680.91	2.19	0.123
Zone x Size	1	2939.50	2939.50	3.21	0.147
Zone x Location (Size)	4	3658.63	914.66	0.43	0.786
Site (Zone x Location (Size))	14	29929.28	2137.81	2.05	**0.032**
Residual	52	54316.67	1044.55		

Source	df	SS	MS	F	Pval
(e) Reef 25 m targeted species					
Zone	1	133.38	133.38	0.43	0.548
Size	1	6769.80	6769.80	4.33	0.106
Location (Size)	4	6252.29	1563.07	3.81	**0.027**
Zone x Size	1	10.78	10.78	0.03	0.861
Zone x Location (Size)	4	1240.86	310.22	0.76	0.571
Site (Zone x Location (Size))	14	5749.50	410.68	1.22	0.288
Residual	52	17469.33	335.95		
(f) Reef 25 m non-targeted species					
Zone	1	1.28	1.28	0.00	0.983
Size	1	610.21	610.21	0.65	0.464
Location (Size)	4	3728.52	932.13	0.30	0.873
Zone x Size	1	3522.44	3522.44	1.39	0.304
Zone x Location (Size)	4	10160.19	2540.05	0.82	0.534
Site (Zone x Location (Size))	14	43426.83	3101.92	2.66	**0.005**
Residual	52	60644.00	1166.23		

Table 2.6. Results of analyses testing for differences in biomass of fish from seagrass habitat among sanctuary zones of different sizes, using measurements from 25-m long transects

Source	df	SS	MS	F	Pval
(a) Seagrass 25 m all fish combined					
Zone	1	864.91	864.91	7.41	0.224
Size	1	5849.08	5849.08	149.80	0.052
Location (Size)	1	39.05	39.05	0.03	0.874
Zone x Size	1	6.25	6.25	0.05	0.855
Zone x Location (Size)	1	116.74	116.74	0.08	0.784
Site (Zone x Location (Size))	10	14738.25	1473.82	2.07	0.060
Residual	31	22099.22	712.88		
(b) Seagrass 25 m targeted species					
Zone	1	0.23	0.23	42.56	**0.007**
Size	1	6.30	6.30	135.45	**0.001**
Location (Size)	3	0.14	0.05	0.02	0.996
Zone x Size	1	0.61	0.61	113.22	**0.002**
Zone x Location (Size)	3	0.02	0.01	0.00	1.000
Site (Zone x Location (Size))	6	14.00	2.33	5.22	**0.001**
Residual	31	13.85	0.45		
(c) Seagrass 25 m non-targeted species					
Zone	1	1.37	1.37	9.45	0.054
Size	1	1.66	1.66	4.94	0.113
Location (Size)	3	1.01	0.34	0.21	0.888
Zone x Size	1	0.03	0.03	0.19	0.694
Zone x Location (Size)	3	0.44	0.15	0.09	0.963

Site (Zone x Location (Size))	6	9.74	1.62	3.27	**0.013**
Residual	31	15.42	0.50		

Table 2.7. Results of analyses testing for differences in density of fish from seagrass habitat with size of sanctuary zone, using measurements from 25-m long transects

Source	df	SS	MS	F	Pval
(a) Seagrass 25 m all fish combined					
Zone	1	864.91	864.91	0.74	0.454
Size	1	5849.08	5849.08	24.71	**0.016**
Location (Size)	3	710.12	236.71	0.13	0.937
Zone x Size	1	21.70	21.70	0.02	0.900
Zone x Location (Size)	3	3518.47	1172.82	0.66	0.606
Site (Zone x Location (Size))	6	10649.99	1775.00	2.49	**0.044**
Residual	31	22099.22	712.88		
(b) Seagrass 25 m targeted species					
Zone	1	0.61	0.61	0.01	0.935
Size	1	1814.19	1814.19	69.77	**0.004**
Location (Size)	3	78.00	26.00	0.04	0.989
Zone x Size	1	28.40	28.40	0.37	0.586
Zone x Location (Size)	3	230.77	76.92	0.11	0.951
Site (Zone x Location (Size))	6	4182.29	697.05	4.12	**0.004**
Residual	31	5248.58	169.31		
(c) Seagrass 25 m non-targeted species					
Zone	1	819.51	819.51	1.22	0.350
Size	1	1148.26	1148.26	9.43	0.055
Location (Size)	3	365.34	121.78	0.40	0.756
Zone x Size	1	99.76	99.76	0.15	0.726
Zone x Location (Size)	3	2015.34	671.78	2.23	0.185
Site (Zone x Location (Size))	6	1807.03	301.17	0.77	0.601
Residual	31	12168.63	392.54		

Table 2.8. Results of analyses testing for differences in biomass of fish from reef habitat among sanctuary zones of different sizes, using measurements from 50-m long transects

Source	df	SS	MS	F	Pval
(a) Reef 50 m all fish combined					
Zone	1	2.24	2.24	1.40	0.302
Size	1	2.95	2.95	5.87	0.073
Location (Size)	4	2.01	0.50	0.23	0.918
Zone x Size	1	1.91	1.91	1.20	0.336
Zone x Location (Size)	4	6.39	1.60	0.73	0.589
Site (Zone x Location (Size))	14	30.79	2.20	1.10	0.382
Residual	52	104.25	2.00		
(b) Reef 50 m targeted species					
Zone	1	0.04	0.04	0.05	0.836
Size	1	0.79	0.79	2.30	0.204
Location (Size)	4	1.38	0.34	0.70	0.604
Zone x Size	1	0.00	0.00	0.01	0.943
Zone x Location (Size)	4	3.24	0.81	1.65	0.218
Site (Zone x Location (Size))	14	6.89	0.49	0.90	0.568
Residual	52	28.56	0.55		
(c) Reef 50 m non-targeted species					
Zone	1	1.68	1.68	2.11	0.220
Size	1	0.68	0.68	0.61	0.479
Location (Size)	4	4.50	1.13	0.73	0.588
Zone x Size	1	1.72	1.72	2.16	0.215
Zone x Location (Size)	4	3.19	0.80	0.51	0.726
Site (Zone x Location (Size))	14	21.69	1.55	1.24	0.275
Residual	52	64.87	1.25		

Table 2.9. Results of analyses testing for differences in density of fish from reef habitat with size of sanctuary zone, using measurements from 50-m long transects

Source	df	SS	MS	F	Pval
(a) Reef 50 m all fish combined					
Zone	1	76.01	76.01	3.57	0.132
Size	1	84.46	84.46	3.36	0.141
Location (Size)	4	100.61	25.15	1.29	0.322
Zone x Size	1	16.77	16.77	0.79	0.425
Zone x Location (Size)	4	85.27	21.32	1.09	0.399
Site (Zone x Location (Size))	14	273.56	19.54	0.68	0.782
Residual	52	1492.00	28.69		
(b) Reef 50 m targeted species					
Zone	1	3.71	3.71	0.56	0.497
Size	1	16.77	16.77	2.62	0.181
Location (Size)	4	25.63	6.41	2.14	0.130
Zone x Size	1	0.30	0.30	0.04	0.842
Zone x Location (Size)	4	26.63	6.66	2.22	0.119
Site (Zone x Location (Size))	14	41.94	3.00	0.48	0.933
Residual	52	324.00	6.23		
(c) Reef 50 m non-targeted species					
Zone	1	46.15	46.15	6.77	0.060
Size	1	25.96	25.96	1.18	0.338
Location (Size)	4	87.86	21.97	1.09	0.398
Zone x Size	1	12.59	12.59	1.85	0.246
Zone x Location (Size)	4	27.29	6.82	0.34	0.847
Site (Zone x Location (Size))	14	281.28	20.09	1.20	0.304
Residual	52	871.33	16.76		

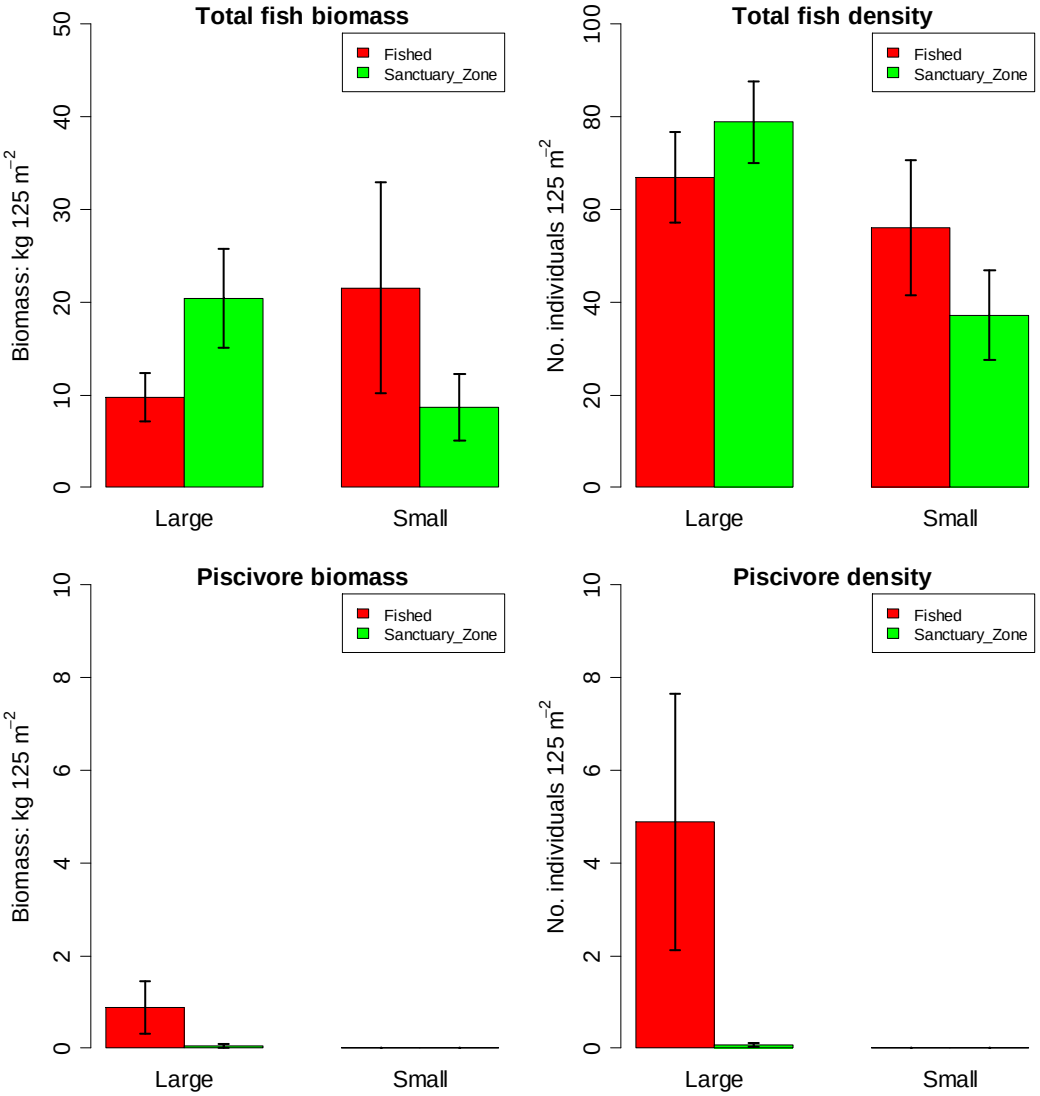

Figure 2.4. Biomass and density of fish from reef habitat in Sanctuary Zones and adjacent fished areas measured from 25 metre transects, contrasting measurements from large (>100 ha) and small (<30 ha) Sanctuary Zones. Separate plots are shown for all fish combined, three key trophic groups of fish (piscivores, herbivores and invertivores), targeted and non-targeted species.

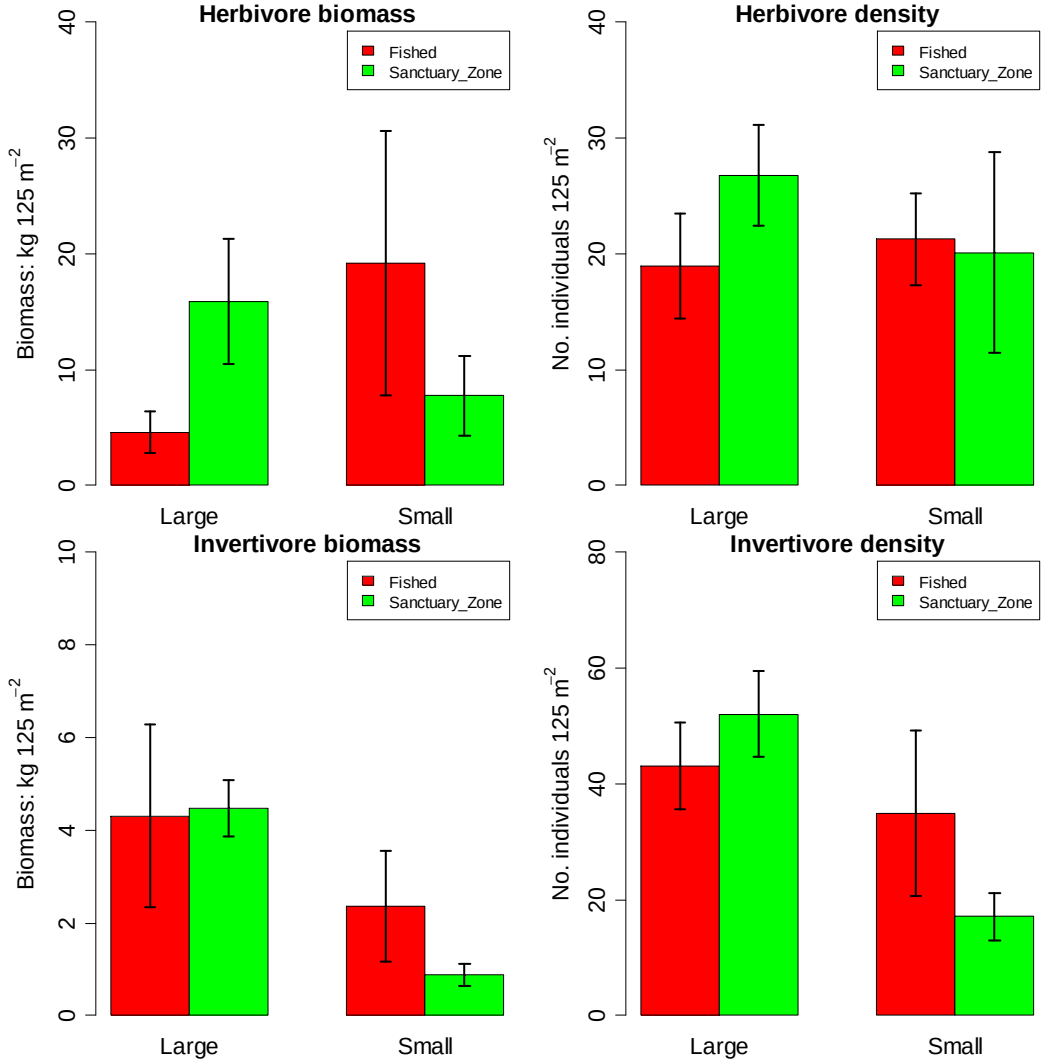

Figure 2.4 contd

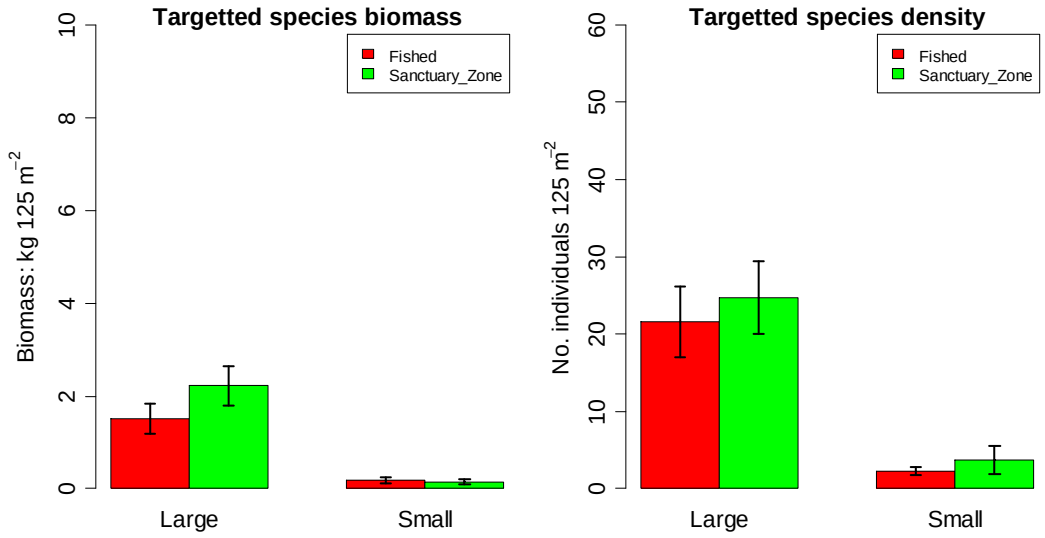

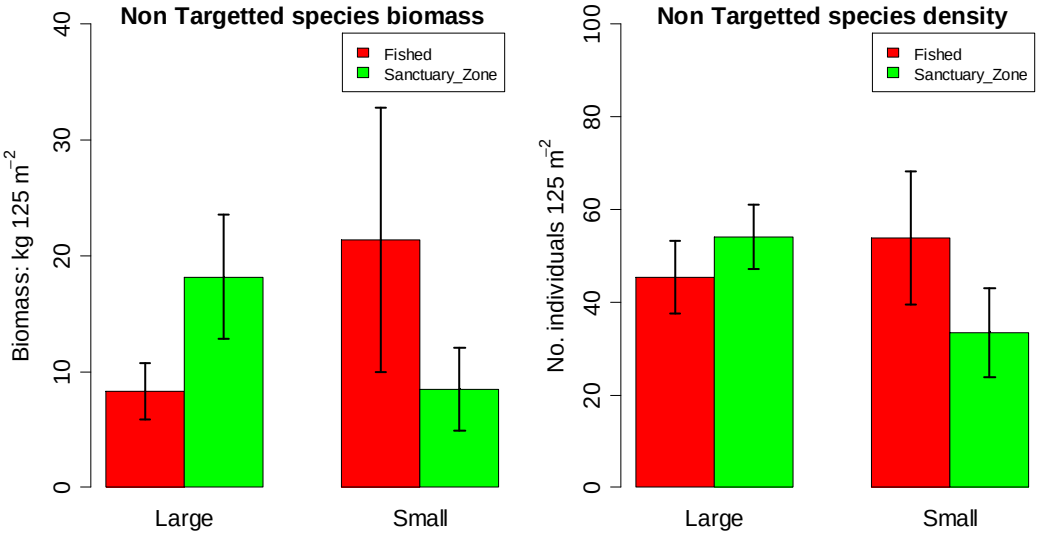

Figure 2.4 contd

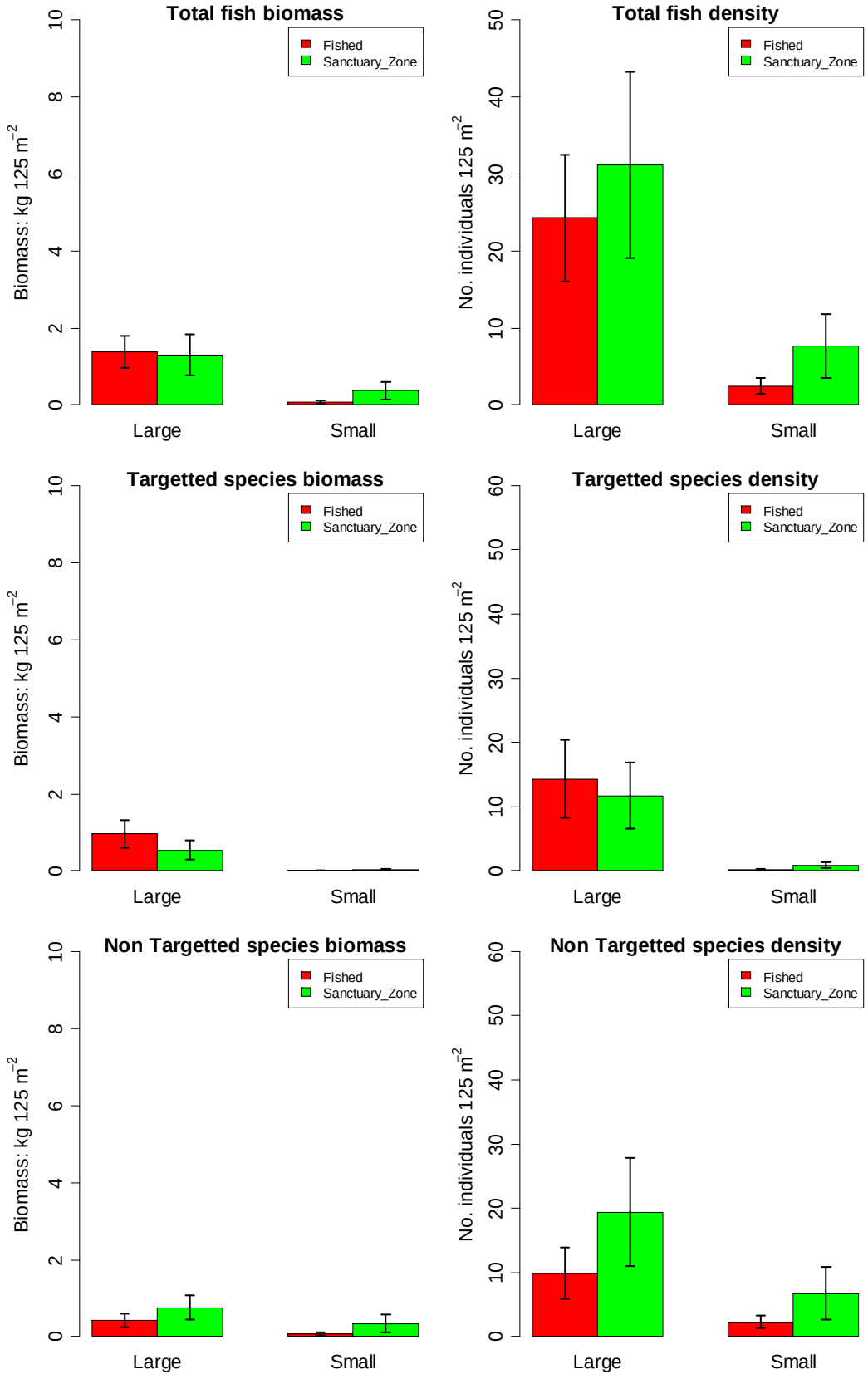

Figure 2.5. Biomass and density of fish from seagrass habitat in Sanctuary Zones and adjacent fished areas measured from 25 metre transects, contrasting measurements from large (>100 ha) and small (<30 ha) Sanctuary Zones. Separate plots are shown for all fish combined, and targeted and non-targeted species.

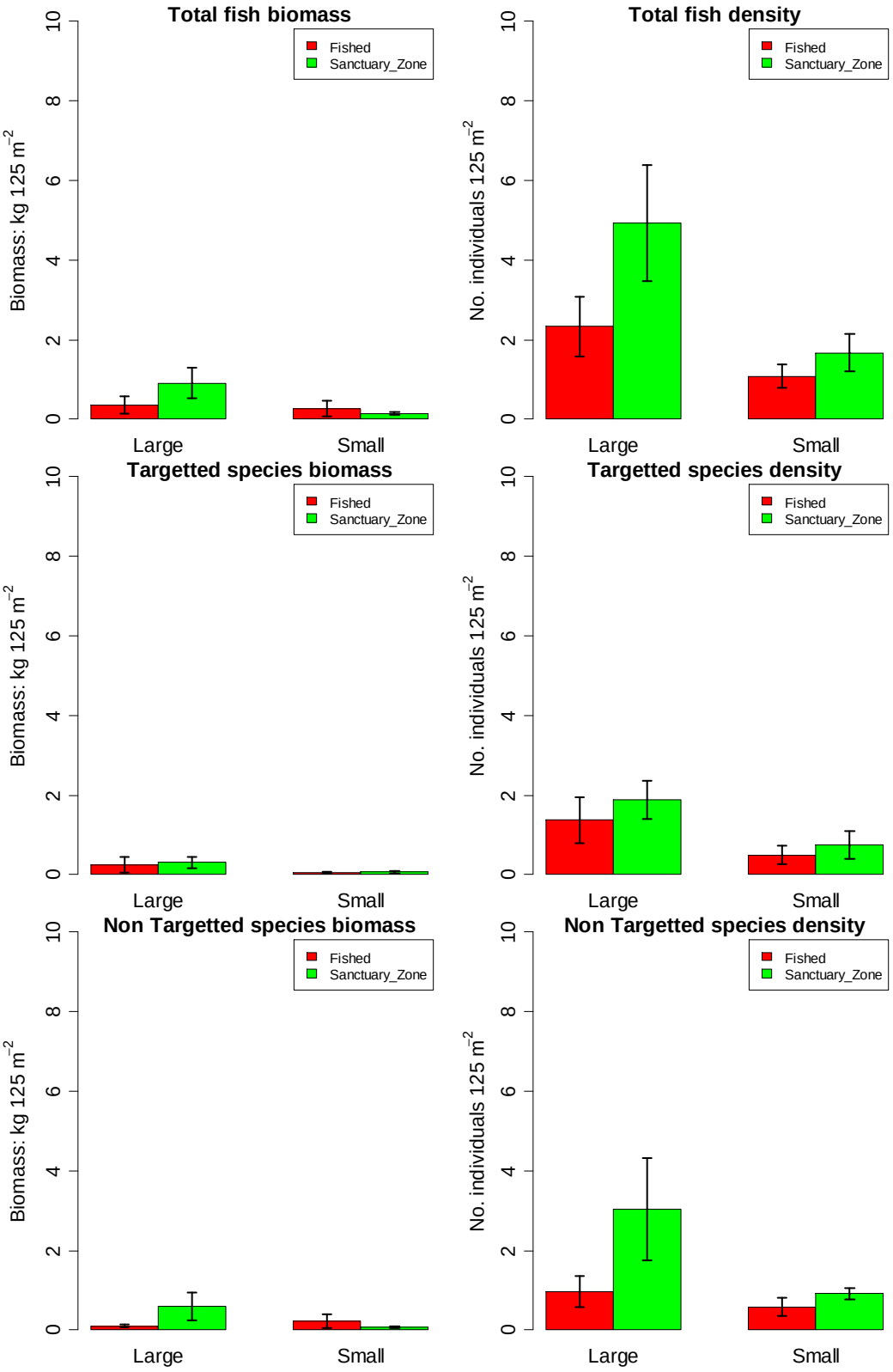

Figure 2.6. Biomass and density of fish from reef habitat in Sanctuary Zones and adjacent fished areas measured from 50 metre transects, contrasting measurements from large (>100 ha) and small (<30 ha) Sanctuary Zones. Separate plots are shown for all fish combined, and targeted and non-targeted species.

2.3.2 Western rock lobster

The biomass of western rock lobsters *Panulirus cygnus* was higher overall in SZs (Table 2.10). The magnitude of the difference between SZs and adjacent fished areas did vary between large and small SZs, but there was no statistically significant interaction between Zone and Size (Table 2.10, Figure 2.7). There was also a higher overall density of lobsters in SZs, but in this case the interaction between Zone and Size was statistically significant, with a higher density of lobsters recorded in large SZs (Table 2.10, Figure 2.7).

Table 2.10. Results of analyses testing for differences in biomass and density of western rock lobster with size of sanctuary zone

Source	df	SS	MS	F	Pval
(a) Biomass					
Zone	1	25.00	25.00	7.73	**0.050**
Size	1	12.57	12.57	8.97	**0.040**
Location (Size)	4	5.60	1.40	0.35	0.839
Zone x Size	1	6.63	6.63	2.05	0.225
Zone x Location (Size)	4	12.94	3.23	0.81	0.537
Site (Zone x Location (Size))	15	59.79	3.99	4.05	**0.000**
Residual	54	53.09	0.98		
(b) Density					
Zone	1	606.03	606.03	48.32	**0.002**
Size	1	707.87	707.87	5.65	0.076
Location (Size)	4	500.83	125.21	0.47	0.755
Zone x Size	1	174.27	174.27	13.90	**0.020**
Zone x Location (Size)	4	50.17	12.54	0.05	0.995
Site (Zone x Location (Size))	15	3970.33	264.69	10.26	**0.000**
Residual	54	1392.67	25.79		

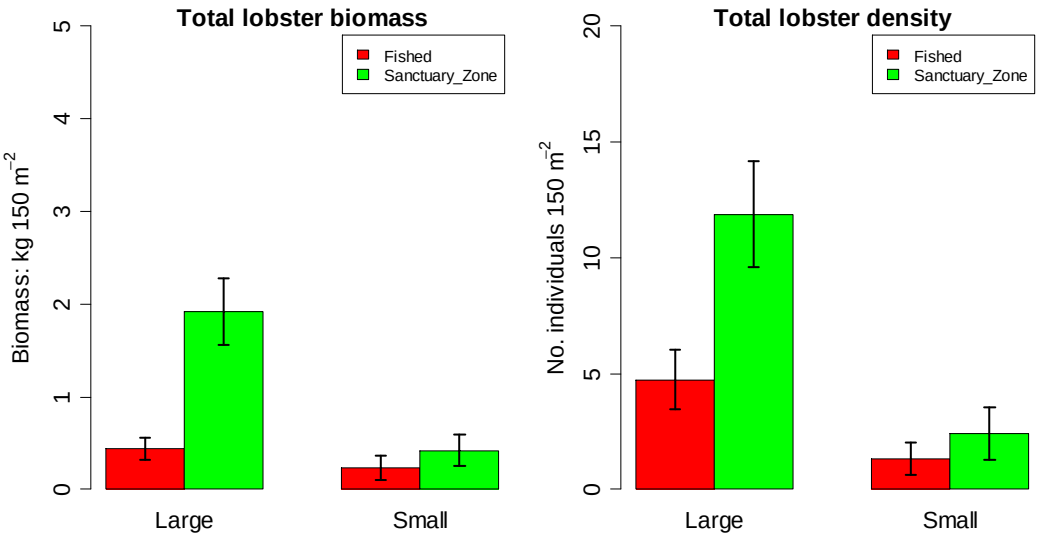

Figure 2.7. Biomass and density of western rock lobster in Sanctuary Zones and adjacent fished areas, contrasting measurements from large (>100 ha) and small (<30 ha) Sanctuary Zones.

2.4 Discussion

There is strong evidence that the overall biomass and density of fish is usually higher within marine reserves than in areas where fishing is allowed. This is supported by results of numerous surveys contrasting sanctuaries with adjacent fished areas globally (see reviews by Rowley 1994, Mosquera *et al.*, 2000) and within Western Australia (e.g. Babcock *et al.*, 2007, Kleczkowski *et al.*, 2008). Our results are generally consistent with this finding although we did not find a ubiquitously higher biomass or density inside SZ for all the metrics evaluated. An important extension of this finding is that several of the metrics provided evidence that large SZs better achieved the goals of higher biomass and density than small SZs.

There was a trend for higher density of western rock lobsters, and higher biomass of targeted species on reef habitat, inside large SZs. This pattern is consistent with the pattern expected if individuals inside small SZs are more susceptible to fishing mortality. This conclusion is further strengthened by the fact that both groups are heavily fished in Western Australia. In the case of western rock lobsters, a higher biomass and density was found in both small and large SZ than adjacent fished areas, but the magnitude of the difference in density was much greater for large SZs. In the case of targeted fish, the difference in biomass between SZs and adjacent fished areas was only detected in large SZs, and was not detected in small SZs.

A meta-analysis by Halpern (2003) found that size was not a good predictor of the effect of protection from fishing. However, this result was yielded by a compilation of results from many different studies, conducted in different habitats and geographical regions, and using a variety of methods. Our results are one of the few to explicitly contrast SZs of different sizes in a single biogeographical region using consistent methods.

Small SZs in this study ranged from 5 ha (Parker Point) to 28 ha (The Lumps). At these sizes, the distance from the centre of the reserve to the nearest edge cannot exceed a few hundred metres. Such a distance is within the nightly foraging range of western rock lobsters (MacArthur *et al.*, 2008), and is also likely to be within the foraging range of many of the targeted fish species most commonly observed in this study, although the foraging ranges of most species remain unknown.

Perhaps the most compelling result is the observation that the metrics that showed the strongest patterns related to size of SZ were for the two most heavily-fished groups of species. This result suggest that, where sanctuary zones are established with the aim of increasing the biomass and/or density of species targeted by fishers, it is likely that large reserves will be most likely to achieve their aim. Although we found some evidence that small reserves did yield higher measurements for some metrics, the difference was smaller than that yielded by large reserves, and was present for fewer metrics. One inference from this is that, while small reserves might achieve aims of increasing biomass or density, they are less likely to do so.

2.5 References

Babcock RC, Phillips JC, Lourey M, Clapin G (2007) Increased density, biomass and egg production in an unfished population of Western Rock Lobster (Panulirus cygnus) at Rottnest Island, Western Australia. Marine and Freshwater Research 58:286-292

Halpern BS (2003) The impact of marine reserves: do reserves work and does reserve size matter? Ecological Applications 13:S117-S137

Kleczkowski M, Babcock RC, Clapin G (2008) Density and size of reef fishes in and around a temperate marine reserve. Marine & Freshwater Research 59:165-176

Levin PS, Kaplan I, Grober-Dunsmore R, Chittaro PM, Oyamada S, Andrews K, Mangel M (2009) A framework for assessing the biodiversity and fishery aspects of marine reserves. Journal of Applied Ecology 46:735-742

MacArthur LD, Hyndes GA, Babcock RC, Vanderklift MA (2008) Nocturnally active western rock lobsters Panulirus cygnus forage close to shallow coastal reefs. Aquatic Biology 4:201-210

Mosquera I, Côté IM, Jennings S, Reynolds JD (2000) Conservation benefits of marine reserves for fish populations. Animal Conservation 4:321-332

Rowley RJ (1994) Marine reserves in fisheries management. Aquatic Conservation: Marine and Freshwater Ecosystems 4:233-254

3. AN ASSESSMENT OF LIKELY DISPERSAL PATTERNS FOR MARINE ORGANISMS BASED ON HYDRODYNAMIC AND POPULATION GENETIC MODELS

Phillip England, Deryn Alpers, Asta Audzijonyte, Ming Feng, Dirk Slawinski, Nicole Murphy and Thomas Wernberg*

CSIRO Marine and Atmospheric Research

*School of Plant Biology & UWA Oceans Institute, The University of Western Australia (M096) and Australian Institute of Marine Science, Crawley 6009 WA

3.1 Introduction

Connectivity between populations is a key ecological process that is attracting increasing attention in marine systems. Its maintenance should be an important goal in marine biodiversity management yet it is difficult to characterise and monitor. Many marine organisms, particularly invertebrates and plants, rely upon ocean currents to disperse their larvae, so spatial population connectivity in these species is likely to reflect the prevailing hydrodynamic patterns at small and large scales.

The difficulty of observing dispersing larvae makes several indirect approaches important aids to understanding population connectivity. Oceanographic modelling is a powerful tool for generating predictions about population connectivity over short periods (Condie *et al.,* 2005). On the other hand, genetics provides a picture of long term, multi-generational population connectivity integrating realised dispersal across seasonal and inter-annual variations in ocean currents.

The approach we take here consists of combining hydrodynamic modelling with genetics. Multidisciplinary approaches have the potential to reveal aspects of spatial and temporal connectivity that are not evident from analysis of individual datasets and recent investigations have yielded important insights in studies of marine connectivity (Galindo *et al.,* 2006; Banks *et al.,* 2007; White *et al.,* 2010; Coleman *et al.,* 2011).

Here we predict oceanographic connectivity among four geographical locations in the south west of Western Australia using hydrodynamic modelling of larval dispersal and test these predictions against genetic descriptions of population structure, population boundaries and estimates of larval migration in two co-distributed sea urchin species.

Sea urchins are excellent models for characterising marine population connectivity because of their commonness, diversity of larval life histories, ease of sampling, and ecological importance as grazers in coastal benthic habitats. Our study sampled two species, *Heliocidaris erythrogramma* and *Phylocanthius irregularis. H. erythrogramma* spawns predominantly in summer (Stuart-Andrews 2005; Wright & Steinberg 2001) and its lecithrotrophic larvae are free swimming for 3-4 days in

laboratory observations (Stuart-Andrews 2005). In contrast, little is known about spawning time and larval duration in *P. irregularis*.

The south-west corner of Australia is dominated by the Leeuwin current system, the world's only poleward-flowing western continental boundary current. The Leeuwin current (LC) is particularly strong in the late autumn and winter months and is weaker in the summer (Feng *et al.,* 2003). Strong seasonal contrasts in the LC flow pattern make it possible to generate testable predictions about the predominant direction of larvae-mediated gene flow in *H. erythrogramma*. Comparison of genetic structure with oceanographic model predictions allowed us to make predictions about the possible larval biology of the less well characterised urchin *P. irregularis*.

3.2 Methods

3.2.1 Sample collection

Two urchin species (*Heliocidaris erythrogramma* and *Phylacanthus irregularis*) with ranges encompassing the lower west coast and southern coasts of Western Australia were collected by diving in coastal waters at four locations (Figure 3.1). Samples were either frozen for later processing in the laboratory or dissected in the field to extract gonads for placement into 95% ethanol.

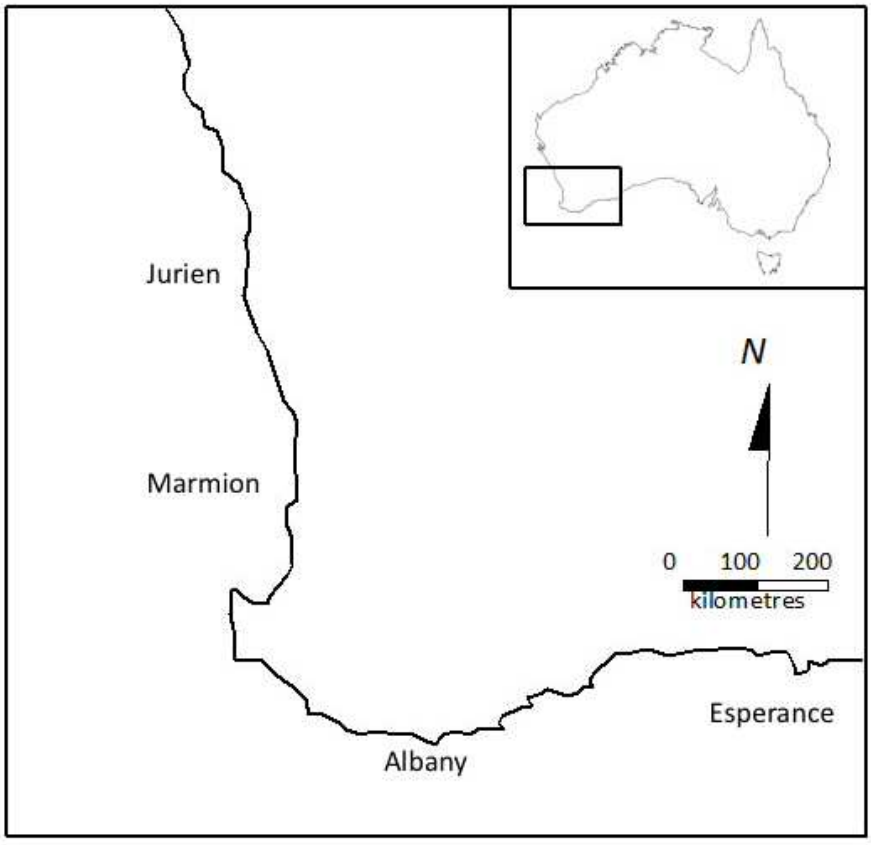

Figure 3.1. Sampling locations of urchins used in this study.

3.2.2 Genetic analysis

A total of 60 *H. erythrogramma* and 53 *P. irregularis* specimens were used in the genetic analyses. We obtained sequence from both mitochondrial (mtDNA) and nuclear DNA. For mtDNA analyses, a fragment of the mitochondrial cytochrome oxidase I subunit gene (COI) was amplified via the polymerase chain reaction (PCR) and sequenced using the LCO1490 and HCO2198 primers (Folmer *et al.,* 1994). To obtain nuclear markers we targeted introns of seven single-copy genes, using universal coelomate primers designed by Jarman *et al.,* (2002). Sequencing was performed by Macrogen Ltd. (South Korea).

Out of seven nuclear intron primer sets tested, only two provided reliable DNA sequences. The primer set for ADP/ATP translocase (ANT) provided reliable sequences in *H. erythrogramma*, whereas the primer set for ANT synthetase subunit α (ATPS α) yielded readable intron sequences in both urchin species. Codon Code Aligner 2.0.6 software (CodonCode Corp. 2002-2007) was used to examine chromatograms. Single nucleotide polymorphisms (SNPs) were scored as heterozygous when two peaks occurring in the sequence trace differed by less than 25% in intensity and were repeatable in the forward and reverse direction sequences. The ATPS α gene of *H. erythrogramma* contained many examples of nucleotide insertions and deletions (indels), which made sequences unreadable from the point of the indel forward. The total length of the intron was *ca*. 400 bp, but in our analyses we divided the gene into four parts, each 80 to 120 bp long to avoid the indels and treated each as independant loci due to the inability of reconstructing haplotypes.

Sequences of the mitochondrial COI gene contained no indels or stop codons to indicate sequencing errors or amplification of pseudogenes. The amplified nuclear genes contained a number of heterozygous sites and their haplotypes (gametic phase) were inferred using a Bayesian approach, as implemented in PHASE 2.1 (Stephens 2001; Stephens and Donnelly 2003) run through DnaSP 5.00.07 (Librado and Rozas 2009). Phylogenetic relationships among haplotypes were represented as haplotype networks using a statistical 95% parsimony criterion (Templeton *et al.,* 1992) as implemented in TCS 1.13 (Clement *et al.,* 2000). Nucleotide (π) and haplotype (h) diversity indices (Nei, 1987) were calculated in Arlequin 3.0 (Excoffier *et al.,* 2005). The partitioning of nucleotide diversity among the four sampling sites in each species was assessed for each locus with an analysis of molecular variance (AMOVA) (Excoffier *et al.,* 1992). Pairwise Φst values were also calculated between sampling locations for each locus and each species and their significance assessed with 1000 random permutations of the data.

3.2.3 Migrate

We used a maximum likelihood approach based on coalescent theory and implemented with the program Migrate-N 3.1.6 (Beerli and Felsenstein, 2001) to estimate effective population size and migration among sampling sites. Population and search parameters were varied until quantitatively similar maximum likelihood values were returned from successive runs.

3.2.4 Hydrodynamic modelling

Lagrangian particle dispersal modelling was used to estimate larval connectivity potential among sites. This was nested within a data assimilated hydrodynamic model, BlueLINK (Schiller *et al.*, 2008) with high spatial (0.1 degree) and temporal (6 hours) resolution reconstructing the hydrodynamic history around the Australian region between 1992 and 2006. Neutrally buoyant, passively dispersing particles were released at each site in selected months and allowed to disperse for selected periods under the influence of prevailing hydrodynamics in the time series covered by the model (1992-2006).

As spawning season and larval duration are unknown for *P. irregularis*, larval dispersal was modelled in January and February when the LC is quiescent and in July and August when its flow is strongest. Larval durations of 5, 15 and 30 days were used, where 5 days approximates *H. erythrogramma* and 15 and 30 days were chosen to provide a longer range with which to compare findings from *P. irregularis* with an unknown larval duration.

Modelling was conducted in six years from 1997 to 2002, chosen to encompass both high and low LC flow years associated with el Nino and la Nina. Connectivity matrices were generated that summarised the probability that particles released from a source grid cell passed into or through a destination grid cell during the specified larval period.

3.3 Results

3.3.1 Hydrodynamic Connectivity

Two representative connectivity matrices of probability densities show contrasting patterns between summer and winter (Figure 3.2). In winter measurable dispersal in the prevailing direction of the LC was observed from all sites except Esperance (which is the most easterly site). In summer, this was also true although to a lesser extent (Table 3.1). In summer, northward dispersal was also observed from Marmion to Jurien; in fact this was more substantial than the southward flow from Jurien. Measurable "counter flow" was not observed at any of the other sites in summer or winter. Another general observation was that retention rates (the proportion of particles that did not leave their source grid cell during the dispersal period (identified as the squares on the diagonal) on the south coast sites Albany and Esperance were higher than the west coast sites, Jurien and Marmion.

Table 3.1. Hydrodynamic connectivity probabilities between sites for larval durations of 5, 15 and 30 days averaged across six years of summer (January) and winter (July) dispersal. Jurien (J), Marmion (M), Albany (A) & Esperance (E). Zero probabilities are represented by blank cells.

	Source											
	5day				15day				30day			
	J	M	A	E	J	M	A	E	J	M	A	E
summer												
J	21.4				8.75	1.85			4.15	5.73		
M	0.13	51.6			0.88	23.2			0.32	8.71	0.12	

	A			49.3			33.0		0.03		29.0	
	E				49.4			36.4			0.24	28.7
winter												
	J	26.6				15.5			11.5			
	M	3.30	43.4			14.6	17.1		14.0	10.9		
	A			35.8			0.05	25.9	0.37	0.24	24.7	
	E				36.4			0.07	23.0		0.14	20.3

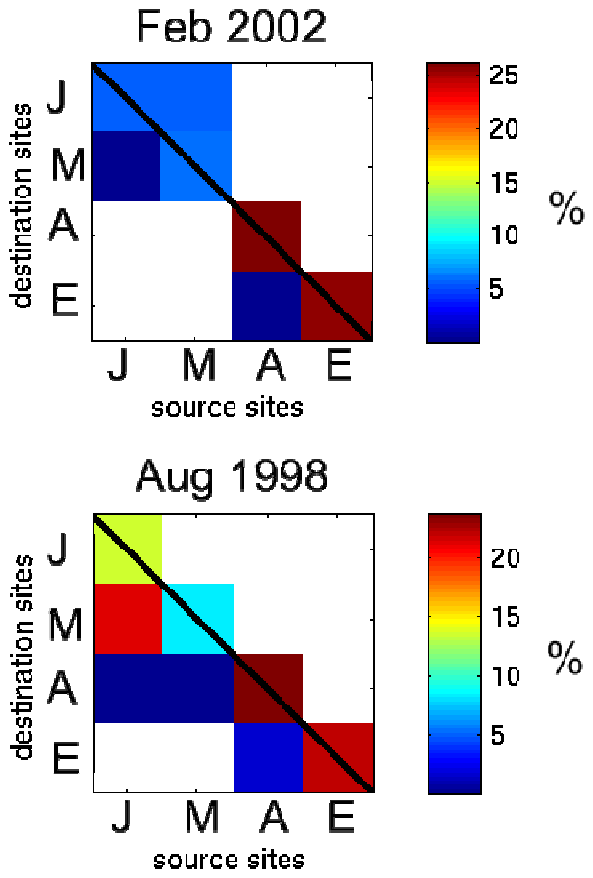

Figure 3.2. Representative summer and winter connectivity matrices from particle dispersal modelling at four sites in W.A.: Jurien (J), Marmion (M), Albany (A) & Esperance (E). Each site was used as a source for particles and a destination for determining the percentage of released particles present at the destination cell after 30 days of dispersal.

The combined northward and southward dispersal at Marmion in summer is illustrated in 30 day larval duration maps in which particle densities in all coastal grid cells is indicated (Figure 3.3). In winter the dispersal is entirely in the "downstream" direction with respect to LC flow. In contrast, dispersal from Esperance is almost entirely downstream in both seasons (Figure 3.3).

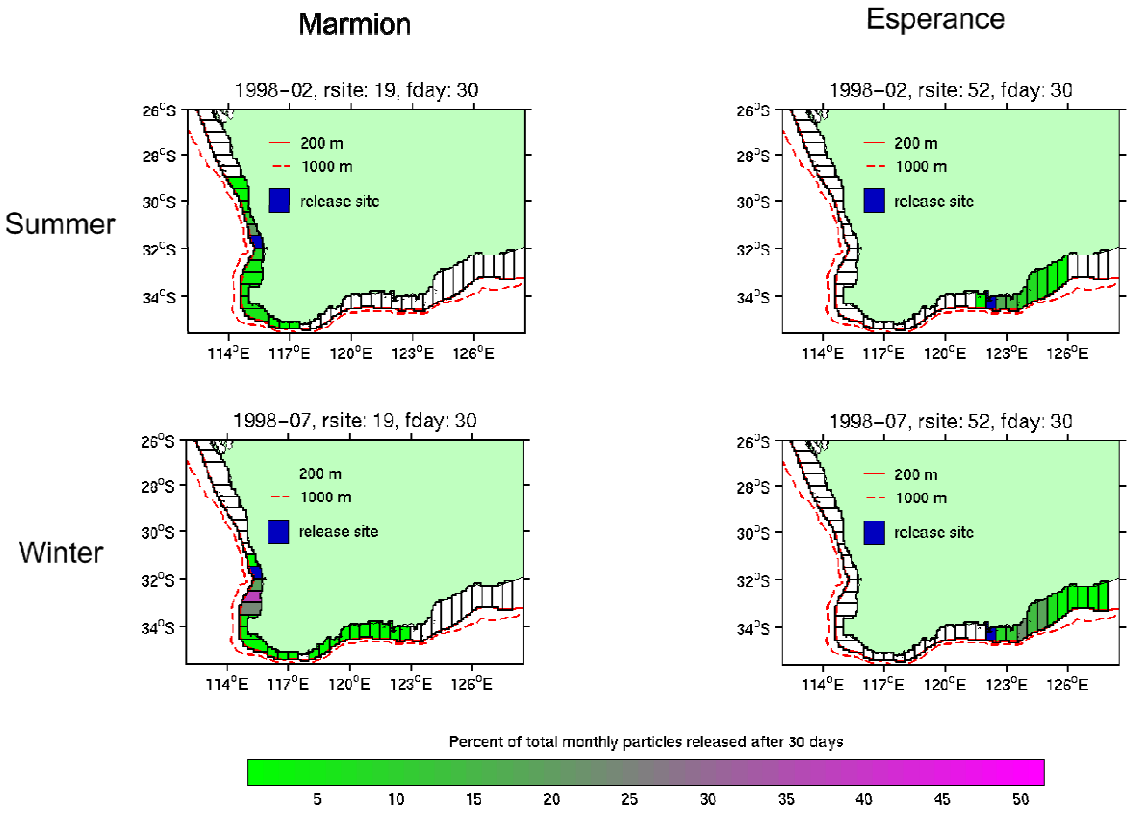

Figure 3.3. Representative 30 day particle dispersal maps for two of the four urchin sampling sites, illustrating the contrast between summer and winter Leeuwin Current influence on the west and south coasts. Grid cells are 0.5 degrees wide.

3.3.2 Genetic Diversity and Connectivity

Substantial DNA sequence diversity was recorded at all sampling sites, however diversity was on average higher in the nuclear genes than the mitochondrial gene COI (Table 3.2). Most of the variation was partitioned among individuals rather than among sampling sites as reflected in Φst values close to or below zero (Table 3.3). No significant differentiation among sites was observed in either species at the COI gene, however, population structure was evident in *H. erythrogramma* at ANT (Table 3.3) and ATPSα (data not shown).

Genetic diversity patterns indicate that substantial gene flow occurs or has in the past occurred between the west and south coasts. Mitochondrial DNA variation, while reasonably high (4.5 & 3.0 haplotypes per site in *H. erythrogramma* and *P. irregularis* respectively), does not resolve structure at this spatial scale. This pattern was also observed with P. irregularis in the nuclear intron ATPSα

despite higher diversity levels (6.75 haplotypes per site), however, significant structure was observed between the west and south coasts in *H. erythrogramma* at the ANT gene.

Table 3.2. DNA sequence statistics obtained from mitochondrial and nuclear genes in two urchin species in at the four sampling regions: number of gene copies, usable sequence length and number of polymorphic sites.

H. erythrogramma

	COI	ANT	ATPSα-1	ATPSα-2	ATPSα-3	ATPSα-4
Jurien	10 603 0	28 249 7	10 83 4	6 122 2	10 108 11	16 47 1
Marmion	22 603 7	38 249 10	26 83 5	20 122 9	22 108 12	36 47 1
Albany	11 603 7	22 248 7	10 83 3	6 122 1	10 108 12	16 47 1
Esperance	7 603 0	32 249 8	14 83 4	8 122 7	2 108 7	18 47 1

P. irregularis

	COI	ATPSα
Jurien	11 641 0	20 240 6
Marmion	17 641 6	34 240 7
Albany	12 641 1	26 240 6
Esperance	10 641 5	26 240 8

Table 3.3. Genetic subdivision (Φst) between sites based on nuclear and mitochondrial genes in two species. Upper half, COI; lower half, ANT (*H. erythrogramma*) and ATPSα (*P. irregularis*).

H. erythrogramma	Jurien	Perth	Albany	Esperance
Jurien	0	-0.032	-0.009	0
Marmion	0.147*	0	-0.008	0
Albany	0.161*	0.074*	0	-0.046
Esperance	0.051	0.022	0.092*	0

P. irregularis	Jurien	Perth	Albany	Esperance
Jurien	0	-0.027	-0.007	0.010
Marmion	-0.004	0	-0.014	-0.007
Albany	0.027	0.004	0	0.013
Esperance	0.047	0.009	0.013	0

* not significantly different from zero (P < 0.05)

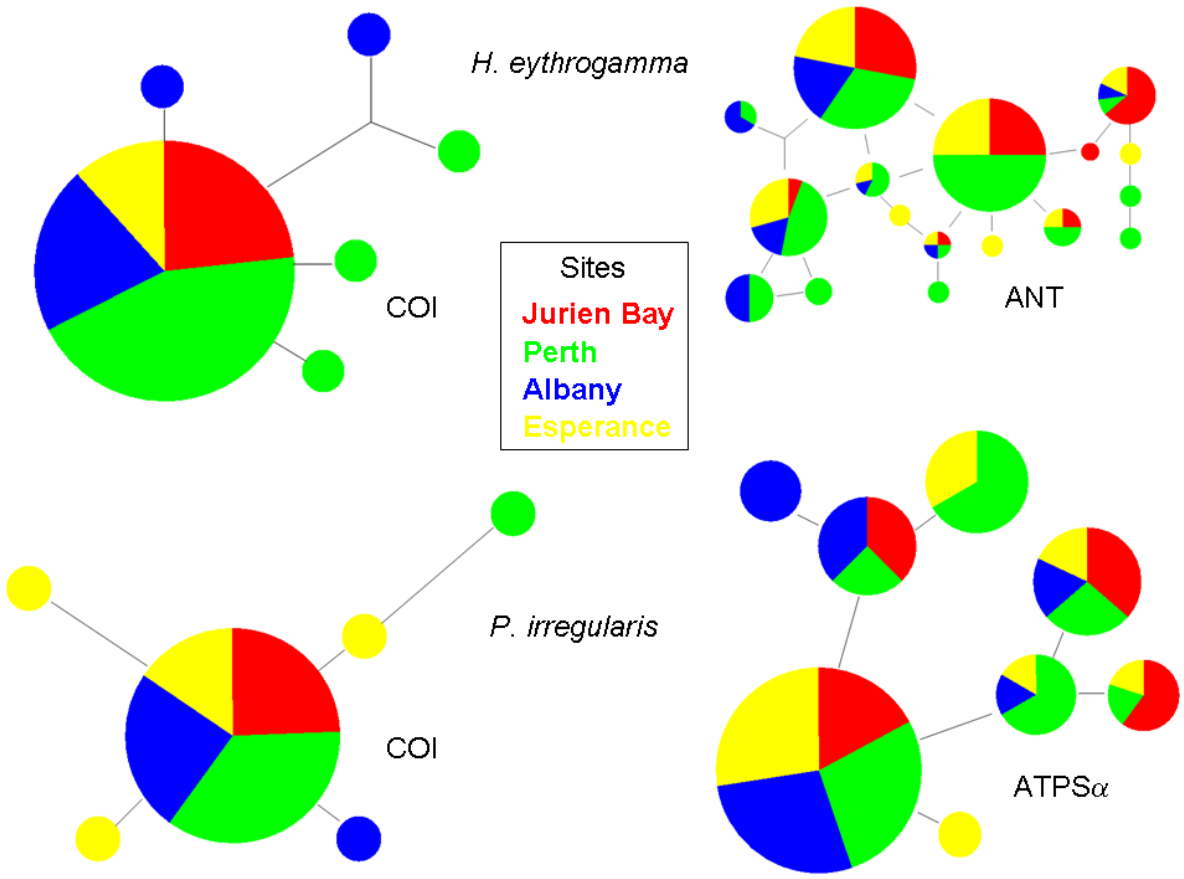

Figure 3.4. Haplotype networks from two genes per species showing the proportion of haplotypes from each region (relative slice size), mutational distance between haplotypes (relative stem length) and relative sample size (pie size). Note, most haplotypes are represented at all sample sites.

Coalescent-based estimation of migration rates suggests that realised gene flow in both species is predominantly northward from Marmion to Jurien with values an order of magnitude higher than the opposite direction (Table 3.4). Connectivity between other sites is in the prevailing downstream direction with respect to the LC.

Table 3.4. Maximum likelihood estimates (MLE) of mutation-scaled migration rates (M) and theta (Θ) with 95% confidence intervals assuming stepping stone migration among sites: Jurien (J), Marmion (M), Albany (A) & Esperance (E).

	H. erythrogramma			*P. irregularis*		
	MLE	0.025	0.975	MLE	0.025	0.975
Θ J	0.0009	0.0006	0.0016	0.00008	0.00006	0.0001
Θ M	0.0101	0.0085	0.0126	0.0064	0.0049	0.0097
Θ A	0.0062	0.0045	0.0098	0.00042	0.0003	0.0006
Θ E	$2.48x10^{11}$	0.0351	$2.48x10^{11}$	0.0013	0.0006	0.0030
M_{JM}	263	179	408	1488	1070	2190
M_{MJ}	12646	9380	17900	17423	12500	25700
M_{MA}	7922	7050	9100	9098	7160	12200
M_{AM}	2395	2120	2810	2859	2260	3800
M_{AE}	9179	6860	13500	4893	3090	8190
M_{EA}	$7.459x10^{-12}$	$5.6x10^{-12}$	75.40	0.0003	0.0002	1.26

3.4 Discussion

Hydrodynamic modelling predicted that summer spawning species should disperse predominantly northward from Perth and eastward from Albany. Dispersal in winter spawning species should be strongly biased downstream with the prevailing LC flow. *H. erythrogramma* is a summer spawner with a relatively short larval duration period (5 days), which appears from the modelling to be sufficiently long to connect adjacent sampled locations in a single dispersal generation. Estimates of genetic connectivity reflect this, with apparently northward geneflow from Perth and an absence of clear phylogeographic boundaries across the sampled range.

Lower population differentiation in *P. irregularis* is consistent with, although not necessarily the result of, longer larval duration and/or winter spawning promoting increased connectivity. These factors are sufficient to explain the reduced population structure, however, other factors might also be responsible or involved, including higher establishment success for larvae across the range, or historical processes not reflected in contemporary estimates of hydrodynamic connectivity.

Coalescent-based maximum likelihood estimates of geneflow magnitude and direction concur with hydrodynamic estimates of connectivity. In summer, when the south-eastward flowing LC is quiescent and eddy activity is greater than it is during winter, greater dispersal northward from Perth is predicted. The number of northward migrants was several orders of magnitude higher from Perth to Jurien than the reverse. Inferred geneflow between other sites is also consistent with hydrodynamic connectivity, being negligible westwards from Esperance to Albany and strongly biased from Albany to Perth.

The larval life history of *P. irregularis* is unknown, but like *H. erythrogramma* geneflow appears to be predominantly northward from Perth and it exhibits qualitatively similar asymmetry between other sites. As with the genetic structure results, this is consistent with summer spawning. This is not an unreasonable expectation in temperate Australian urchins although winter spawning has been reported in *Centrostephanus rodgersii* (Ling *et al.*, 2008).

Coastal wind-driven currents including the capes current on the lower west coast of Western Australia prevail in summer and these may also be driving the northward dispersal from Perth (Feng *et al.,* 2010). This inshore process is undoubtedly important, but its spatial resolution is poorly resolved by the hydrodynamic model used in our study (Condie *et al.,* 2011). Offshore eddys that might move larvae northward are prominent features of the LC system and have the potential to be important dispersers of urchins although to date, study has focussed on their role in fish larval dispersal (Muhling *et al.,* 2007)

Our findings need to be interpreted in the light of a number of assumptions and model limitations. The hydrodynamic model grid has a resolution of 10km, which inevitably limits its accuracy inshore where bathymetric and shoreline variation occurs at a finer scale. This approach therefore cannot model accurately the stage between larval release and entrainment in deeper waters further offshore nor the stage leading to larval settlement and establishment in shallow water urchin habitats. Further fine-scale, shallow water hydrodynamic modelling focussed on larval dispersal will improve our capacity to determine the role of these two important stages in explaining connectivity patterns in coastal organisms.

Assumptions of the coalescent-based inference of gene flow are also important to consider when interpreting our results especially that all populations have been sampled and included in the analysis, i.e. there are no “ghost” populations contributing migrants to the sampled populations. As this assumption is obviously breached in the case of the two continuously distributed urchin species in our study we are unable to discount the possibility that gene flow estimates reflect the influence of unsampled locations and possible cryptic source-sink dynamics rather than or as well as simply describing realised connectivity among the four sites in our study.

Our findings provide further evidence of the dominance of the Leeuwin Current in WA marine ecosystems. In this case, physical transport dynamics appear to drive patterns of connectivity throughout the very broad range (hundreds to thousands of kilometres) of two coastal marine invertebrates. It would be surprising if this observation is not widespread in other species with larval life histories and other strategies dependent upon passive transport e.g. vegetative reproduction. By combining predictive oceanographic modelling of larval dispersal with directional analysis of gene flow we have been able to generate and test hypotheses relating to population connectivity in two species of sea urchins. In one species for which little is known of its reproductive ecology, we have made predictions of spawning time and duration that invite experimental testing in the future.

3.5 Summary

Broad scale ocean currents play an important role in determining marine population connectivity through the dispersal of planktonic larvae. Combining physical oceanography with genetics can yield important insights into this process through the combination of hypothesis generation via larval dispersal modelling and hypothesis testing via measurement of population genetic structure and inference of realised gene flow patterns. We compared population structure, delineated using mitochondrial and nuclear gene sequences, in two co-occurring sea urchin species found in southwest Australia with predictions of oceanographic connectivity derived from modelled larval dispersal. Genetic differentiation among sites (two west and two south coast sites spanning 1130 km of coastline) was observed in nuclear but not mitochondrial genes, consistent with faster rates of intron evolution. Stronger structure and isolation by distance was apparent in *Heliocidaris erythrogramma* compared to *Phylocanthius irregularis*, suggesting the latter may have a longer lived larva than the 3-4 day duration measured in *H. erythrogramma* or some other adaptation counteracting population

differentiation over the scale of this study. Coalescent-based directional estimates of genetic exchange rates were consistent with overall predictions from hydrodynamic particle models that incorporated spawning time and larval duration in *H. erythrogramma* where northward gene flow from Perth predominated. Similar findings in *P. irregularis* imply a similar spawning time and this needs experimental investigation.

3.6 References

Banks SC, Piggott MP, Williamson JE, Bové U, Holbrook NJ, Beheregaray LB (2007) Oceanic variability and coastal topography shape genetic structure in a long-dispersing sea urchin. Ecology 88:3055-3064

Clement M, Posada D, Crandall K (2000) TCS: a computer program to estimate gene genealogies. Molecular Ecology 9:1657-1660

Coleman MA, Roughan M, Macdonald HS, Connell SD, Gillanders BM, Kelaher BP, Steinberg PD (2011), Variation in the strength of continental boundary currents determines continent-wide connectivity in kelp. Journal of Ecology 99: no. doi: 10.1111/j.1365-2745.2011.01822.x

Condie SA, Waring J, Mansbridge ML, Cahill ML (2005) Marine connectivity patterns around the Australian continent. Environmental Modelling and Software. 20: 1149-1157

Condie SA, Mansbridge JV, Cahill ML (2011) Contrasting local retention and cross-shore transports of the East Australian Current and the Leeuwin Current and their relative influences on the life histories of small pelagic fishes. Deep Sea Research Part II: Topical Studies in Oceanography 58(5):606-615

Excoffier L, Smouse PE, Quattro JM (1992) Analysis of molecular variance inferred from metric distances among DNA haplotypes: application to human mitochondrial DNA restriction data. Genetics 131:479-491

Excoffier L, Laval G, Schneider S (2005) Arlequin, Version 3.0: an integrated software package for population genetics data analysis. Evolutionary Bioinformatics Online 1:47–50

Feng M, Meyers G, Pearce A, Wijffels S (2003) Annual and interannual variations of the Leeuwin Current at 32◦S. Journal of Geophysical Research. 108:3355

Feng M, Slawinski D, Beckley LE, Keesing JK (2010). Retention and dispersal of shelf waters influenced by interactions of ocean boundary current and coastal geography. Marine and Freshwater Research 61:1259–1267

Folmer O, Black M, Hoeh W, Lutz RA, Vrijenhoek R (1994) DNA primers for amplification of mitochondrial cytochrome C oxidase subunit I from diverse metazoan invertebrates. Molecular Marine Biology Biotechnology 3:294-299.

Galindo HM, Olsen DB, Palumbu SR (2006) Seascape genetics: a coupled oceanographic-genetic model predicts population structure of Caribbean corals. Current Biology 16:1622-1626

Jarman SN, Ward RD, Elliott NG (2002) Oligonucleotide primers for PCR amplification of coelomate introns. Marine Biothechnology 4:347-355.

Librado P, Rozas J (2009) DnaSP v5: A software for comprehensive analysis of DNA polymorphism data. Bioinformatics 25:1451-1452

Ling SD, Johnson CR, Frusher S, King CK, (2008) Reproductive potential of a marine ecosystem engineer at the edge of a newly expanded range. Global Change Biology 14(4):907-915

Muhling MA, Beckley LE, Olivar MP (2007) Ichthyoplankton assemblage structure in two meso-scale Leeuwin Current eddies, eastern Indian Ocean. Deep Sea Research Part 54:1113-1128

Nei M (1987) Molecular Evolutionary Genetics. Columbia University Press, New York.

Pelcl RA, Warner RR, Gaines SD (2009)Geographical patterns of genetic structure in marine species with contrasting life histories. J. Biogeography 36:1881-1890

Schiller A, Oke PR, Brassington G, Entel M, Fiedler R, Griffin DA, Mansbridge JV (2008) Eddy-resolving ocean circulation in the Asian-Australian region inferred from an ocean reanalysis effort. Progress in Oceanography 76:334-365

Stephens M, Donnelly P (2003). A comparison of bayesian methods for haplotype reconstruction from population genotype data. American Journal of Human Genetics 73:1162-1169

Stephens M, Smith N, Donnelly P (2001) A new statistical method for haplotype reconstruction from population data. American Journal of Human Genetics 68:978-989

Stuart-Andrews C (2005) Spatial and temporal patterns of recruitment of Heliocidaris erythrogramma (Valenciennes, 1846) on the central West Australian coast. Honours thesis, The University of Western Australia

Templeton AR, Crandall KA, Sing CF (1992) A cladistic analysis of phenotypic associations with haplotypes inferred from restriction endonuclease mapping and DNA sequence data. III. Cladogram estimation. Genetics 132:619-633

White C, Selkoe KA, Watson J, Siegel DA, Zacherl DC, Toonen RJ (2010) Ocean currents help explain population genetic structure. Proceedings of the Royal Society B 277:1685-1694

Wright JT, Steinberg PD (2001) Effect of variable recruitment and post-recruitment herbivory on local abundance of a marine alga. Ecology 82(8): 2200-2215

4. ELECTRONIC DELIVERY OF DATA AND MODELS TO MANAGEMENT AGENCIES, BUILDING ON THE DEVELOPMENT OF THE DATA INTERROGATION AND VISUALISATION ENVIRONMENT (DIVE) IN SRFME

Peter Craig, Gary Carroll and Uwe Rosebrock

CSIRO Marine and Atmospheric Research

DIVE is a data access and visualisation package that has been developed through CSIRO's partnership with the WA Government. DIVE enables scientists and managers to view the diverse data sets that have been generated in WAMSI. The data are multidisciplinary and multidimensional, and range from relatively small numbers of field samples through to 4d model output occupying gigabytes of computer storage. DIVE can be installed onto all platforms supporting Java. It is functional on Windows, Linux and Mac OSX computers.

Figure 4.1 shows a typical DIVE screen display, in this case of model output off WA. The narrow left-hand panel provides detail of the data being displayed. The graphics panel is on the right, featuring four different panes. The main pane is a plan view of currents (represented by arrows) overlaid on water temperature (shown by colours). There is a red sample location marker inserted by the user at approximately 32 °S, 114 °E. The graph to the right shows vertical profiles of current speed (black), temperature (red) and salinity (blue) at this location. On the extreme right, there is a vertical depth-slider. The marker on this slider is located at 0 m, indicating the depth at which the plan view is plotted. This marker can be dragged to change the depth of the plan view.

Below the plan view is a time-series, showing the variability of current speed, temperature and salinity at the sample point location, and at the depth indicated by the depth-slider. At the bottom of the panel is an equivalent time-slider, which changes the time of the plan view (and the vertical profiles). The bottom plot on the panel is a cross-section of temperature along the track indicated near the top of the plan view. This track is selected by clicking with the screen cursor.

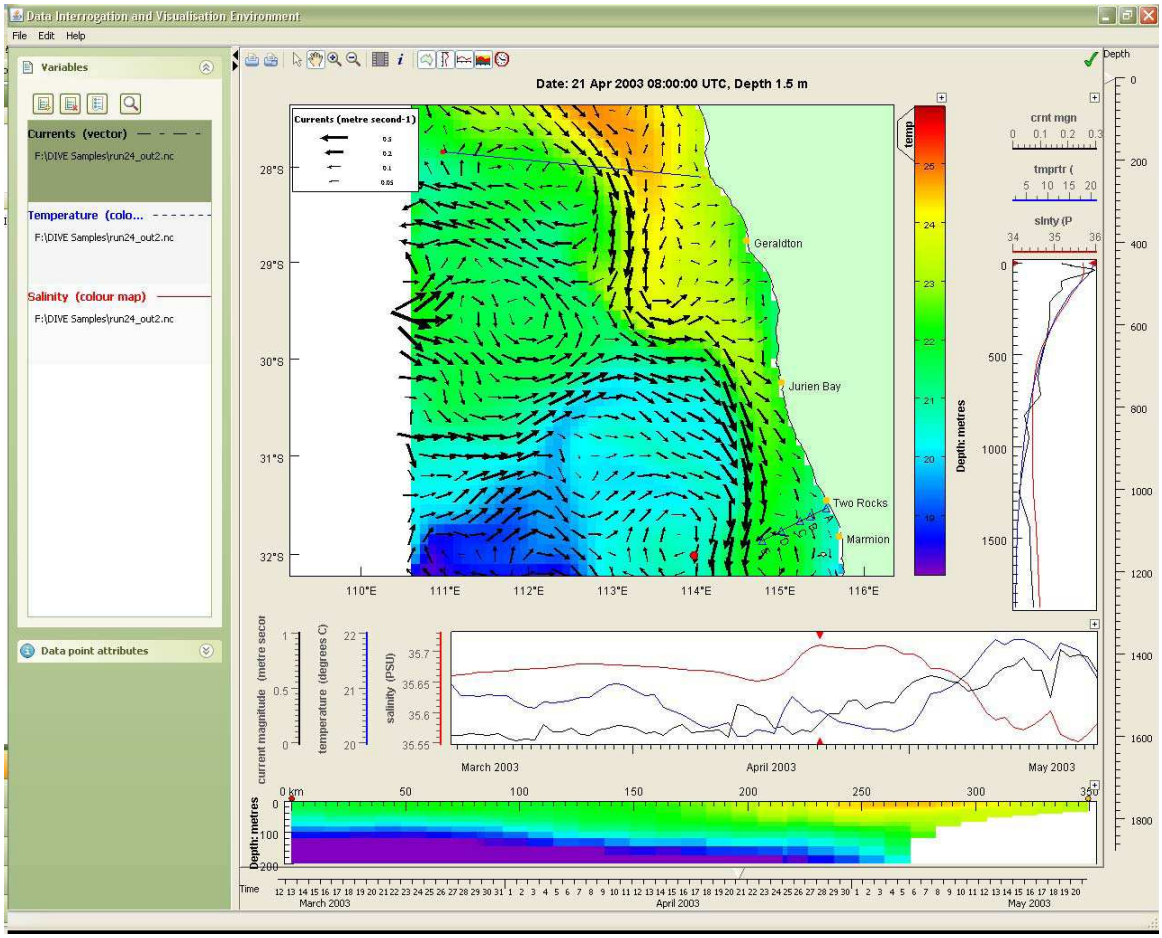

Figure 4.1. Presentation of layered data with one sample point displayed as time-series and profile in conjunction with a vertical section displayed along an arbitrarily drawn transect.

DIVE functionality:

While Figure 4.1 depicts the basic structure of the DIVE display, the full functionality of the package is described in the DIVE user manual. DIVE's features include:

- Selection and display of arbitrarily directed cross-section plots (Figure 4.1).
- Display of data from multiple sample points through the use of distinguishing colour and line styles (Figure 4.2).
- Display of scalar and vector variables (Figure 4.1).
- Expansion of individual panels by utilising a "lift-out" function to assist with examination of the data: the lift-out option is invoked by clicking on the small plus sign at the top-right of each plot, to make the panels appear in their own windows (Figure 4.2).
- User–selection of the time-zone in which the data are displayed: most commonly, this will be UTC, or the local time-zone of the user.

- Single-step viewing through the time-series or vertical layers: that is, the time-slide and depth-slide can be clicked through individual time or depth intervals in the data file.

- Output of animations, over either the whole time-range or user-defined subsets: animations can be saved in AVI, Flash and animated gif formats.

- Ability to read folder-based datasets: if data are held in multiple files within a single folder/directory (as is common with output from large model runs), DIVE can interpret the files as a single data source, enabling, for example, faster access and continuous plots (rather than a new plot for each separate file).

- Plotting of data for sediments and the atmosphere, when they are available: for example, Figure 4.3 shows an overlay of water-column and sediment nitrate from a coupled model, with water-column nitrate shown in red in the graphs, and by the colours on the map view, while sediment nitrate is shown in blue, and by contour lines on the map; data from different sources can also be overlayed on the same profile as shown in Figure 4.4.

- Display of underway datasets including high-resolution glider data (Figure 4.5 and Figure 4.6): hovering the cursor over the track produces detail of the data, as shown.

DIVE accepts data in self-describing format, in particular NetCDF, which is the standard for oceanographic data and model output. For model results, it has been tailored to handle:

- box-model output, for example from CSIRO's ecosystem model (Atlantis) as shown in Figure 4.7.

- z-coordinate models, such as CSIRO's SHOC, shown in Figure 4.1.

- sigma-coordinate models, such as Rutger's University's ROMS (Figure 4.8). (ROMS is one of the hydrodynamic models used in WAMSI, in Nodes 1, 3 and 6. The vertical sigma coordinate varies in time with the surface elevation.)

DIVE can also read:

- HTF (Hydrographic Transfer Format) described at www.hydro.gov.au/tools/htf/htf.htm

- CFF (Column File Format Files) an in-house CMAR text-based spreadsheet-like format. This format is described in an appendix to the DIVE manual.

DIVE can connect to MEST (Metadata Entry and Search Tool) servers, select from available on-line datasets, and download and plot these datasets. MEST servers are based on OGC (Open Geospatial Consortium) Catalogue Services standards to access data sets across the web. This capability will enable DIVE to access data sets archived by the Australian Oceanographic Data Network (AODN), and the Australian Integrated Marine Observation System (IMOS), which have both adopted OGC standards. The capability will be available in DIVE when the national MEST servers are fully functional.

The DIVE installer can be freely downloaded from the WAMSI website http://www.wamsi.org.au/category/region/research/data-management which links to http://software.cmar.csiro.au/

The DIVE Manual is available on the web site.

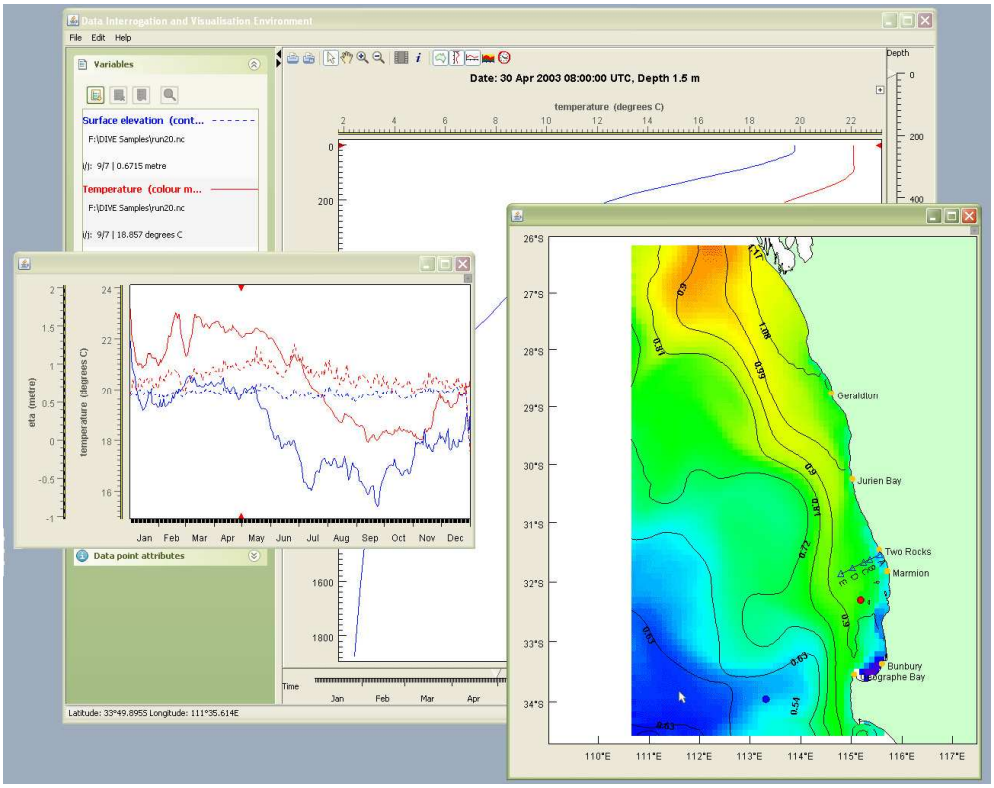

Figure 4.2. Demonstration of multiple sample points and the 'lift-out' functionality on the time-series and map plot.

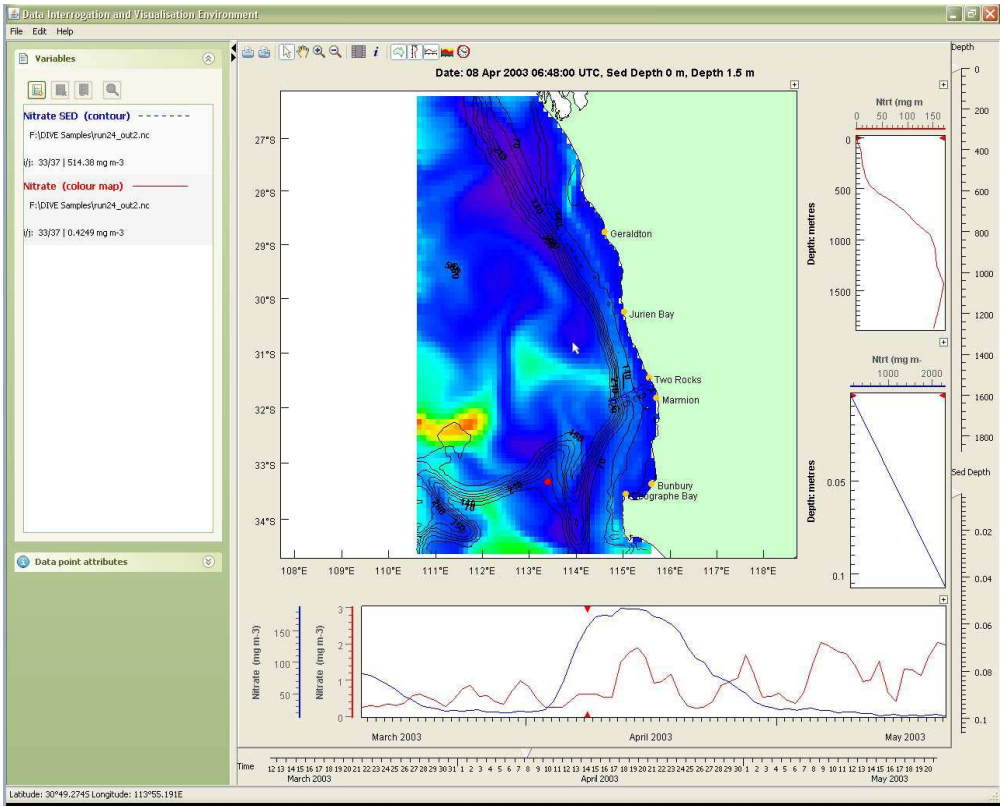

Figure 4.3. Display of data from different vertical grids, showing separate nitrogen profiles in water and sediment.

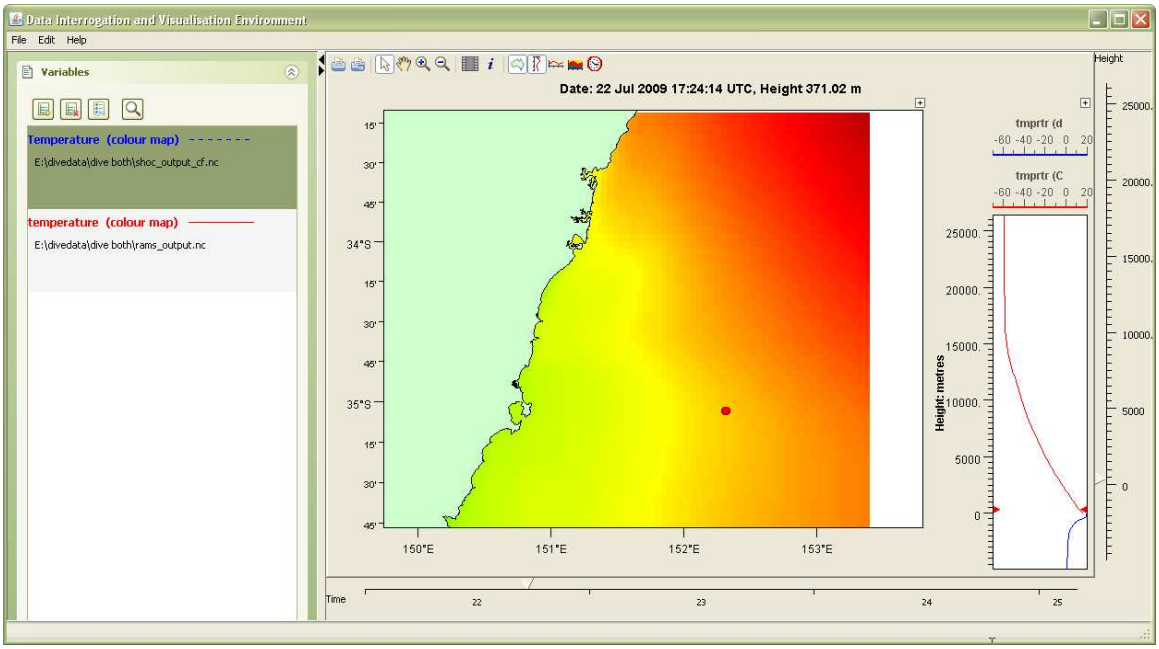

Figure 4.4. Simultaneous ocean and atmospheric model output showing combined temperature profiles at the sample point (red dot)

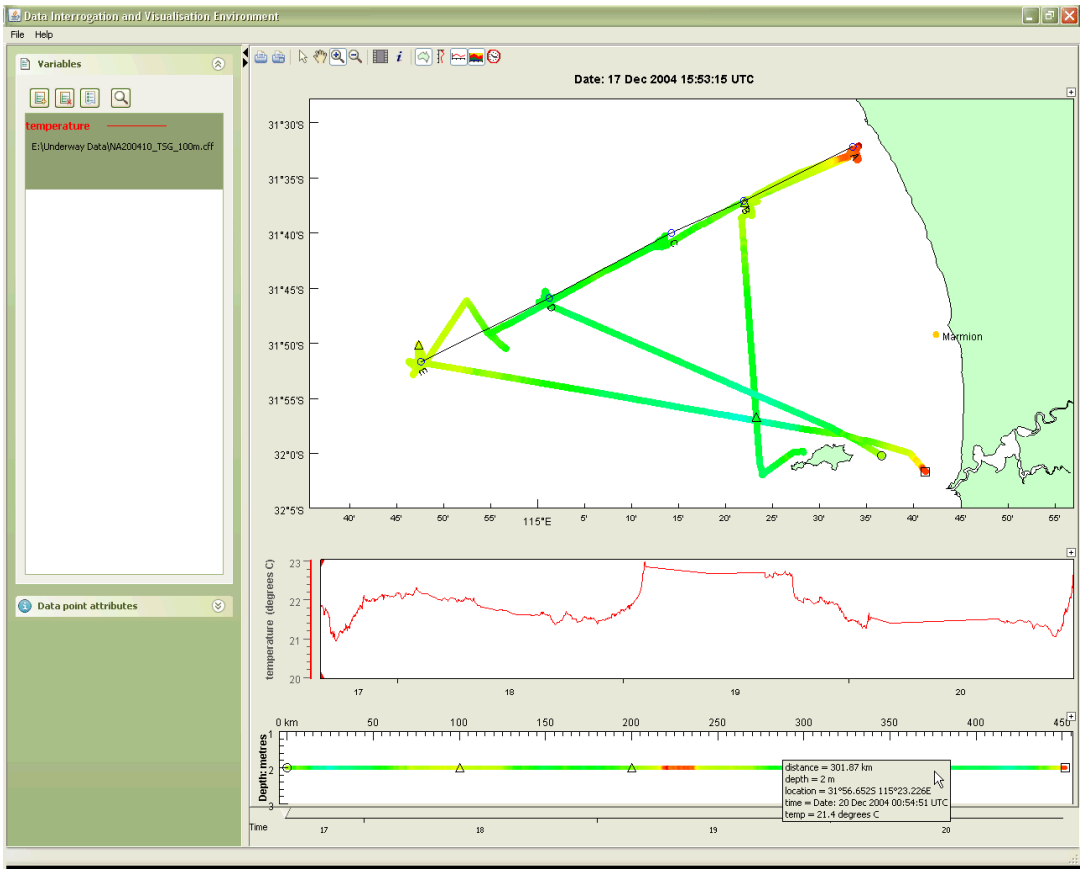

Figure 4.5. Display of underway data, showing the information panel activated by hovering the cursor over a reference point

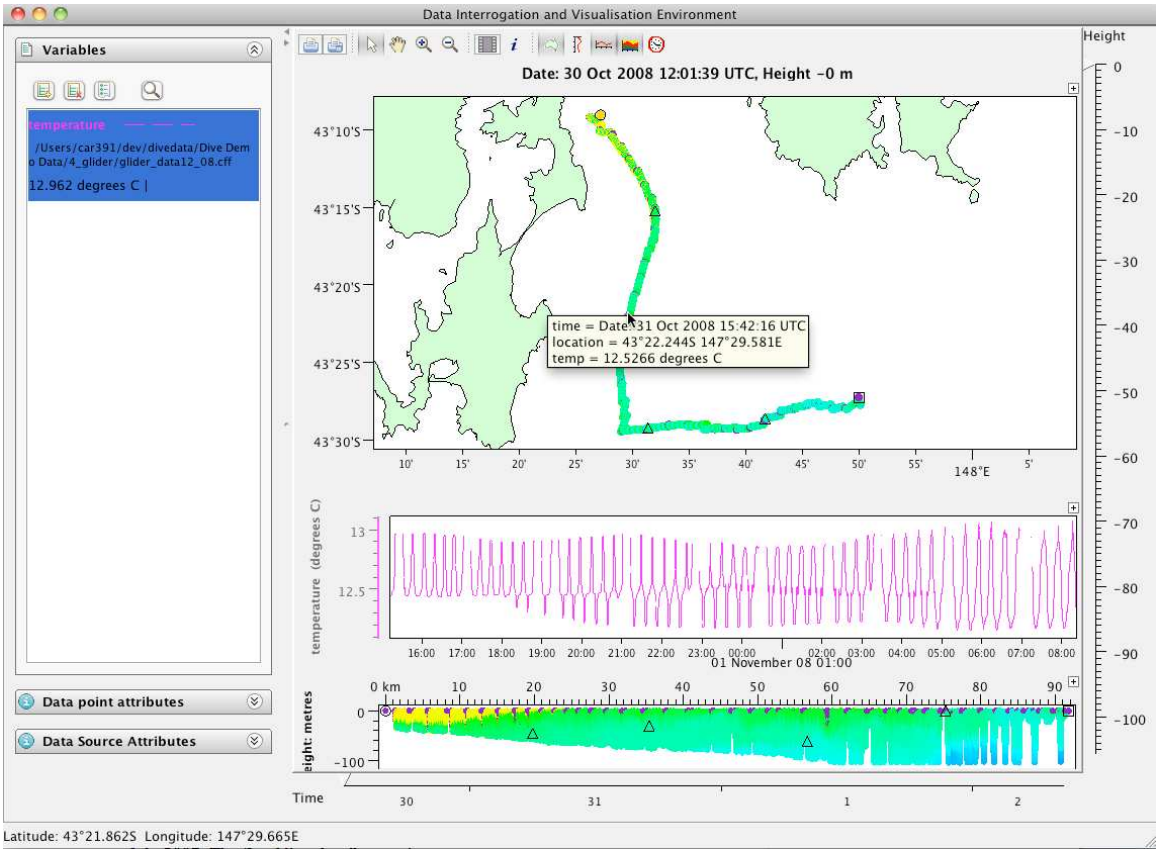

Figure 4.6. Display of glider data, showing information panel activated by hovering the cursor over a reference point

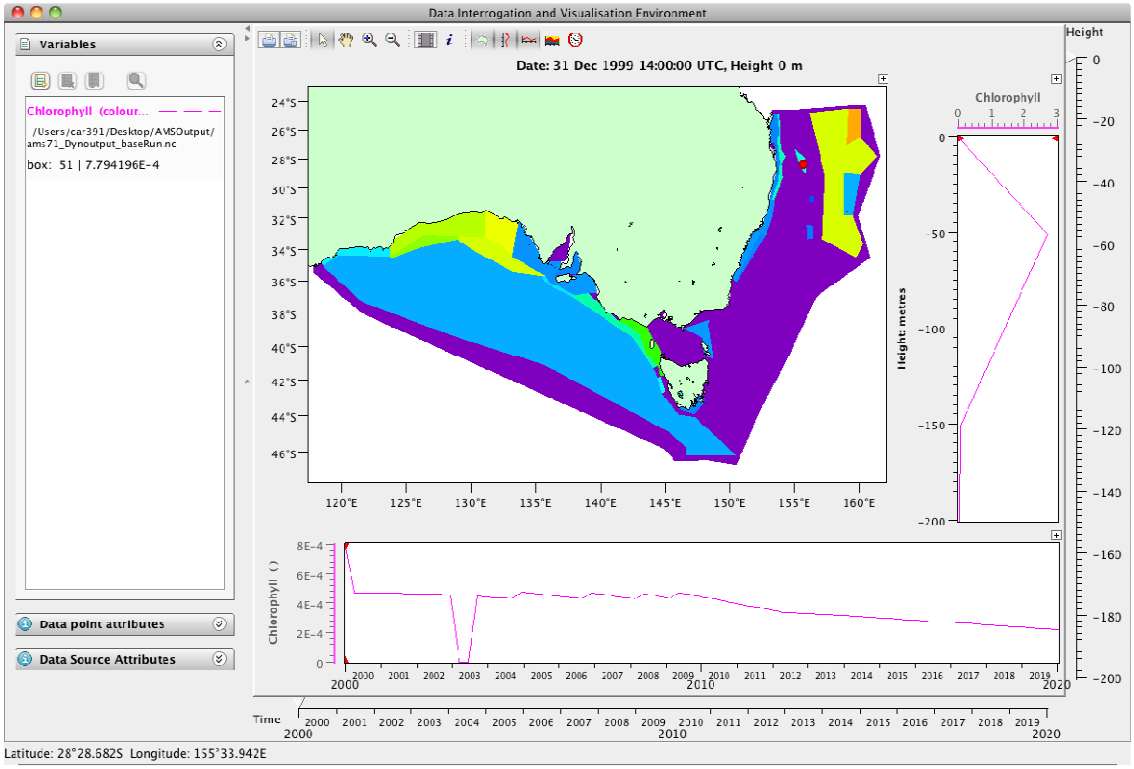

Figure 4.7. Box Model output from Atlantis

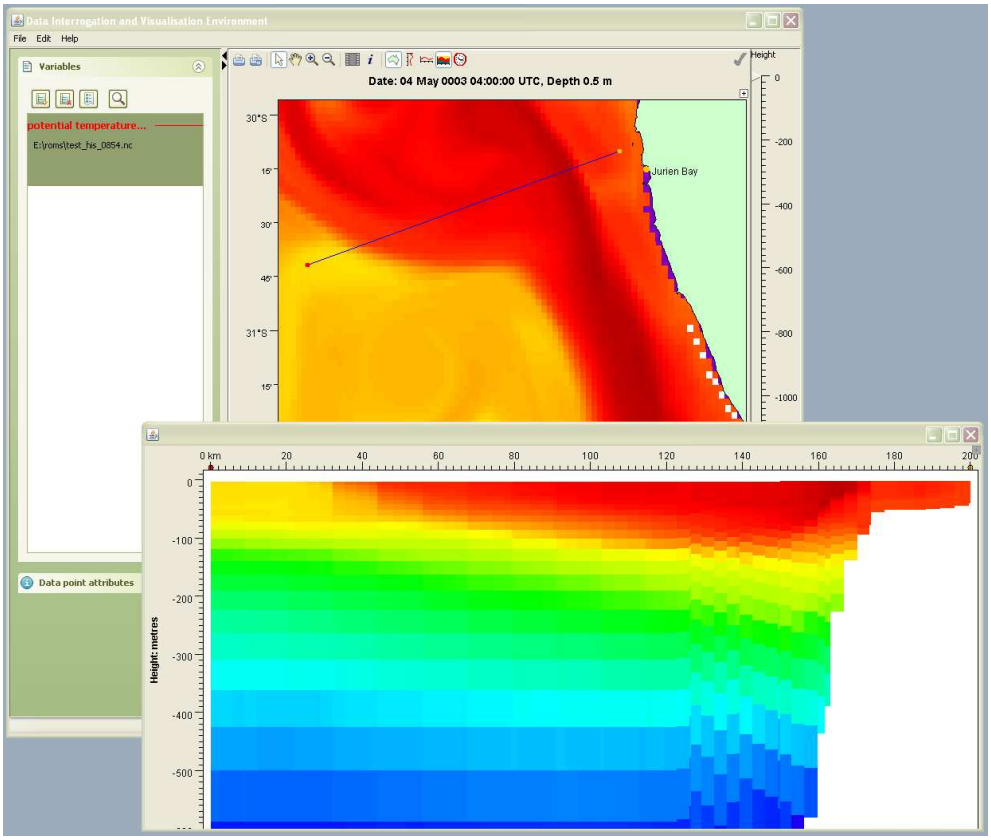

Figure 4.8. ROMS model output showing a cross section with sigma levels

Contact Us
Phone: 1300 363 400
+61 3 9545 2176
Email: enquiries@csiro.au
Web: www.csiro.au

Your CSIRO

Australia is founding its future on science and innovation. Its national science agency, CSIRO, is a powerhouse of ideas, technologies and skills for building prosperity, growth, health and sustainability. It serves governments, industries, business and communities across the nation.